Function of Lin9 *in vivo*

and

MAP3K4-p38 signaling regulates p53 mediated cell cycle arrest after defective mitosis

Dissertation zur Erlangung des

naturwissenschaftlichen Doktorgrades

der Bayerischen Julius-Maximilians-Universität Würzburg

vorgelegt von

Tanja Ulrich

aus Würzburg

Würzburg, 2012

Eingereicht am:

……

Mitglieder der Promotionskommission:

Vorsitzender:
1. Gutachter: Prof. Dr. Stefan Gaubatz
2. Gutachter: Prof. Dr. Georg Krohne

Tag des Promotionskolloquiums:

……

Doktorurkunde ausgehändigt am:

……

Contents

1 Introduction

1.1 The human cell cycle

The human cell cycle is a complex process which is essential for cell growth, proliferation, survival and development. Different series of events regulate the proper division of one cell into two daughter cells, thereby transmitting the genetic information equally to the next cell generation. Precise regulation of cell cycle progression is fundamental for cell proliferation and genomic integrity as alterations in cell division can lead to tumor formation.

The cell cycle can be divided into four major phases: G1 phase (gap1), S phase (synthesis) and G2 phase (gap2), that are collectively termed interphase, and M phase (mitosis) (Vermeulen et al., 2003). The two main phases are the S phase, that is characterized by DNA replication and chromosome duplication, and the M phase, where the separation of the duplicated chromosomes and the division into two cells takes place. Between S and M phase, the gap phases allow the cells to prepare for the next cell cycle stage. In G1 and G2, the cells are metabolically active and synthesize proteins that are required to enter the subsequent cell cycle phase. Progression through the cell cycle is dependent on external mitogens that stimulate proliferation in early G1 phase. Absence of growth signals triggers cells to exit the cell cycle in G1 and enter a non-proliferating quiescent state termed G0 phase. In humans, the majority of cells are non-proliferating, non-growing cells in G0 (Johnson and Walker, 1999; Vermeulen et al., 2003).

1.1.1 Cell cycle regulation

Progression through the cell cycle is mediated by two distinct classes of molecules, cyclins and cyclin-dependent kinases (CDK) (Sánchez and Dynlacht, 2005). CDKs are heterodimeric serine/threonine kinase proteins that require association with a specific regulatory cyclin subunit to become active. The four main CDKs in humans, CDK1, CDK2, CDK4 and CDK6 remain stable throughout the cell cycle whereas the various cyclins have an unique oscillating expression pattern during the cell cycle and determine the activity of their associated CDK. Cyclin/CDK complexes regulate progression through the different stages of the cell cycle by phosphorylating specific substrates that are involved in DNA replication and mitosis. To achieve full kinase activity the CDKs are further phosphorylated by CDK activating kinases (CAK) (Lees, 1995; Morgan, 1997; Vermeulen et al., 2003).

At the beginning of the cell cycle, in G1, expression of cyclinD is induced by extracellular mitogenic signals like growth factors (Hunter and Pinest, 1994). CyclinD preferentially binds to CDK4 and CDK6 to regulate progression through G1 by phosphorylating the tumor

suppressor protein pRB (Sherr, 1996). pRB acts as a negative regulator of cell proliferation by binding to the transcription factor E2F (E2F1-3), which regulates the expression of genes that are important for G1/S transition. Hyperphosphorylation of pRB by CDK4/6 results in the release of E2F from its repressive complex (Sherr, 1996; Stevaux and Dyson, 2002). Once E2F proteins are no longer repressed by pRB, the cells bypass the restriction point (R-point). Now, independent on extracellular growth signals, the cells are committed to divide (Planas-Silva and Weinberg, 1997). This emphasizes the important role of pRB, the product of the first identified tumor suppressor gene *RB-1*, in controlling cell cycle progression. The fact that pRB is found to be mutated in one third of human tumors also underlines the essential function of this protein (Lee et al., 1987; Sherr, 1996). E2Fs induce the transcription of cell cycle regulators like the S phase cyclins E and A, and of genes that are essential for DNA replication and nucleotide synthesis (Trimarchi and Lees, 2002). CyclinE-CDK2 complexes mainly regulate the G1-S transition (Ohtsubo et al., 1995), whereas the cyclinA-CDK2 composition is required later during S phase (Girard et al., 1991). In G2 and early M phase cyclinA and cyclinB associate with CDK1 to facilitate entry into mitosis. The mitotic cyclinB-CDK1 complex, also known as mitosis promoting factor (MPF), regulates the activation of substrates necessary for chromosome segregation and mitotic spindle assembly. Ubiquitination and following degradation of cyclinB in late mitosis is mediated via the E3

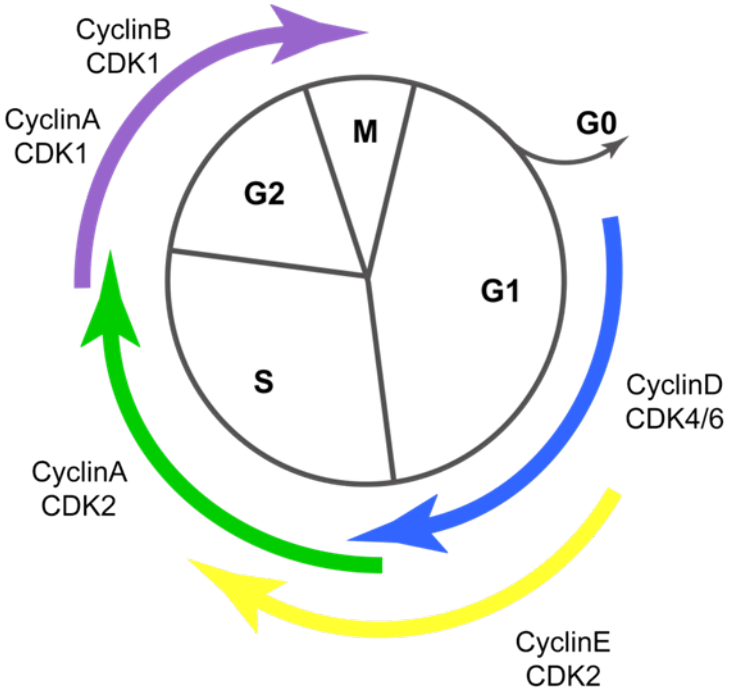

Fig. 1.1: The human cell cycle
The cell cycle consists of the four distinct phases G1, S, G2 and M phase. Progression through the mitotic cycle is regulated by the activity of different Cyclin-CDK complexes. See text for detailed description.

ligase APC/C. CyclinB degradation results in mitotic exit and in the restart of the cell cycle (King et al., 1994; Zachariae, 1999).

CDK inhibitors:
CDK activity is antagonized by two classes of CDK inhibitors, the INK4 and the CIP/KIP family of CDK inhibitors. The INK4 proteins p16INK4a, p15INK4b, p18INK4c and p19INK4d inhibit the activation of G1 phase cyclin-CDK complexes by preventing association of CDK4/6 to cyclinD (Lees, 1995; Vermeulen et al., 2003). Without active cyclinD-CDK4/6 complexes the cell is unable to proceed through the cell cycle and arrests in G1 phase. The INK4a locus encoding for p16 is altered in a high percentage of human tumors by hypermethylation or deletion (Kamb, 1998), pointing out the important function of these CDK inhibitors in preventing uncontrolled proliferation by inducing cell cycle arrest. The second class of CDK inhibitors, the CIP/KIP family, consists of p21(Waf1/Cip1), p27(Cip2) and p57(Kip2) (Harper et al., 1995; Lee et al., 1995; Carnero and Hannon, 1994). Unlike the INK4 inhibitors, the CIP/KIP proteins show a higher affinity to already formed cyclin-CDK complexes than to monomeric CDK subunits (Lees, 1995). p21, which is transcriptionally activated by the tumor suppressor protein p53 (El-Deiry et al., 1993), further inhibits DNA replication by binding to the proliferating cell nuclear antigen (PCNA) (Pan et al., 1995).

Checkpoints:
In order to maintain genomic integrity, cell cycle progression has to be tightly controlled at specific checkpoints (Hartwell and Weinert, 1989). In mid-late G1 phase the restriction point (R-point) marks the transition between early-mid G1 and the subsequent cell cycle. After passing the R-point cells are independent of extracellular stimuli and are committed to complete the cell cycle (Planas-Silva and Weinberg, 1997).
In response to DNA damage, cells arrest in the cell cycle at the G1/S checkpoint before entering S phase, or at the G2/M checkpoint after DNA replication. DNA damage, that occurs as a result of external stimuli like UV-irradiation triggers activation of ATM (ataxia telangiectasia mutated) and ATR (ataxia telangiectasia related) kinases. Their downstream targets Chk1 and Chk2 block cell cycle progression by inhibiting the phosphatase CDC25, which acts as activator of CDKs (Sancar et al., 2004). Another target of the DNA damage signaling pathway is p53 which promotes transcription of cell cycle arresting genes like p21, DNA repair genes or apoptotic genes (Vousden and Lu, 2002).
In mitosis, the spindle assembly checkpoint (SAC) detects improper alignment of chromosomes and holds the cell cycle in metaphase by inhibiting the anaphase promoting complex (APC/C) (see 1.1.2.1).

All these mechanisms make sure that cells are either repaired after damage or, if the defects are too severe undergo apoptosis or senescence to prevent genomic instability which has been linked to carcinogenesis (Kastan and Bartek, 2004; Kuilman et al., 2010).

1.1.2 Mitosis and cytokinesis

Mitosis is divided into five subphases: prophase, prometaphase, metaphase, anaphase and telophase. During prophase the chromosomes, containing two sister chromatids that are held together by cohesin, condense in the nucleus and the duplicated centrosomes separate and migrate to the opposite cell poles to form the mitotic spindle. Prometaphase is initiated with the breakdown of the nuclear envelope. Then the chromosomes become attached by spindle microtubules at the kinetochor, a multiprotein complex in the centromeric region. In metaphase the chromosomes align at the spindle equator which is called the metaphase plate. When all chromosomes are attached by microtubules, cells proceed to anaphase where the sister chromatides get separated and are pulled to the spindle poles by microtubule shortening. After complete chromosome segregation cells enter telophase where chromosomes decondense, the nuclear membrane is reformed and the first steps of cytokinesis are initiated (Alberts, 2002).

Cytokinesis, the final step of cell division, results in the cytoplasmic separation of the newly formed daughter cells. A contractile ring, which is built up of actin and myosin filaments, forms the cleavage furrow which closes the cytoplasmic connection between the two daughter nuclei by furrow ingression. The remaining cytoplasmic bridge is called the midbody, a dense structure consisting of microtubules from the central spindle and of regulatory proteins. Finally, abscission of the midbody completes cytokinesis (Glotzer, 2003; Skop et al., 2004).

1.1.2.1 The spindle assembly checkpoint

The spindle assembly checkpoint (SAC) is an important surveillance mechanism in mitosis that ensures fidelity of chromosome segregation by sensing unattached kinetochors. The activated SAC inhibits the anaphase promoting complex/cyclosome (APC/C) until all sister chromatid pairs have become bipolarly attached to microtubules and have aligned in the metaphase plate. APC/C, a multi-subunit E3 ubiquitin ligase, is required for sister chromatid separation and regulates the transition from metaphase to anaphase. Unattached kinetochores activate the SAC, which interferes with the function of Cdc20, the substrate recognition subunit of APC/C. The SAC consists of the core component proteins Bub3, BubR1, Mad2, Bub1, Mad1 and Msp1. Bub3, BubR1 and Mad2 are recruited to unattached kinetochors, where they form the mitotic checkpoint complex (MCC) by binding to Cdc20 and thereby inhibiting APC/C. As soon as all chromatides have achieved attachment to the mitotic spindle, the SAC is switched off and APC/C is activated. The two main targets of APC/C, Securin and cyclinB, become ubiquitinated and degraded via the proteasome. Degradation of Securin releases the protease Separase that cleaves Cohesin, a protein ring that pairs sister chromatids. CyclinB degradation inactivates CDK1 and thus enables mitotic exit (Kang and Yu, 2009; Musacchio and Hardwick, 2002; Yu, 2002).

1.1.2.2 Aurora kinases

The Aurora protein kinase family (Aurora A, B and C) plays a crucial role in the regulation of mitosis and cytokinesis. Aurora A and B share over 70% homology but have diverse subcellular localizations and functions.
Aurora A localizes to the spindle poles and regulates centrosome maturation and separation, which is necessary for bipolar spindle assembly and mitotic entry (Carmena and Earnshaw, 2003; Vader and Lens, 2008). Aurora B is the catalytic component of the chromosomal passenger complex (CPC) which consists of the scaffolding protein INCENP and the subunits Survivin and Borealin (Vader et al., 2006). The CPC features a dynamic localization pattern during mitosis: during prometaphase and metaphase the complex associates with chromosome arms and the inner centromeres and is transferred to the central spindle midzone and to the midbody in late mitosis and cytokinesis (Ruchaud et al., 2007; Vader et al., 2006). The main function of Aurora B is the regulation of chromosome bi-orientation in the metaphase plate by correcting microtubule-kinetochor misattachments, and the formation and stability of the mitotic spindle (Ditchfield et al., 2003; Hauf et al., 2003). Aurora B supports the spindle assembly checkpoint function by recruiting the SAC proteins BubR1, Mad2 and CenpE to unattached kinetochors and by phosphorylating BubR1 (Ditchfield et al., 2003). In cytokinesis Aurora B plays an essential role by targeting several substrates that are necessary for correct cell division (Carmena and Earnshaw, 2003; Fu et al., 2007). Furthermore, Aurora B controls the timing of abscission by preventing furrow regression in cells with incompletely segregated chromosomes, thereby protecting cells against tetraploidization (Steigemann et al., 2009).
The activity of Aurora kinases A and B is tightly regulated by phosphorylation and degradation. Aurora A reaches its highest activity during G2/M transition and falls during exit of mitosis. Aurora B protein levels peak in G2/M phase and highest kinase activity is found from metaphase to the end of mitosis (Katayama et al., 2003; Fu et al., 2007). Degradation of Aurora A and B is mediated via the APC/C ubiquitin ligase after exit of mitosis (Castro et al., 2002; Nguyen et al., 2005).
The third member of the Aurora kinase family, Aurora C shows a localization pattern similar to Aurora B but mainly functions in meiosis (Yang et al., 2010).

Aurora kinases are frequently overexpressed in human tumors emphasizing their crucial function as regulators of mitosis and cytokinesis. As uncontrolled expression of these mitotic regulatory proteins promotes tumorigenesis by induction of chromosomal instability, Aurora kinases have become potential targets for cancer therapy approaches (Katayama et al., 2003; Vader and Lens, 2008). A number of small molecule inhibitors that block the catalytic activity of Aurora kinases is already in preclinical or clinical trials to date. Inhibition of Aurora induces tetra- and polyploidy which results in cell cycle arrest or apoptosis and inhibition of tumor growth (Gautschi et al., 2008; Katayama and Sen, 2010).

1.1.3 Aneuploidy and tumorigenesis

Most cancer cells are characterized by aneuploidy, an abnormal karyotype with structural and numerical aberrations of chromosomes. Although Theodor Boveri proposed that cancer is caused by aneuploidy over 100 years ago (Boveri, 2008), the role of aneuploidy in cancer is still poorly understood and it is still controversially discussed if aneuploidy is cause or consequence of tumorigenesis (Thompson et al., 2010; Weaver and Cleveland, 2006). The majority of aneuploid tumors have chromosome numbers between 40 and 60 chromosomes indicating that an imbalance in the chromosome number through chromosomal instability (CIN) - the missegregation of whole chromosomes - can be regarded as the most common pathway to aneuploidy (Thompson et al., 2010). In several tumor types including colon, lung and breast, CIN has been shown to be associated with aneuploidy (Lengauer, 1997; Yoon et al., 2002; Haruki et al., 2001).

There are two routes to the formation of aneuploid cells: they can either arise directly from diploid cells by loss or gain of chromosomes during mitosis or through a tetraploid intermediate.
Chromosome missegregation in diploid cells can occur through partial inactivation of the spindle checkpoint by reduced expression of spindle checkpoint proteins, or through centrosome amplification. Mice that are heterozygous in spindle checkpoint genes show high frequencies in aneuploidy but the type of aneuploidy and the development of spontaneous tumors are different: for instance, mice with reduced levels of Bub3 and BubR1 do not develop spontaneous tumors (Baker et al., 2004, 2006), but mice that are heterozygous for Mad1 or Mad2 are more tumor prone although these mice develop tumors after a long latency (Michel et al., 2001; Iwanaga et al., 2007). The variability in tumor formation found in the different mouse models could be due to the additional nonmitotic functions of several mitotic checkpoint proteins and it is therefore proposed that aneuploidy generated by a weakened mitotic checkpoint drives tumorigenesis only if other cellular pathways are affected (Weaver and Cleveland, 2009).
An intermediate tetraploid status is often found in tumor cells at early stage and it is assumed that tetraploidy increases chromosomal instability and is a precursor of aneuploidy and cancer (Barrett et al., 2003; Olaharski et al., 2006; Storchová et al., 2006). Unstable tetraploid cells can arise from mitotic slippage due to prolonged mitotic arrest, from cell fusion or failures in cytokinesis (Storchova and Pellman, 2004; Ganem et al., 2007). As consequence, the increased number of centrosomes in tetraploid cells can lead to the formation of multipolar spindles and defects in chromosome segregation (Gisselsson et al., 2008). Amplification of centrosomes has been linked to chromosomal instability and aneuploidy in various studies (Rajagopalan and Lengauer, 2004; Saunders, 2005), for instance 80 % of invasive breast tumors harbor abnormal centrosome numbers and/or structures (Lingle et al., 2002).

Proliferation and survival of tetraploid precursor cells is limited by the tumor suppressor protein p53. Tetraploid cells derived from failed cell division have been shown to arrest in the following G1 phase by p53-dependent mechanism in order to prevent chromosomal instability and tumorigenesis (Ganem and Pellman, 2007; Stukenberg, 2004).

1.2 Cellular stress response pathways

Cells are continuously exposed to various forms of endogenous and exogenous stress stimuli like DNA damage, oxidative stress, osmotic stress, hypoxia, inflammation or oncogene activation. Dependent on the cellular context the stress signals activate complex pathways that mediate cell cycle control and survival or cell death.

1.2.1 MAP kinase stress signaling pathways

Mitogen-activated protein kinase (MAPK) cascades are highly conserved signaling transduction pathways that regulate several processes like proliferation, differentiation, metabolism, survival and apoptosis (Hommes et al., 2003).
Fundamental for each MAP kinase pathway is a three-tiered core signaling module consisting of the MAP-kinase-kinase-kinase (MAPKKK, MAP3K), MAP-kinase-kinase (MAPKK, MAP2K) and MAP-kinase (MAPK). The first component acting in the MAPK signaling cascade is the serin/threonine protein kinase MAPKKK that is activated either by phosphorylation or by interaction with regulatory proteins in response to diverse stimuli. Activated MAPKKKs phosphorylate and activate MAPKKs which then specifically stimulate MAPK activity through dual phosphorylation of threonine and tyrosine residues. MAPKs activate multiple downstream effectors like MAPK activated kinases (MAPKAPKs) and transcription factors to finally generate the biologic responses.
The three main MAP kinase signaling transduction cascades are the ERK1/2, the JNK and the p38 MAPK pathways. The ERK1/2 MAPK pathway responds to mitogenic stimuli and cytokines and plays a central role in cell growth, proliferation and survival. The JNK and p38 MAPK signaling pathways are activated upon different kinds of cellular stresses and regulate multiple cellular processes like inflammation, apoptosis, cell differentiation and cell growth (Hommes et al., 2003; Kyriakis and Avruch, 2001; Pearson et al., 2001).

p38 MAPK:
The p38 MAPK signaling pathway belongs to the mammalian stress response pathways and has important functions in inflammation processes, cell differentiation, cell survival and cell death.
This family of MAP kinases consists of the four isoforms p38α, p38β, p38γ and p38δ and each shares about 60% identity within the p38 family. The p38 MAP kinase family can

be divided into two subgroups: p38α and p38β on the one hand and p38γ and p38δ on the other. This classification is based on the different expression patterns, the higher homology of the isoforms within one subgroup, the substrate specificity of these kinases and their sensitivity to pharmacological inhibitors (Cuenda and Rousseau, 2007). While p38α and p38β are ubiquitously expressed, p38γ and p38δ are expressed tissue specifically: p38γ is predominantly found in skeletal muscle, p38δ is mainly expressed in the lungs, kidney, pancreas, small intestine and testis (Ono and Han, 2000).
The p38 signaling pathway is activated by a wide range of different stress stimuli. p38 responds to inflammatory cytokines (e.g. TNFα , TGFβ), pathogens (e.g. LPS, Herpes simplex virus 1), growth factors and environmental factors such as heat shock, osmotic shock, UV irradiation or hypoxia. Activation of p38 is mediated by the upstream MAP2 kinases (MAPKK) MKK3 and MKK6. MKK6 phosphorylates and activates all four p38 isoforms whereas MKK3 has been shown to preferentially activate p38α, p38γ and p38δ but not p38β (Enslen et al., 2000; Keesler et al., 1998). In addition, p38α and p38δ can also be phosphorylated by the JNK activator kinase MKK4 (Brancho et al., 2003; Jiang, 1997). MKK3/6 on their part are activated by a large group of MAP3 kinases (MAPKKK). Among other MEKK3, MEKK4, DLK1, TAK1, MLK3 and ASK1 are responsible for p38 activation (Cuevas et al., 2007). The wide range of MAP3 kinases that is implicated in the regulation of the p38 signaling pathway explains the diversity of stimuli that can trigger p38 activation. Downstream targets of p38 are either other protein kinases or transcription factors that mediate the cellular behavior upon different stress signals (Ono and Han, 2000).

JNK:
The second stress responsive MAPK signaling pathway besides p38 is the JNK pathway that regulates cell death but also cell proliferation and survival. The three isoforms within this MAPK family JNK1, JNK2 and JNK3, show different expression patterns: JNK1/2 are widely expressed in many tissues, whereas JNK3 is mainly found in neuronal tissue, testis and heart (Bode and Dong, 2007).
Like p38, JNK is activated upon various kinds of cellular stress signals including heat shock, osmotic stress, UV-irradiation and cytokines. JNKs are phosphorylated and activated by their upstream MAP2 kinases MKK4 and MKK7 (Lawler et al., 1998) which on their part are regulated by several MAP3 kinases like MEKK 1-4, MLK 1-3, TAK1 and DLK1 (Cuevas et al., 2007). Dependent on the stimulus JNK can activate several transcription factors and proteins (Bogoyevitch and Kobe, 2006). Due to their shared upstream MAP3 kinases, p38 and JNK pathways are simultaneously activated in response to stress stimuli.

A simplified model of the p38 and JNK MAPK signaling pathways with the participating MAP kinases is illustrated in Fig. 1.2.

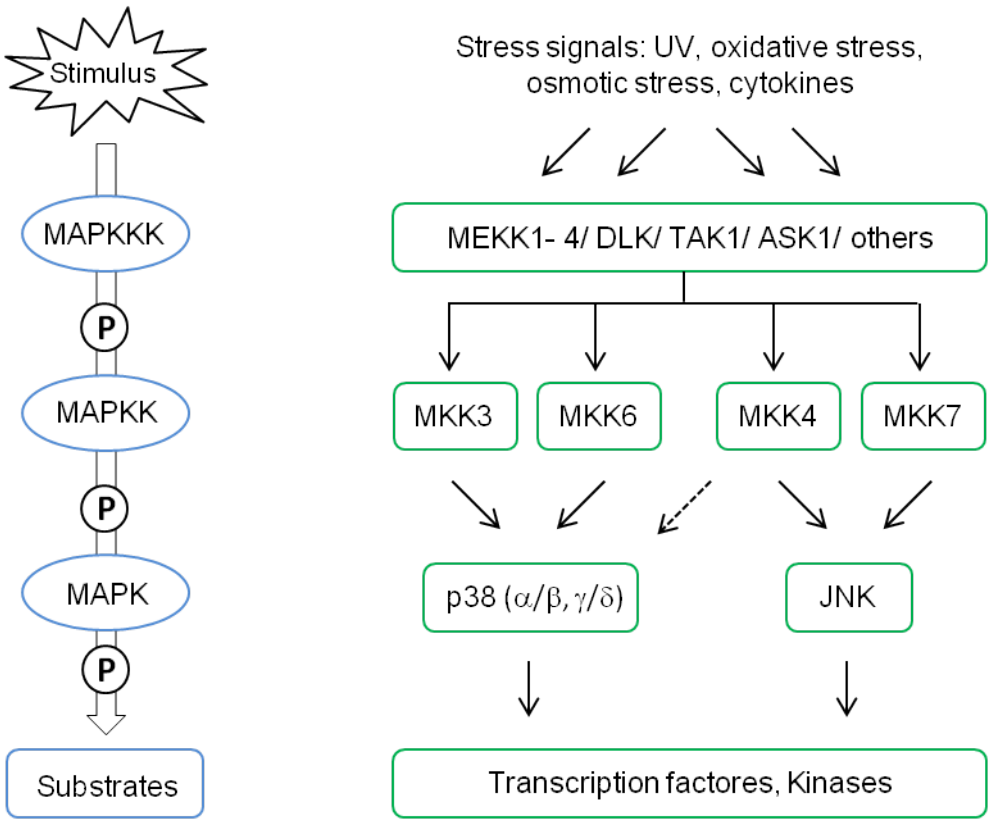

Fig. 1.2: Stress activated p38 and JNK MAPK signaling pathways
Different kinds of stress stimuli activate p38 and JNK through a conserved kinase cascade. Dependent on the stress signal a MAPKKK activates a downstream MAPKK that triggers the signal to the MAPKs p38 and JNK. Activation of p38 and JNK results in phosphorylation of transcription factors and other proteins. P = phosphorylation

1.2.2 The p53 tumor suppressor pathway

The tumor suppressor p53 is one of the most important proteins regulating genomic integrity and preventing tumorigenesis by coordinating cellular responses to multiple stress factors. Its cellular gatekeeper function becomes apparent as p53 is mutated in over half of all human tumors. Additionally, tumors that retain wild-type p53 often exhibit alterations in p53 regulatory proteins (Vogelstein et al., 2000; Vousden and Lu, 2002).

In response to various forms of stress, p53 regulates the expression of a large number of target genes that determine the cellular outcome by inducing apoptosis, cell cycle arrest or senescence. The particular cell fate is thereby dependent on the cell type, the environment and the nature of stress. Low levels of stress activate p53 to mediate a temporary cell cycle arrest that allows cells to pause and repair the occurred damage. If the stress signal is sustained or too severe, p53 triggers an irreversible cell cycle arrest (senescene) or apoptosis

(Ashcroft et al., 2000; Riley et al., 2008; Vogelstein et al., 2000). Different stress signals like UV irradiation, hypoxia or oncogenic stimuli can utilize diverse and independent signaling pathways to regulate p53 activity, which reflects the complexity of the p53 network (Horn and Vousden, 2007; Murray-Zmijewski et al., 2008).

The activation of p53 includes three main steps: stabilization of p53 by preventing its degradation, promoter-specific binding and transcriptional activation. In these processes different post-translational modifications as well as several regulatory proteins and interacting partners of p53 are involved.

In unstressed cells the negative regulator of p53, the ubiquitin E3 ligase Mdm2, controls the stability of p53 by targeting it for proteasomal degradation (Fang et al., 2000). Disruption of the p53-Mdm2 interaction is the crucial step in the stabilization of p53 and can be achieved by different mechanisms. Phosphorylation of serine residues in the N-terminal domain of p53, that inhibits the interaction of p53 and Mdm2, has been regarded as the first step of p53 stabilization. Several kinases like ATM, ATR, Chk1, Chk2, JNK and p38 are known to phosphorylate p53 at specific serine residues. These phosphorylation events facilitate the recruitment of p53 coactivators, such as p300/CBP, that further enhance p53 stabilization and activation by acetylating the C-terminal domain of p53 (Bode and Dong, 2004; Lavin and Gueven, 2006). Besides the post-translational modifications on p53 that prevent Mdm2 binding, several proteins can directly control the levels and function of Mdm2 and influence p53's stability. For instance, upon oncogenic stress the Mdm2 regulator p19ARF is induced and binds to Mdm2, thereby inactivating its activity as ubiquitin ligase (Kruse and Gu, 2009; Lavin and Gueven, 2006).

Once stabilized, p53 translocates to the nucleus and binds as tetramer to sequence-specific responsive elements (RE) in promoter regions of target genes where it becomes transcriptionally activated. Several factors are involved in the complex regulation of promoter-specificity and transcriptional activation of p53. Dependent on the type of stress stimulus, post-translational modifications, such as acetylation or methylation, and recruitment of coactivators and binding partners affect the activity of p53 and the induction of specific target genes.

Thus, a special kind of 'barcode' of precise combinations of post-translational modifications and interacting cofactors is likely to be required in order to determine the transcriptional program of p53 and thus the cellular stress response (Beckerman and Prives, 2010; Kruse and Gu, 2009; Murray-Zmijewski et al., 2008).

1.2.3 Senescence as consequence of cellular stress

One type of cellular response to severe stress stimuli is the induction of cellular senescence, an irreversible arrest of cell growth. Besides the programmed cell death apoptosis, senescence seems to be another self-defense mechanism to prevent tumorigenesis.
Senescent cells that arrest in the G0/G1 phase of the cell cycle loose the ability to respond to mitogenic stimuli, alter their gene expression, undergo morphological changes and are resistant to apoptosis (Ben-Porath and Weinberg, 2005; Zhang, 2007).
Cellular senescence can be categorized into two distinct classes: replicative senescence that is induced by telomere shortening during cell aging (Allsopp and Harley, 1995), and stress induced premature senescence that is activated by various different stress conditions like oncogenic or oxidative stress (Chen et al., 1995; Serrano et al., 1997).
The central tumor suppressor pathways that are involved in the induction of the senescence program are the p53-21 and the p16-pRB pathways. p16 activates pRB by inhibiting cyclinD-CDK4/6 complexes. p53, that can be activated by p19ARF, induces expression of p21, that in turn can mediate activation of pRB by inhibiting cyclinD-CDK4/6 and cyclinE-CDK2. Hypophosphorylated pRB represses the transcription of E2F target genes, thereby inducing growth arrest. Dependent on the cell type and the nature of stress p53 and pRB can either be activated as one linear pathway (ARF-p53-p21-pRB) or as two parallel pathways (p53-p21, p16-pRB) (Ben-Porath and Weinberg, 2005; Dimri, 2005; Itahana et al., 2004). For instance, in response to telomere shortening senescence is mediated through a linear p53-p21-pRB pathway in human fibroblasts (Wei et al., 2003). In mouse fibroblasts oncogenic stimuli initiate the senescence response through one linear pathway (ARF-p53-p21-pRB), whereas in human cells oncogenic activation induces both senescence pathways in parallel (p53-p21, p16-pRB) (Serrano et al., 1997).
Mitotic stress - mediated through inhibition or altered expression of mitotic proteins - has also been linked to premature senescence. Reduced levels of the spindle checkpoint protein Bub1 or BubR1 can induce premature senescence in mouse fibroblasts (Baker et al., 2004; Schliekelman et al., 2009). Similary, reduction of the centromere protein CENP-A in human fibroblasts causes p53 dependent cellular senescence (Maehara et al., 2010).

1.3 The DREAM complex

Proper progression through mitosis is essential in order to avoid genomic instability. Therefore, the expression of G2/M genes has to be well coordinated. Recently, our group identified the DREAM (or LINC) complex, a multi-protein complex that is required for the transcriptional regulation of specific G2/M genes (Osterloh et al., 2007; Schmit et al., 2007).
DREAM is a stable complex consisting of the core subunits Lin9, Lin37, Lin52, Lin54 and the chromatin associated protein RbAp48 (Schmit et al., 2007). This complex is highly conserved and the protein subunits of DREAM are related to that of the dREAM/Myb-MuvB complex in Drosophila melanogaster (Korenjak et al., 2004; Lewis et al., 2004) and the DRM/synMuv complex in Caenorhabditis elegans (Harrison et al., 2006).
During the cell cycle DREAM shows a dynamic cell cycle dependent interaction with the repressor proteins E2F4 and p130 in G0 phase and the transcription factor B-Myb in S phase (Litovchick et al., 2007; Pilkinton et al., 2007; Schmit et al., 2007). In quiescent cells DREAM binds together with E2F4/p130 to E2F regulated promoters and represses cell cycle dependent genes (Litovchick et al., 2007). The assembly of the DREAM repressor complex was shown to be regulated by the kinase DYRK1A that phosphorylates the DREAM subunit Lin52 resulting in activity of DREAM and entry in quiescence (Litovchick et al., 2011).
The DREAM complex composition switches when cells re-enter the cell cycle: DREAM dissociates from G1/S gene promoters and remains at specific G2/M gene promoters in S phase where it associates with B-Myb (Osterloh et al., 2007; Schmit et al., 2007). RNAi mediated knockdown experiments revealed the important function of DREAM in cell cycle progression: Depletion of the core subunit Lin9 resulted in impaired proliferation with cell accumulation in G2 and a delayed entry into mitosis. A cluster of DREAM target genes that is required for regulation of mitosis and cytokinesis has been identified with microarray analyses (Fig. 1.3): these genes have functions in mitotic entry (e.g. cyclinA2, B1, cdc2, AuroraA), in the mitotic spindle checkpoint and chromosome segregation (e.g. Plk1, Bub1, CENP-E, Survivin) as well as in cytokinesis and the mitotic exit (e.g. CENP-F, Ubch10, Cep55) (Osterloh et al., 2007; Reichert et al., 2010). The importance of the transcriptional regulation of mitotic genes by DREAM was demonstrated by severe defects in mitosis and cytokinesis that are found after deletion of Lin9 in mouse embryonic fibroblasts (MEFs): Lin9 knockout leads to binucleated and tetraploid cells with abnormal nuclei shape, multipolar spindles and supernumary centrosomes. These phenotypes results from defective spindle assembly, chromosomal missegreagation and cytokinesis defects. As consequence of these serious defects in mitosis MEFs undergo premature senescence to avoid further progression through the cell cycle (Reichert et al., 2010).

Lin9 is also essential for embryonic development. Homozygous Lin9-/- embryos at embryonic day 6.5 and 7.5 depict severe phenotypic abnormalities and die shortly after implantation

(Reichert et al., 2010). This developmental defect might be explained by the loss of Lin9 target gene expression, as several DREAM targets such as Plk1, CENP-A, and Fbxo5/Emi1 have been shown to be essential for early embryogenesis in mice (Howman et al., 2000; Lee et al., 2006; Lu et al., 2008). In contrast, heterozygous Lin9+/- mice develop normally with no obvious defects. However, these haploinsufficient Lin9 animals show increased numbers of tumors and reduced survival in a small cell lung tumor model (BXB-Raf), suggesting that Lin9 might function as a haploinsufficient tumor suppressor (Reichert et al., 2010).

In summary, these *in vivo* and *in vitro* studies emphasize the important role of the DREAM complex in the regulation of mitotic genes. (Reichert et al., 2010).

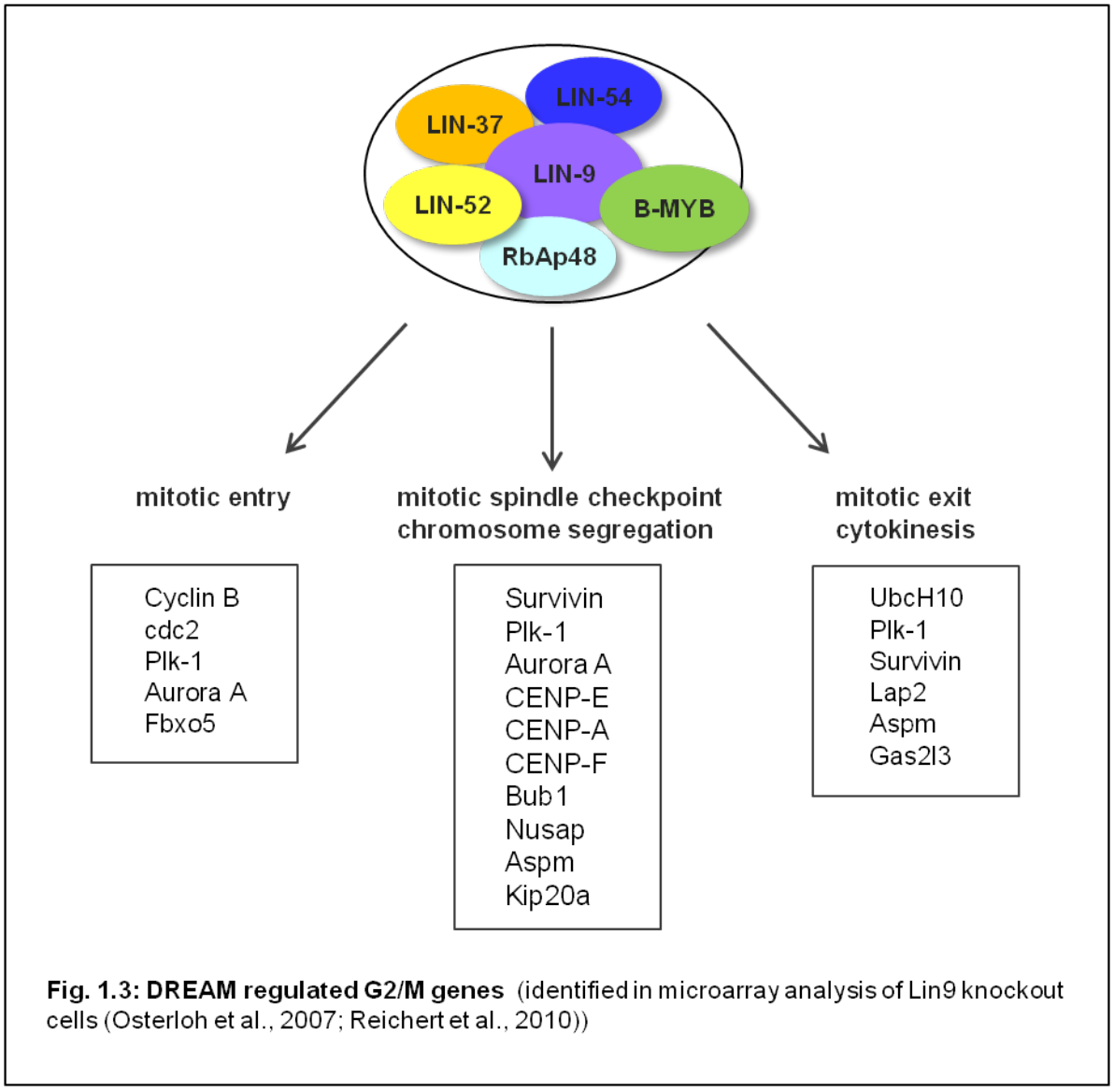

Fig. 1.3: DREAM regulated G2/M genes (identified in microarray analysis of Lin9 knockout cells (Osterloh et al., 2007; Reichert et al., 2010))

1.4 Aim of this project

From previous studies it was known that the DREAM complex is an essential regulator of mitotic gene expression. Downregulation of Lin9, one subunit of the DREAM complex, results in delayed entry into mitosis and impaired cell proliferation (Osterloh et al., 2007; Schmit et al., 2007).
Analysis of a constitutive Lin9 knockout mouse model revealed an important role of Lin9 in mouse development as complete loss of Lin9 caused early embryonic lethality. In order to study the function of Lin9 *in vitro* and *in vivo* with an inducible system, a conditional Lin9 knockout mouse model was generated. Conditional deletion of Lin9 in mouse embryonic fibroblasts (MEFs) leads to severe defects in mitosis and cytokinesis and cells display a premature senescence phenotype (Reichert et al., 2010).

The first aim of this project was to study the function of Lin9 by using the conditional knockout mouse model: MEFs generated from these mice were used to investigate the molecular pathways leading to senescence after Lin9 deletion. This Lin9 knockout mouse model was further used to analyzed the role of Lin9 in proliferation *in vivo*.

The second goal was to examine the pathways leading to p53-mediated cell cycle arrest after defective mitosis/cytokinesis in more detail. Therefore, a high throughput siRNA screening of the human kinome was performed in order to identify proteins that act in these pathways.

2 Materials and Methods

2.1 Materials

2.1.1 Chemical stocks and reagents

Unless otherwise indicated, commonly used chemicals were purchased from Applichem, Roth, Invitrogen or Sigma with analysis quality.

Chemicals	**Stock concentration**
Ammonium Persulfate (APS)	10 % in H_2O
Blasticidin	10 mg/ml in 10 mM Hepes, pH 7.4
Bovine serum albumin (BSA)	20 mg/ml in H_2O
DAB (BD Biosciences)	ready to use
DMSO	ready to use
dNTPs	2 mM dATP, dCTP, dGTP, dTTP each
Ethidium bromide	10 mg/ml in H_2O
Glutaraldehyde solution, Grade I, 25 %	ready to use
Hoechst 33258	10 mg/ml in H_2O
4-Hydroxytamoxifen (4-OHT)	10 mg/ml in ethanol
ImmuMount (Shandon)	ready to use
Luminol	250 mM in DMSO
Nocodazole	1 mg/ml in DMSO
p-Coumaric acid	90 mM in DMSO
Polybrene (Hexadimethrine bromide)	4 mg/ml in H_2O
Ponceau S solution	0.1 % Ponceau S in 5 % acetic acid
Propidium Iodide (PI)	1 mg/ml in H_2O
Protease Inhibitor Cocktail Sigma	ready to use
Random Primer	500 µg/ml in H_2O
RNase A	10 mg/ml in 10 mM Tris-HCl pH 7.4 150 mM NaCl
SB 202190 (p38-Inhibitor)	10 mM in DMSO
Temed 99 % p.a	ready to use
Trizol/Trifast (total RNA isolation reagent) (Peqlab/Thermo)	ready to use
Tamoxifen	10 mg/ml in peanut oil
Xylole	ready to use
ZM 447439 (Aurora kinase Inhibitor)	10 mM in DMSO

2.1.2 Buffers

2.1.2.1 General buffers

Phosphate buffered saline (PBS) (1 X)	13.7 mM NaCl 0.3 mM KCl 0.64 mM Na_2HPO_4 0.15 mM KH_2PO_4 adjust pH to 7.4 with HCl
TAE buffer (1X)	40 mM Tris base 5 mM glacial acetic acid 10 mM EDTA, pH 8.0
2 X HBS	280 mM NaCl 1.5 mM Na_2HPO_4 50 mM HEPES-KOH, pH 7.05
5 X DNA Loading Buffer	15 % Ficoll 0.05 % Bromphenol blue 0.05 % Xylene Cyanol 0.05 M EDTA in 1 X TAE

2.1.2.2 Buffers for whole cell lysates

TNN buffer	50 mM Tris-HCl, pH 7.5 120mM HCl 5 mM EDTA 0.5 % NP-40 10 mM $Na_4P_2O_7$ 2 mM Na_3VO_4 100 mM NaF ad 500 ml H_2O Protease Inhibitors (PI) 1:500 (add freshly)

Bradford Solution	50mg Coomassie Brilliant Blue G250 23.75 ml Ethanol 50 ml 85 % (v/v) ortho-phosphoric acid ad 500 ml H_2O filter twice

2.1.2.3 Buffers for immunoblot

Acrylamide solution for SDS gels	30 % (w/v) Acrylamide 0.8 % (w/v) N,N´-Methylenbisacrylamide
SDS running buffer	576 g Glycine 120 g Tris 40 g SDS ad 4 l H_2O
Blotting buffer (1 X)	0.6 g Tris base 2.258 g Glycine 150 ml Methanol ad 1 l H_2O
Blocking Solution	3 % (w/v) milk powder in TBST or 5 % BSA in TBST
3 X Electrophoresis sample buffer (3 X ESB)	300 mM Tris-HCl pH 6.8 15 mM EDTA 150 mM DTT 12 % (w/v) SDS 15 % (w/v) glycerol 0.03 % (w/v) bromphenol blue
TBS (1 X)	50 mM Tris, pH 7.5 150 mM NaCl adjust to pH 7.4
TBST	0.1 % Tween in 1 X TBS

Substrate Solution	10 ml 100 mM Tris-HCl pH 8.5 50 µl 250 mM Luminol 22 µl 90 mM p-coumaric acid 3 µl 30 % H_2O_2

2.1.2.4 Buffers for chromatin Immunoprecipitation (ChIP)

Cell lysis buffer	5 mM PIPES, pH 8.8 85 mM KCl 0.5 % NP-40 PI 1:1000 (add freshly)
Nuclei lysis buffer	50 mM Tris, pH 8.1 10 mM EDTA 1 % SDS PI 1:1000 (add freshly)
Dilution buffer	0.01 % SDS 1.1 % Triton 1.2 mM EDTA 16.7 mM Tris, pH 8.2 167 mM NaCl PI 1:1000(add freshly)
Elution buffer	50 mM Tris, pH 8.0 1 % SDS 10 mM EDTA
LiCl wash buffer	0.25 M LiCl 0.5 % NP-40 0.5 % Sodium deoxycholate (DOC) 1 mM EDTA 10 mM Tris, pH 8.0
Blocking buffer	3 ml Dilution buffer 30 µl BSA (100 mg/ml) 30 µl ssDNA (10 mg/ml)

2.1.2.5 Buffers for luciferase assay

Lysis buffer	25 mM Glycyl-Glycine 15mM K3PO4 pH 8.0 15 mM MgSO4 4 mM EGTA 1 mM DTT 1% TritonX
Firefly buffer	25 mM Glycyl-Glycine 15mM K3PO4 pH 8.0 15 mM MgSO4 4 mM EGTA 1 mM DTT 1% TritonX 1 mM ATP 75 µM luciferin
Renilla buffer	1.1 M NaCl 2.2 mM EDTA 0.22 M K3PO4 pH 5.0 1.3 mM NaN3 0.44 mg/ml BSA 1.43 µM coelenterazine

2.1.2.6 Buffers for flow cytometry (FACS)

Sodium Citrate	38 mM in H_2O
Annexin V Binding Buffer	10 mM HEPES 140 mM NaCl 2.5 mM $CaCl_2$

2.1.2.7 Buffers for immunohistochemistry

4 % Paraformaldehyd (PFA)	4 % PFA in PBS adjust pH to 7.0 with NaOH
Citrate Buffer	100 mM, pH 6.0
Blocking Solution	3 % BSA in PBS

2.1.2.8 Buffers for immunofluorescence

PSP	15 g paraformaldehyde 10 g sucrose ad 500 ml 1 X PBS, store at -20°C
PBST	0.1 % Triton-X-100 500 ml PBS, store at 4°C
PBS/ 0.1 M Glycine	3.75 g glycine in 500 ml 1 X PBS
PBS/ 0.1 % NP-40	500 µl NP-40 in 500 ml 1 X PBS
Blocking Solution	5 % BSA in PBST or 5 % FCS in PBS/ 0.1% NP-40

2.1.2.9 Buffers for genomic DNA extraction

Base Buffer	25 mM NaOH 0.2 mM EDTA pH 12.0
Neutralisation Buffer	40 mM Tris-HCl pH 5.0

2.1.2.10 Buffers for centromere Fluorescence in situ Hybridisation (c-FISH)

Denaturation Solution	2 X SSC 70 % Formamide
Wash Buffer I	0,4 X SSC 0,3 % NP-40
Wash Buffer II	2 X SSC 0,1 % NP-40

2.1.3 Enzymes

Enzymes	Company
Absolute QPCR SYBR Green Mix	Thermo Fisher
M-MLV-RT Transcriptase (200 U/µl)	Promega / Thermo Fisher
RNase A (10 mg/ml)	Sigma-Aldrich
RiboLock RNase-Inhibitor (40 U/µl)	Fermentas

2.1.4 Antibiotics

Antibiotic	Stock concentration	Final concentration	Cell line
Blasticidin	10 mg/ml	10 µg/ml	U2OS EcoR neo
Neomicin	200 mg/ml	400 µg/ml	MEFs

2.1.5 Staining Solutions

SA-β-Galactosidase Staining Solution (prepare fresh in PBS, pH 6.0)	1 mg/ml X-Gal 0.12 mM $K_3Fe(CN)_6$ 0.12 mM $K_4Fe(CN)_6$ 1 mM $MgCl_2$
Crystal Violet Staining Solution	0.1 % Crystal violet in 20 % Ethanol

2.1.6 Antibodies

2.1.6.1 Primary antibodies

Antibody against	Company	Origin	Application and Dilution	Internal number
β-actin (C-4)	Santa Cruz	mouse monoclonal	WB 1:5000	#196
p16 (M-156)	Santa Cruz	rabbit polyclonal	WB 1:1000	#34
p21 (C-19)	Santa Cruz	rabbit polyclonal	WB 1:1000 IF 1:100	#178
phospho-p38	cell signaling	rabbit polyclonal	WB 1:1000	#202
phospho-JNK	cell signaling	rabbit polyclonal	WB 1:500	#230
p53 (DO-1)	Santa Cruz	mouse monoclonal	WB 1:1000 IF 1:100 ChIP 3µg	#239
phospho-p53 (Ser33)	cell signaling	rabbit polyclonal	WB 1:1000	#229
phospho-p53 (Ser15, 20, 37, 46, 392)	cell signaling (p53 Sampler Kit)	rabbit polyclonal	WB 1:1000	#228
MAP3K4 (K-7)	Santa Cruz	mouse monoclonal	WB 1:500	#238
phospho H3	Upstate	rabbit polyclonal	WB 1:1000	#57
BrdU	AbD Serotec	rat polyclonal	IHC 1:200	#175
BrdU-FITC	BD Bioscience	mouse monoclonal	IF 1:100	non
Ki-67	Thermo Scientific	rabbit monoclonal	IHC 1:200	#185
IgG	Sigma Aldrich	mouse monoclonal	ChIP 2µg	non

2.1.6.2 Secondary antibodies

Antibody against	Company	Application and Dilution
anti-mouse HRP linked	GE Healthcare	WB 1:5000
anti-Protein A HRP linked	GE Healthcare	WB 1:5000
anti-rabbit HRP linked	Santa Cruz	WB 1:5000
anti-rabbit HRP linked	Invitrogen	IHC 1:200
anti-rat HRP linked	GE Healthcare	IHC 1:100
anti-mouse Alexa 594	Invitrogen	IF 1:500
anti-rabbit Alexa 594	Invitrogen	IF 1:500

2.1.7 Primers

Primer oligonucleotides were purchased from Metabion or MWG.

2.1.7.1 Primers for quantative real time PCR

human sequences:

Primer number	Sequences	Application	
SG 645	GCCCAATACGACCAAATCC	Gapdh	antisense
SG 646	AGCCACATCGCTCAGACAC		sense
SG 628	TCACTGTCTTGTACCCTTGTGC	p21	antisense
SG 629	GGCGTTTGGAGTGGTAGAAA		sense
SG 580	CCCCACCACGGTTACATTAT	Lin9	antisense
SG 581	CGGCGACTGTCCTAATAAAGG		sense
SG 1460	GGGACCTCCTTATAGATGAGTGG	p38α	antisense
SG 1461	GGACTCCATCTCTTCTTGGTCA		sense
SG 1462	CATGCTCAACTGGATGCATTA	p38β	antisense
SG 1463	CGCTTCAGCTGGTCAATGTA		sense
SG 1527	GCCTTGAGAGTGACCCAAAG	MAP3K4	antisense
SG 1528	GCTTCATTCTTCATCTGTGCAA		sense
SG 572	GGTACTGAAGTCCGGGAACC	cyclin A2	antisense
SG 573	GAAGATCCTTAAGGGGTGCAA		sense
SG 574	CGCCTGAGCCTATTTTGGT	cyclin B1	antisense
SG 575	GCACATCCAGATGTTTCCATT		sense

SG 682	GAACCACCAAAGTTACCACGA	p107	antisense
SG 683	ATTAAACAGATCCTTAACACTGCAAG		sense
SG 731	CCTGTTCTCCTCGTGTAAAAGC	cdc6	antisense
SG 732	GTGTTGCATAGGTTGTCATCG		sense
SG 568	GCCCAGTGTTTCTTCTGCTT	Birc5	antisense
SG 569	CCGGACGAATGCTTTTTATG		sense
SG 570	GGAGAACGCTCTGTCAGCA	Bub1	antisense
SG 571	TCCAAAAACTCTTCAGCATGAG		sense
SG 1572	GAATGGATTCTTGTTGACTTCATAGAT	Tp53inp	antisense
SG 1573	TCAGTAGGTGACTCTTCACTGATGT		sense
SG 1574	AAGAACCTGGCCAACAAGATT	Alox5	antisense
SG 1575	CATCTCCCGGGATTTGGT		sense
SG 1570	AGCGTTTACAAGGTGCTGCT	Rrad1	antisense
SG 1571	CAATGGAGCGATCATAGGTG		sense

mouse sequences:

Primer number	**Sequences**	**Application**	
SG 1225	ATGACGAACCAGTCACC	Gus	antisense
SG 1226	CCTCCAGTATCTCTCTCGCAAA		sense
SG 785	CCTGGTTCATCATCGCTAATC	Lin9	antisense
SG 786	GAAGGCCGCTGTTTTTGTC		sense
SG 1026	GATGGAGGCCGAGAGAGG	Aspm	antisense
SG 1027	CAGCTTCCACTTTGGATAAGTATTTC		sense
SG 1030	TCTAAACTTGGGAACAATAAAAGGA	Nusap	antisense
SG 1031	TGGATTCCATTTTCTTAAAACGA		sense
SG 1034	GCAGCCTGCAATCCAAGT	Gas2l3	antisense
SG 1035	AGGGGACACCTGGGACTTA		sense
SG 1167	CCCAACGCCCCGAACT	p16	antisense
SG 1168	GCAGAAGAGCTGCTACGTGAA		sense
SG 1015	AACATCTCAGGGCCGAAA	p21	antisense
SG 1016	TGCGCTTGGAGTGATAGAAA		sense

2.1.7.2 Primers for chromatin immunoprecipitation

Primer number	Sequences	Application	
SG 540	GGCAGCAAGAGTCACTCCA	Gapdh2	antisense
SG 541	TGTCTCTTGAAGCACACAGGTT	promoter	sense
SG 1585	CTGGACTGGGCACTCTTGTC	p21	antisense
SG 1586	CTCCTACCATCCCCTTCCTC	promoter	sense

2.1.7.3 Primers for mouse genotyping

Primer number	Sequences	allele	Product size(bp)
SG 722	GCAAAAGCTGCAAGTCCTCT	floxed(fl) lin9	fl lin9 770
SG 893	CCTGGCTGCCTAGCATTTAC		wt 541
			Δfl lin9 289
SG 1113	TGGGATACAGAAGACCAATGC	$CreER^{T2}$	Cre 300
SG 1114	ACGGACAGAAGCATTTTCCA		wt 240
SG 1115	GTCTCTGCCTCCAGAGTGCT		
SG 1403	GCAGTGTTGCAGTTTGAACCC	p16	wt 500
SG 1404	TGTGGCAACTGATTCAGTTGG		ko 600

2.1.8 Plasmids

Internal number	Plasmid name	Description
# 746	pBabe-H2B GFP	GFP control vector
# 1053	pBabe-neo	empty vector
# 923	pBabe-neo Large T	retroviral expression of Large T antigen
# 940	pBabe-neo Large T K1 mutant	retroviral expression of LT-K1
# 1085	pBabe-neo Large T Δ 434-444	retroviral expression of LT Δ 434-444
# 652	pMSCV480 Blasticidin	empty vector
# 679	pMSCV480-shp53 Blasticidin	retroviral expression of shp53

# 270	PG13-Luc	p53-responsive luciferase construct (wt p53 binding sites)
# 271	PM15-Luc	p53-responsive luciferase construct (mutant p53 binding sites)
# 1088	pRL-TK Renilla	Renilla luciferase construct

2.1.9 siRNA sequences

siRNA sequences were purchased from Metabion.

siRNA against	Sequence 5'to 3'	Target
ctrl	UAGCGACUAAACACAUCAA	non targeting
p21	AGAUUUCUACCACUCCAAA	Lindström and Nistér, 2010
p38α#1	GCUGUUGACUGGAAGAACA	Wälchli et al., 2008
p38α#2	CUGCGGUUACUUAAACAUA	Wälchli et al., 2008
p38β#1	AAGGACCUGAGCAGCAUCUU	Wälchli et al., 2008
p38β#2	AAGUGUACUUGGUGACCACC	Wälchli et al., 2008
MAP3K4#1	GGAGAGCUGUGCUGAAUUU	Dharmacon smart pool
MAP3K4#2	GGAAGUGGAUGAAUUAUGU	Dharmacon smart pool
MAP3K4#3	GAGCACAACUUUCAAAUUA	Dharmacon smart pool
MAP3K4#4	GAAAUGAGGAGAAAGAAUA	Dharmacon smart pool
Lin9 -4	GGAAGAGAGAUCAGCAUUAUU	Schmit et al., 2007

2.1.10 Markers

1 Kb DNA Ladder	Fermentas
SDS Page Ruler	Mix Fermentas

2.1.11 Cell culture medium and cell lines

DMEM (4.5 g Glucose/L-Glutamine)	Gibco®, life technologies
OptimeM	Gibco®, life technologies
Penicillin/Streptomycin (10 U/µl each)	Lonza
Trypsin (EDTA) (200 mg/l)	Gibco®, life technologies
TrypLE Express	Gibco®, life technologies
Foetal Bovine Serum (FCS)	Gibco®, life technologies

$Lin9^{fl/fl}CreER^{T2}$ MEFs	MEFs (mouse embryonic fibroblasts) with floxed Exon 7 of the Lin9 allele and $CreER^{T2}$ recombinase
U2OS	human osteosarcoma tumor cell line
U2OS-EcoR neo	U2OS cells with ecotropic receptor for retroviral infection (neomycin resistance cassette)
Phoenix	retroviral packaging cell line for stable infection

2.1.12 Mouse strains

$Lin9^{fl/fl}CreER^{T2}$ mice	mice carrying a floxed Lin9 allele and the $CreER^{T2}$ recominase allele (Reichert et al., 2010)
$Lin9^{+/+}CreER^{T2}$ mice	mice carrying wildtype Lin9 allele and the $CreER^{T2}$ recominase allele
$p16^{-/-}$ mice	mice with p16 knockout allele (Krimpenfort et al., 2001)
$p16^{-/-}$ $Lin9^{fl/fl}CreER^{T2}$ mice	$Lin9^{fl/fl}CreER^{T2}$ mice with p16 knockout allele

2.2 Methods

2.2.1 Cell culture methods

2.2.1.1 Passaging cells

Eukaryotic cells were cultivated in a tissue culture incubator at 37°C with 5 % CO_2. For passageing, cells were washed once with PBS and incubated with TrypLE Express (MEFs, U2OS cells) or Trypsin/EDTA (PlatE cells) for a few minutes at 37°C. The detached cells were plated on new cell culture dishes.

2.2.1.2 Freezing and thawing cells

To freeze cells, cells on 10 cm dishes were trypsinized and transferred into a 15 ml falcon with 10 ml fresh media. Cells were then centrifuged for 3 min at 1000 rpm, the supernatant was discarded and the cells were resuspended in 1 ml ice-cold freeze medium (DMEM media containing 10 % DMSO) and transferred into cryotubes. Cells were stored at -80°C for short term or in liquid nitrogen for long term.

For thawing cells, cells were quickly thawed in a 37°C water bath. The cell suspension was mixed with 10 ml fresh medium and centrifuged for 3 min at 1000 rpm. The supernatant was discarded and pellets were resuspended in 10 ml fresh medium and seeded into 10 cm dishes.

2.2.1.3 Counting cells

Cell counting was performed using a Neubauer Chamber. The number of cells per ml in suspension was calculated using the following formula:

$$\text{Cells/ml} = (\text{Cells counted/ number of counted large squares}) \times 10^4$$

2.2.1.4 Cell treatment with different reagents

4-OHT:	To induce Lin9 knockout in MEFs 0.5 µM of 4-Hydroxytamoxifen (4-OHT) was added to the cells. 48 hours later cells were harvested for genotyping and knockout control.
BrdU:	To label cells in S-phase U2OS cells were treated with 15 µg/ml for 2 hours before cell fixation.
ZM 447439:	U2OS cells were treated with different concentrations (0.5 µM or 1 µM) of the Aurora inhibitor for different time points.

SB 202190: U2OS cells were pretreated with 10 µM SB (p38 kinase inhibitor) 2 hours before additional treatment.

Nocodazole: For cell synchronization in G2/M phase U2OS cells were treated with 100 ng/ml for 18 hours.

2.2.1.5 Generation of MEFs

Murine embryonic fibroblasts (MEFs) were isolated from 13.5 dpc embryos from timed pregnancy. Embryos were prepared in PBS and rinsed in PBS. The yolk sac, placenta, head and the blood containing organs were removed. For genotyping a small piece of the head was used and further processed (s. 2.2.2.5). The remaining body was cut into small pieces with razorblades, transferred to a 10 cm dish containing 2 ml TrypLE Express and was incubated for 10 min at 37°C. Next, 2 ml of fresh Trypsin were added, the cells were separated by pipetting them up and down and incubated for further 10 min at 37°C. Then 6 ml cell culture medium was added and the cells were transferred into falcon tubes and centrifuged for 3 min at 1000 rpm. Finally, the supernatant was discarded and the cell pellet was resuspended in 10 ml fresh media and transferred into 10 cm dishes. The following day, these cells (passage 0) were split 1:4 (passage 1). One or two days later, when the cells were grown to 90 - 100 % density, they were trypsinized and frozen (passage 2).

2.2.1.6 Transient transfection

2.2.1.6.1 Plasmid transfection with Calcium phosphate

Phoenix cells were transfected using calcium phosphate. 20-30 µg of plasmid DNA was mixed with 50 µl of 2.5 M $CaCl_2$ and with H_2O to a final amount of 500 µl. 500 µl of 2 X HBS were continuously vortexed while DNA/$CaCl_2$ mixture was added drop wise. This solution was added slowly to the cells. After 16-18 h incubation, cells were washed with PBS and fed with fresh medium. 24 hours later the produced virus supernatent was harvested for cell infection (see 2.2.1.7).

2.2.1.6.2 Plasmid transfection with JetPEI

For luciferase reporter assay U2OS cells were transfected using JetPEI transfection reagent in a 24 well format. 250ng of firefly plasmid and 100ng of Renilla-plasmid was mixed with 50 µl 150 nM NACl and in parallel 1 µl JetPEI was mixed with 50 µl 150 nM NaCl. Both approaches were incubated for 5 min at room temperature. Afterwards the JetPEI solution was added to the plasmid/NaCl mix and further incubated for 20 min. The solution was then

dropped to the cell dishes containing antibiotic free DMEM. 24 h after transfection cells were harvested for luciferase assay (see 2.2.1.12). Luciferase assay was performed in triplicates.

2.2.1.6.3 siRNA transfection with Dharmafect

U2OS cells were transfected with 50-75 nM siRNA using Dharmafect I (DFI) solution (Thermo scientific Dharmacon). For 6 cm dishes 5 µl of siRNA was mixed with 495 µl OptimeM medium and 2.5 µl of DFI was mixed with 497.5 µl OptimeM medium. Both approaches were incubated for 5 min at room temperature. Afterwards the DFI solution was added to the siRNA/OptimeM mix and further incubated for 15-20 min. The solution was then dropped to the cell dishes containing antibiotic free DMEM. 24-36 h or 72-96 h after transfection cells were either harvested for RNA expression analysis or for protein analysis.

2.2.1.6.4 Reverse siRNA transfection with Dharmafect

For siRNA screen reverse siRNA transfection was performed in 96 well plates using 25 nM siRNA each. In each well 2.5 µl of siRNA (1 µM stock) was mixed with 7.5 µl OptimeM medium and incubated for 5 min at RT. Separately 0.1 µl of DFI was incubated with 9.9 µl of OptimeM medium for 5 min. Afterwards the DFI solution was added to the siRNA dilution and this mixture was further incubated for 20 min at RT. Following, U2OS cells in antibiotic free DMEM medium were seeded at a number of 8000 cells per well.

2.2.1.7 Cell infection

For production of ecotrophic virus supernatant, Phoenix cells carrying the ecotrophic receptor were transiently transfected with the plasmid of interest using calcium phosphate (see 2.2.1.6.1). 36-48 h after transfection, the virus supernatants were harvested and used immediately or were frozen in liquid nitrogen and stored at -80°C. Cells (U2OS EcoR neo or MEFs) were splitted 1:5 the day before infection. For infection, the viral supernatant was mixed with 10 µg/ml polybrene, filtered (0.45 µm) and added to the cells. 24 h after infection, the cells were fed with fresh medium and selection was started 48 h after infection.

2.2.1.8 Immunofluerescence staining

For immunofluorescence studies, cells were plated on cover slips in 6-well plates. After washing once with PBS cells were fixed with PSP for 10 min at RT. Cells were washed again with PBS, permeabilized in PBS/ 0,2 % Triton-X-100 for 5 min at RT and washed again twice in PBS/ 0,1 % Triton-X-100 (PBST). Unspecific staining was minimized by blocking for 20-30 min with PBST/3 % BSA. The cells were washed 3 times in PBST (p21-staining) or PBS/5 mM $MgSO_4$ (BdrU-staining) and incubated with the primary antibody diluted in

PBST or PBS/5 mM $MgSO_4$ for 1 h in a humified chamber. The coverslipes were then washed with PBST and incubated with the secondary antibody for 30 min in a humified chamber. After washing with PBS cells were stained with Hoechst33258 (1:1000) and mounted with ImmuMount.

2.2.1.9 siRNA screen

The siRNA screen was performed with the human siRNA library against 779 kinases and 130 phosphatases. A pool of 4 different single siRNA was used against each target.
U2OS cells were reversely transfected with the siRNA pools (s. 2.2.1.6.4).
For immunofluorescence staining cells were fixed with 4% PFA for 15 min and washed twice with PBS. Two 10 min washing steps in PBS/0.1 M Glycine followed. After washing twice with PBS/0.1% NP-40 for 5 min cells were blocked in PBS/0.1% NP-40/5% FCS (blocking buffer) for 45 min at RT. Antibody staining was performed in blocking buffer (1:200 delution) for 45 min at 37°C. Cells were washed three times for 5 min with blocking buffer and then incubated with secondary antibody (1:500) and Hoechst33258(1:1000) deluted in blocking buffer for 45 min at RT. Cells were washed three times with PBS/0.1% NP-40 for 5 min and stores in PBS at 4°C.

For automated immunofluorescent data acquisition the BD Pathway^{TM} 855 bioimager (BD Biosciences) in Marburg was used. p21 levels were quantified using the BD AttoVision^{TM} software (BD Biosciences). Data quality was assessed with Z-factor analysis and the relative changes in p21 levels were calculated using the Z-score.

Z-factor: 1 - 3 x σ (neg.ctrl) + σ (pos.ctrl) / μ (neg.ctrl) - μ (pos.ctrl)

Z-score: X (well) - median (all wells) / σ (all wells)

2.2.1.10 Flow cytometry (FACS)

2.2.1.10.1 Propidium Iodide (PI) FACS

For determination of cell cycle phases with PI-FACS cells were harvested by trypsinization and centrifuged for 5 min at 1200rpm at 4°C. After washing the cell pellet with cold PBS the cells were fixed with 1 ml ice-cold 80 % ethanol. After fixation at -20°C for at least one night, cells were again washed with cold PBS and the cell pellet was resuspended in 500 µl 38 mM Sodium citrate and 25 µl 10 mg/ml RNase A. Cells were incubated for 30 min at 37°C and stained with 30 µl 1 mg/ml propidium iodide (PI) directly before FACS measurement.

2.2.1.10.2 Annexin V FACS

To analyse apoptotic cells by annexin V staining, cells were trypsinized and centrifuged for 5 min at 1200 rpm at 4°C. The cell pellet was resuspended in 100 µl Annexin buffer and 5 µl Annexin-FITC was added. After 15 min incubation at room temperature (RT) 300 µl annexin buffer was added and cells (put back on ice) were immediately measured by flow cytometry.

2.2.1.11 Centromere Fluorescence in situ Hybridisation (c-FISH)

Cells were trypsinized and centrifuged for 3 min at 1000 rpm. The cell pellet was resuspended in 0,8 % sodium-citrate and incubated at 37°C for 30 min. After a further centrifugation step cells were fixed in a 3:1 methanol:glacial acetic acid solution and stored O/N at 4°C. The fixed cells were dropped onto a slide and air dried at least for 24 h.
Denaturation of the cells were performed at 72°C in preheated denaturation solution for 2 min. Afterwards the slides were dehydrated in ice-cold 70 %, 85 %, 100 % ethanol for 2 min each and air dried. The probe mix for c-FISH against chromosome 7 and chromosome 8 (Kreatech diagnostics) was denaturated at 90°C for 10 min. The probe was applied to the denaturated slide, covered with a coverslip and sealed. Hybridization took place in a humified chamber at 37°C O/N.
After removing the coverlips the slides were first washed in preheated wash buffer I at 72°C for 2 min, then washed in wash buffer II at RT for 1 min. After a dehydration series (70 %, 85 %, 100 % ethanol) for 1 min each slides were counterstained with Hoechst33258, washed with PBS and mounted with ImmuMount.

2.2.1.12 Luciferase reporter assay

Cells were lysed directly in 24 wells with 150 µl lysis buffer for 10 min while shaking. Lysates were transferred to reaction tubes and cell debris was centrifuged for 10 min at 14.000rpm. Supernatant was taken into 96-well plate and firefly and renilla luciferase activity was measured using a luminometer.

2.2.1.13 SA-β-galactosidase staining

To stain cells for SA - β - galactosidase (SA - β - Gal) they were fixed for 10 min with 0.5 % glutardealdehyde and washed twice with PBS/ 1 mM $MgCl_2$. Staining solution was given to the cells and staining was performed O/N at 37°C. Cells were washed twice with PBS and PBS were given to the dish. The dishes were sealed with parafilm and kept at 4°C.

2.2.1.14 Colony forming assay

U2OS cells were plated in a very low density on 10 cm dishes (6000 cells). Treatment of the cells with different drugs (ZM 447439, SB 202190) was performed for 3 days. After 10 - 14 days cells were fixed for 10 min with 4 % PFA, washed with tap water and air dried. Then the cells were stained with 0.1 % crystalviolet staining solution for 30 min, washed with tap water and air dried again.

2.2.2 Molecular methods

2.2.2.1 RNA isolation

Total RNA was isolated from cells by using the RNA isolation reagent Trizol/Trifast (Peqlab). After removing the medium, 1 ml Trifast was added onto the cell culture plate and cells were scraped into a reaction tube. After 5 min incubation, 200 µl chloroform was added and thoroughly vortexed for 15 sec. The tubes were centrifuged at 14000 rpm and 4°C for 10 min and the upper aqueous phase was transferred to a new reaction tube. RNA was precipitated with 500 µl isopropanol on ice for 30 min and centrifuged for 10 min at 14000 rpm and 4°C. The pellet was washed with 80 % ethanol and resuspended in 20 -25 µl RNase free water.
To isolate RNA from tissue, 1 ml Trifast was added to 50-100 mg tissue and homogenized with an Ultra-Turrax. Isolation with chloroform and isopropanol was performed as described above.

2.2.2.2 Reverse transcription (RT)

To transcribe RNA into cDNA, 1-2 µg RNA were mixed with 0.5 µl random primer [0.5 µg/µl] and brought to 10 µl with water. After incubation at 70°C for 5 min the samples were left for 1 min at 4°C and then mixed with 5 µl M-MLV 5 x reaction buffer, 6.25 µl dNTPs [2 mM], 0.5 µl Ribolock RNase inhibitor [40 U/µl], 0.5 µl M-MLV-RT [200 U] and 2.75 µl H_2O. For cDNA synthesis, the samples were incubated at 37°C for 60 min and then inactivated for 15 min at 70°C.

2.2.2.3 Quantitative real-time PCR (qPCR)

To determine the amount of a specific mRNA compared to a housekeeping gene, the following reaction was prepared:

Reaction mix:	12.5 µl Absolute Q-PCR Sybr Green Mix
	10.5 µl H_2O
	1µl fw/rev primer mix (10 pmol/µl each)
	1µl cDNA
PCR program (40 cycles):	95°C 15 min
	95°C 15 sec
	60°C 1 min

The relative expression of a gene compared to a housekeeping gene was calculated with the formula:

$2^{-\Delta\Delta Ct}$

with Ct = ΔCt (sample) - ΔCt (reference)

and ΔCt = Ct (gene of interest) - Ct (housekeeping gene)

The standard deviation of ΔΔCt was calculated with the formula:

$s=\sqrt{s_1}^2 + s_2{}^2$

with s_1 = standard deviation (gene of interest)

and s_2= standard deviation (housekeeping gene)

The margin of error for $2^{-\Delta\Delta Ct}$ was determined with the formula: $2^{-\Delta\Delta Ct\ +/-s}$

and the error used for the error bars was calculated with: $2^{-\Delta\Delta Ct\ +/-s}$ - $2^{-\Delta\Delta Ct}$

2.2.2.4 Microarray Analysis

Microarray analysis was performed using the two color Quick-Amp Labeling Kit (Agilent). 1 µl of total RNA was used for cDNA synthesis, mRNA amplification and labeling according to manufacturer's instructions. Transcriptional profiling was done on a human gene expression 4x44k array (Agilent) and quantified with Feature Extraction software (Agilent). Microarray data were analyzed by F.Finkernagel, Marburg.
For experimental comparison, genes showing more than 2-fold change were chosen.

2.2.2.5 Genomic DNA PCR

For genotyping mouse tails or for knockout control in tissue or cells genomic DNA (gDNA) PCR was performed. The samples were lysed in 75µl base buffer for 30 min at 95°C, cooled down for 5 min and 75µl neutralisation buffer was added. 5 µl of gDNA was used for PCR. The standard gDNA PCR mix and PCR program was the following:

PCR mix	**PCR program(30cycles)**
5 µl gDNA	94°C 5 min
2.5 µl ReproFast buffer	94°C 30 sec
2.5 µl dNTPs [2mM]	58-60°C 0.5-1 min
1 µl forward primer [10 µM]	72°C 1 min
1 µl reverse primer [10 µM]	72°C 5 min
0.2 µl His Taq Polymerase [15U]	
ad 25 µl H_2O	

The samples were mixed with 5 µl gel loading buffer and loaded on a 1 % or 2 % agarose gel for 60 min at 100 Volt.

2.2.3 Biochemical methods

2.2.3.1 Whole cell lysates

Cells were scraped with cold PBS and centrifuged for 5 min at 3000 rpm and 4°C. The pellet was lysed in 10 times its amount of TNN buffer (with freshly added PI [1:500]) by vortexing and incubated on ice for 20 min. The lysates were spun down at 14000 rpm for 10 min at 4 °C to remove the cell debris. The supernatant was transferred in a new reaction tube and immediately used for immunoprecipitation or boiled in 3 X ESB for 5 min and frozen at -20°C.

2.2.3.2 Determination of protein concentration (Bradford)

Protein concentration was measured with Bradford solution on the basis of a known BSA straight calibration line as described by Bradford (Bradford 1976). 5 µl of the whole lysate were mixed with 1 ml Bradford solution. Extinction was measured at 595 nm and compared to a standard BSA dilution series.

2.2.3.3 SDS polyacrylamide gel electrophoresis (SDS-PAGE)

SDS-PAGE analysis was performed using the discontinuous method (Laemmli, 1970). For electrophoretic separation of proteins a 8 - 12 % separating gel was prepared. After polymerization, the stacking gel was poured on the top. The gels were prepared as follows:

Separating gel (10 %)	**Stacking gel**
6.1 ml H_2O	6.9 ml H_2O
3.7 ml 1.5 M Tris pH 8.8	1.4 ml 0.5 M Tris pH 6.8
5 ml Acrylamid/Bisacrylamid	1.6 ml Acrylamid/Bisacrylamid
75 µl 20 % SDS	50 µl 20 % SDS
100 µl 10 % APS	50 µl 10 % APS
10 µl TEMED	10 µl TEMED

Electrophoresis was carried out in 1 X SDS running buffer for 60 - 90 min at 35 mA/gel. The gels were then used for immunoblotting.

2.2.3.4 Immunoblotting

The transfer of proteins to a PVDF membrane was done via electro blotting using a BioRad Wet Blot gadget. The PVDF membrane was preincubated for 1 min with methanol and rinsed with blotting buffer. The membrane was placed onto a layer of Whatman filter paper and the SDS-polyacrylamide gel was laid on the membrane, followed by a second layer of filter paper. This sandwich was clasped on both sides by sponges and placed in a cooled wet blotting tank (Biorad). The transfer occurred for 60 - 90 min at 300 mA in 1 X Blotting Buffer. The equal and complete transfer of proteins was visualized by staining the membrane with a Ponceau S solution and destaining with H_2O. To detect specific proteins with their respective antibodies, the membranes were transferred into blocking solution for 1 - 2 h to avoid unspecific antibody binding. As blocking solution either 3 % milk powder in TBST (most antibodies) or 5 % BSA in TBST (phospho - specific antibodies) was used. Incubation of the membrane with the primary antibody diluted in adequate blocking solution was performed overnight (O/N) at 4°C. Afterwards, the membrane was washed 3 times for 10 min in TBST and incubated with the secondary HRP-conjugated antibody for 1 h at RT. After 3 more washing steps of 10 min in TBST, specific bands were detected using a Luminol - substrate - solution. The membrane was wrapped in plastic foil and exposed to an ECL-film.

2.2.3.5 Chromatin immmunoprecipitation (ChIP)

Cells for ChIP analysis were trypsinized and the cell number was determined. In 20 ml medium cellular proteins were crosslinked with 540 µl of 37 % formaldehyde for 10 min. The reaction was stopped by adding 2.5 ml 1 M glycine and incubated for 5 min at RT. Afterwards cells were pelleted at 4 °C and the cells was washed twice with cold PBS. According to the cell number 2×10^7 cells were lysed in 1 ml lysis buffer for 10 min. After centrifugation the nuclei was lysed in 800µl nuclei lysis buffer for 10 min. Lysed nuclei were sonicated for 10 min using the Bioruptor with 30 sec on/ 30 sec off cycle with high intensity. Thereby chromatin was fractured into 250 - 1000 bp fragments. To remove cell debris chromatin was centrifuged and 20 µl of the supernatant was used to check the chromatin size. 2µl of 5 M NaCl was added to the chromatin and incubated O/N at 65° C. After 2 h treatment with 4 µl Proteinase K (10 mg/ml) the chromatin size was analyzed on a 1.2 % agarose gel.
The remaining chromatin was diluted 1:10 with dilution buffer and separated for 4 immunoprecipitations (5×10^6 cells each). 20 µl of the diluted chromatin was removed as input and stored at 4 °C O/N. The chromatin was precleared with 50 µl blocked Protein-G sepharose beads for 15 min on a rotating wheel at 4 °C. After addition of the antibodies the samples were incubated at 4 °C O/N on a rotating wheel. The following day the pull down of the proteins was performed by adding 50 µl Protein-G sepharose beads to the chromatin for 1 - 2 hours at 4 °C. The beads were washed 7 times with 1 ml LiCl-washing buffer and eluted with 100 µl elution buffer for 15 min. A second elution step was performed with additional 150 µl elution buffer for 15 min and both supernatants were combined. For reverse crosslink 10 µl 5 M NaCl was added to the eluted mixture as well to the input samples and incubated O/N at 65° C. Proteins were degraded by incubation with 2 µl proteinase K (10 mg/ml) for 2 h at 55 °C. Thereafter a phenol/chloroform extraction was performed by adding 250 µl phenol to the eluted samples. After centrifugation the aqueous phase was transferred into a new tube and the DNA was purified using the Qiagen DNA Purification Kit according to the manufacturers manual.
1 µl of the purified chromatin was used for quantitative PCR analysis and precipitated samples were compared to input chromatin.

2.2.4 Immunohistochemical methods

2.2.4.1 Preparation of paraffin sections

Fixation of tissue samples was performed in 4 % PFA O/N at 4°C. The following day the fixed tissue was washed twice in PBS and in 0.9 % $NaCl_2$ for 10 min each. Afterwards the samples were dehyrated in an ethanol series (50 %, 70 %, 80 %, 90 %). Incubation took place for 1 h each. O/N the samples were incubated in 95 % at 4°C. Next the tissue was transferred into

100% ethanol twice for 1 h at RT, Followed by 1 h incubation in ethanol/xylol (1:1), twice in xylole (1 h), and finally in xylole/paraffin (1:1) for 1 h 65°C. The next day the paraffin was changed twice and the tissue was embedded in paraffin.
The paraffin blocks were sectioned to a thick of 5 µm with a rotation mikrotom Hydrax M40 (Zeiss).

2.2.4.2 H&E staining

The slides were first deparaffinized twice in xylol for 10 min and then incubated in a rehydrating ethanol series (100 %, 70 %, 50 %) for 3 min each. After washing in H_2O staining of nuclei was performed in haematoxyline (Sigma-Aldrich) for 4 min. The slides were rinsed with running tap water for 10 min to develop the blue staining. To counterstain the slides were incubated for 1 min in eosin Y (Sigma-Aldrich) and then dehydrated in 96% ethanol and 100 % ethanol for 3 min. After two additional 10 min incubation steps in xylol the slides were mounted with Roti-Histokitt (Roth).

2.2.4.3 Antibody staining

Slides for antibody staining were first deparaffinized twice in xylol for 5 min and then incubated in a rehydrating ethanol series (100 %, 95 %,80 %, 70 %, 50 %) for 3 min each. After blocking endogenous peroxidase activity with 3 % H_2O_2 (in PBS) slides were washed three times with PBS and afterwards antigen retrival was performed in boiling 10 mM Sodiumcitrate pH 6.0 buffer for 1 - 2 min. After 20 min cooling down slides were washed again and then blocked in 3 % BSA. Primary antibody was incubated O/N in a humified chamber at 4°C. Slides were washed in PBS and the secondary antibody was incubated for 1 h at RT. After washing again the DAB substrate was pipetted on the tissue and the staining developed 5 - 10 min. Slides were washed in H_2O and counterstained with haematoxyline. A dehydrating ethanol series (70 %, 95 %, 100 %) for 2 min each and two xylol incubation steps of 5 min followed. Slides were mounted with Roti-Histokitt.

2.2.5 Mouse intraperitonal injection

For intraperitoneal (i.p.) injection of mice 25 gauge needles was used.

To induce Lin9 knockout in $Lin9^{fl/fl}CreER^{T2}$ mice 1 mg tamoxifen was injected i.p. on three consecutive days.

For BrdU antibody staining in intestinal sections 2 h before sacrificing the mice, 1 mg of BrdU was injected i.p.

3 Results

3.1 Senescence phenotype after Lin9 deletion in MEFs

The DREAM complex works as a master regulator of mitotic gene expression and depletion of DREAM subunits results in reduced expression of G2/M genes leading to impaired cell proliferation (Osterloh et al., 2007; Reichert et al., 2010; Schmit et al., 2007). Depletion analysis of the best characterized subunit Lin9 in mouse embryonic fibroblasts (MEFs) revealed binucleated cells and multilobular nuclei that later undergo senescence due to defects in mitosis and cytokinesis (Reichert et al., 2010). The aim of this work was to analyze which tumor suppressor pathways are activated to induce irreversible cell cycle arrest when Lin9 is depleted. For this purpose the conditional Lin9 knockout mouse model (Reichert et al., 2010) was used.

3.1.1 p16 and p21 are upregulated after loss of Lin9

In conditional Lin9 knockout mouse embryonic fibroblasts (MEFs) activation of the Cre recombinase (CreER^{T2}) is induced by adding 4-Hydroxytamoxifen (4-OHT) to the cell culture medium. CreER^{T2} mediates the recombination of loxP sites, that flank exon 7 of the Lin9 allele, thereby generating the Δfl allele (Reichert et al., 2010) (Fig. 3.1 A). Deletion of exon 7 creates a frame shift and this results in a nonfunctional Lin9 protein. The successful deletion of Exon 7 can be determined by a genotyping PCR. Fig. 3.1 B shows the control floxed (fl) allele (770 bp) and the Δfl allele (289 bp).

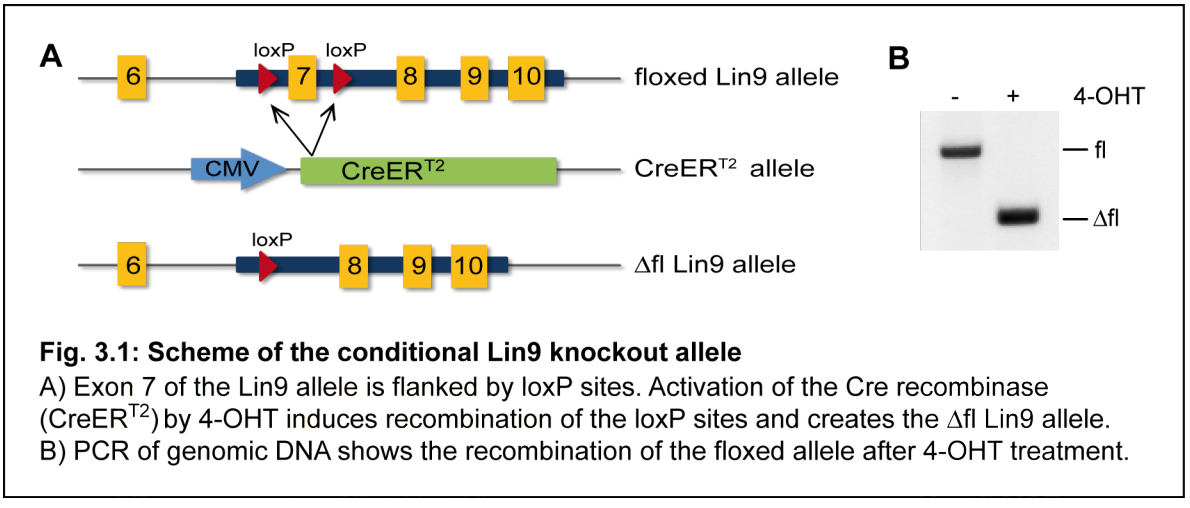

Fig. 3.1: Scheme of the conditional Lin9 knockout allele
A) Exon 7 of the Lin9 allele is flanked by loxP sites. Activation of the Cre recombinase (CreER^{T2}) by 4-OHT induces recombination of the loxP sites and creates the Δfl Lin9 allele.
B) PCR of genomic DNA shows the recombination of the floxed allele after 4-OHT treatment.

To induce the knockout of Lin9, MEFs were treated with 500 nM 4-OHT for 48 hours. 10 days later the cells were stained for SA-β-galactosidase, which is a marker for senescent cells (Dimri et al., 1995). Lin9 knockout cells showed a large and flat morphology and were positive

for SA-β-galactosidase (Fig. 3.2 A). 24 hours after 4-OHT treatment cells were harvested and lysed for immunoblot analysis and the expression of the senescent related proteins $p16^{INK4a}$ and $p21^{Waf1}$ was determined. Both CDK-inhibitors were upregulated on protein level upon loss of Lin9 (Fig. 3.2 B). As loading control β-actin was used. The knockout efficiency of Lin9 on mRNA level was tested by reverse transcription quantitative PCR (RT-qPCR) and showed decrease of Lin9 mRNA level down to 30% (Fig. 3.2 C).

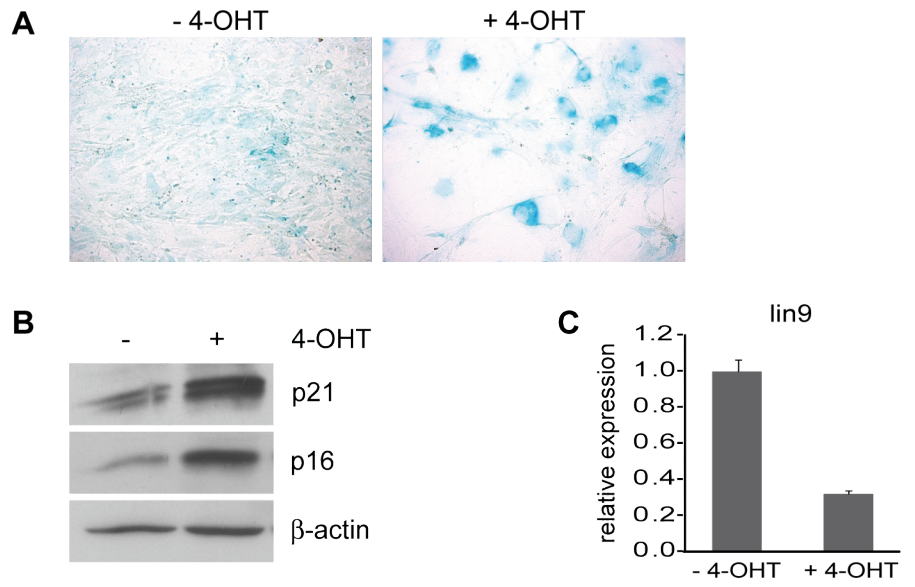

Fig. 3.2: Deletion of Lin9 induces senescence and upregulates p16 and p21 expression
Conditional $Lin9^{fl/fl}$ $CreER^{T2}$ MEFs were treated with 500nM 4-OHT for 48h to induce knockout of Lin9. A) Senescent cells were stained for SA-β-galactosidase 10 days after Lin9 knockout. B) p21 and p16 protein levels in Lin9 knockout MEFs were analyzed 24h after 4-OHT treatment by immunoblotting. C) mRNA expression levels of Lin9 were detected by RT-qPCR.

3.1.2 Senescence can be independently induced by the p53 or the pRB tumor suppressor pathway

In order to find out whether the senescence phenotype induced by loss of Lin9 in MEFs is dependent on the p53-p21 and/or the p16-pRB tumor suppressor pathways, MEFs were infected with retrovirus encoding for the SV40 large T antigen (LT). SV40 LT is able to bind to the tumor suppressors p53 and pRB and thereby inhibits the function of both proteins. As control, wild-type MEFs (wt) were infected with an empty vector. After neomycin selection, cells were treated with 500 nM 4-OHT for 48 hours and SA-β-galactosidase staining was performed 10 days later. Expression of the wild-type SV40 LT (LT wt) antigen no longer resulted in senescent cells when Lin9 was deleted (+ 4-OHT), compared to wild-type (wt)

MEFs (Fig. 3.3 A), suggesting that inhibition of p53 and pRB overcomes the senescent phenotype.

Furthermore, two different mutants of the SV40 LT antigen were used in this assay: the SV40 LT-K1 mutant, which is impaired in binding to pRB and to the related pocket proteins p107 and p130 (Stubdal et al., 1997), and the SV40 LTΔ434-444 mutant that is not able to inhibit p53 anymore (Kierstead and Tevethia, 1993). SA-β-galactosidase staining of Lin9 knockout MEFs showed that cells still become senescent when either only p53 (LT-K1) or pRB (LTΔ434-444) were blocked (Fig. 3.3 A). The expression of SV40 LT wt and the LT mutants was detected by immunoblot analysis (Fig. 3.3 B). The SV40 LTΔ434-444 mutant was only weakly expressed when compared to SV40 LT wt and the SV40 LT-K1 mutant, as described previously (Ye et al., 2007). To determine if the pRB pathway was nevertheless blocked, the phosphorylation status of the pocket protein p130 was checked (Fig. 3.3 B). Immunoblot analysis revealed that the levels of phosphorylated p130 (pp130) and p130 were decreased in cells expressing LT wt or the LTΔ434-444 mutant, confirming that the SV40 LTΔ434-444 mutant completely disrupted the pRB tumor suppressor pathway although it was only weakly expressed. In contrast, high levels of pp130 were observed in cells expressing the pRB binding mutant of LT (LT-K1).

In summary, these data suggest that senescence upon loss of Lin9 can be independently induced by the p53-p21 and the p16-pRB pathway.

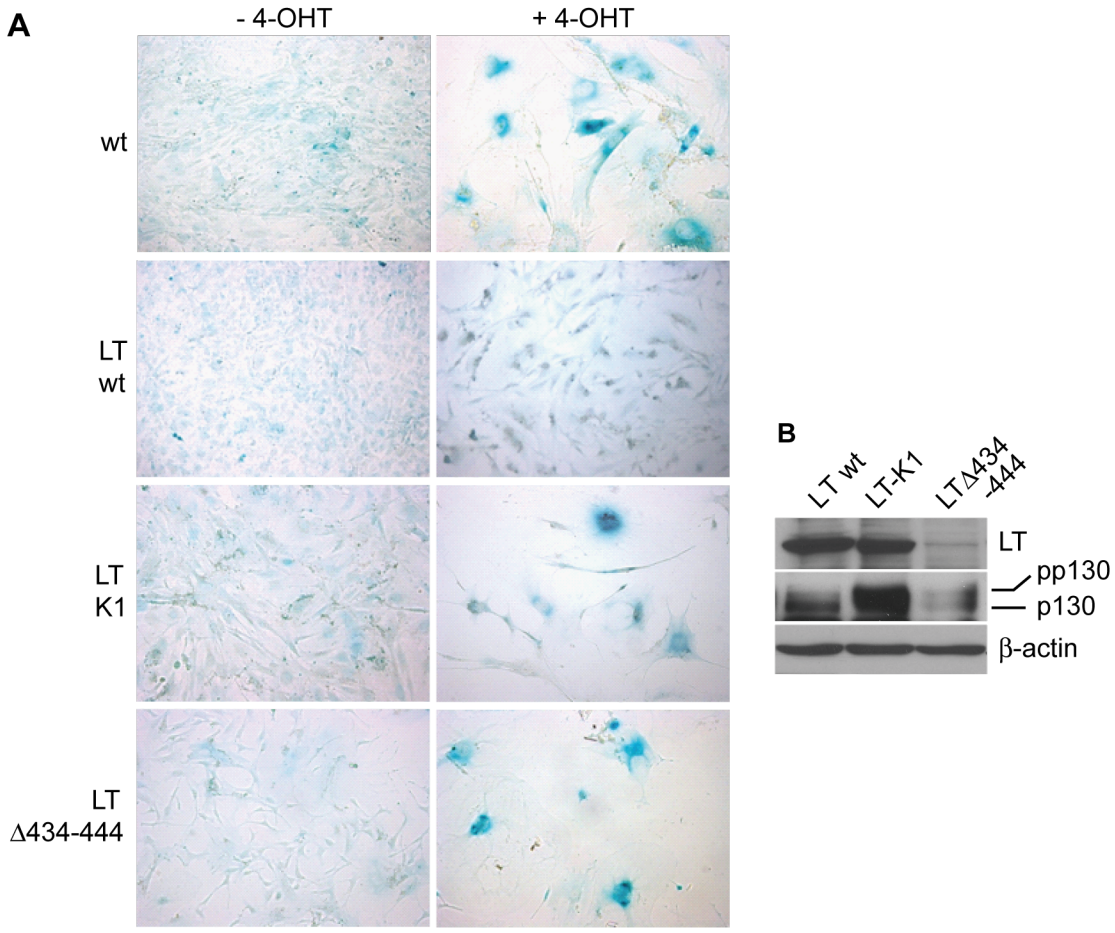

Fig. 3.3: SV40 LT antigen overcomes the senescence induced by Lin9 deletion
Conditional Lin9$^{fl/fl}$ CreER^{T2} MEFs were infected with retroviruses encoding for wildtype SV40 LT (LT wt) or SV40 LT mutants (K1, Δ434-444). Control MEFs were infected with an empty vector (wt). A) Senescence was detected by SA-β-galactosidase 10 days after Lin9 knockout. B) Expression of LT antigen and phosphorylation status of p130 were detected by immunoblot analysis.

3.2 Function of Lin9 *in vivo*

It has been shown previously that Lin9 is essential for mouse development as Lin9 knockout results in early embryonic lethality in mice (Reichert et al., 2010). The aim of part of this project was to study the function of Lin9 in adult mice. Therefore, the conditional Lin9 knockout mouse model (Reichert et al., 2010) was used to examine the effects of deleted Lin9 in somatic tissue of mature mice.

3.2.1 Efficiency of Lin9 knockout in different tissues

First, the efficiency of the Lin9 knockout in different mouse organs was tested. Therefore, 1 mg tamoxifen was applied to 8 week old $Lin9^{fl/fl}CreER^{T2}$ mice via intraperitoneal injection (i.p.) for three consecutive days to induce recombination of the conditional Lin9 allele (fl-allele). Tamoxifen is metabolized to its active form 4-OHT in the liver and enables activation of the $CreER^{T2}$ recombinase (see Fig. 3.1). One day after the last injection the mice were sacrificed and tissue pieces of different organs were taken for genotyping PCR (Fig. 3.4). Almost complete recombination (90-100%) of the conditional Lin9 allele (Δfl-allele) took place in intestine, colon, liver, spleen, testis and kidney. Other tissues like heart, lung, stomach and skin showed about 50% recombination of the Lin9 allele. Only in the brain no recombination occured indicating a limited permeability through the blood-brain barrier.

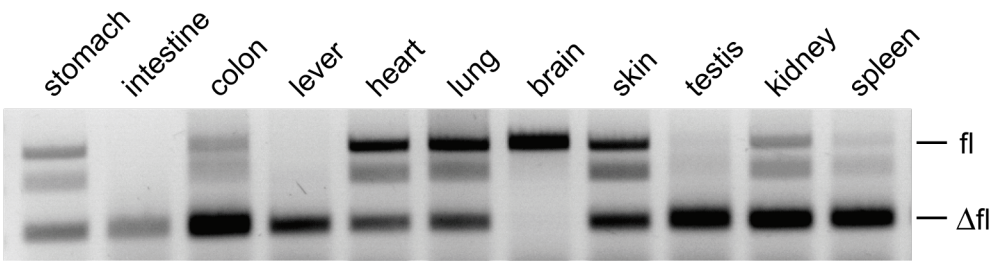

Fig. 3.4: Lin9 deletion in different tissues
$Lin9^{fl/fl}$ $CreER^{T2}$ mice were treated with 1mg tamoxifen by intraperitoneal injection for three consecutive days. One day later the mice were killed and different tissues were taken to anlayze the knockout efficiency of the floxed Lin9 allele.

3.2.2 Loss of Lin9 *in vivo* causes atrophy of the gastrointestinal epithelium

In order to investigate the consequences of Lin9 knockout on different mouse tissues, recombination of the Lin9 allele was induced in $Lin9^{fl/fl}CreER^{T2}$ mice by i.p injection of tamoxifen for three days. To exclude toxic effects of tamoxifen, Lin9 wild-type (wt) mice ($Lin9^{+/+}CreER^{T2}$) were used as controls. Treatment of the mice showed a dramatic effect, as all $Lin9^{fl/fl}CreER^{T2}$ mice died 6-7 days after the first tamoxifen injection, suggesting that Lin9 is essential for the

survival of adult mice. Histological analysis of tissues of the gastrointestinal tract revealed that deletion of Lin9 caused severe effects on the gastrointestinal epithelium. Tissues were taken on the indicated days post first tamoxifen injection (3dpi-6dpi), fixed in 4% PFA and embedded in paraffin. Afterwards, tissue sections of the small intestine, colon and stomach were stained with H&E to monitor the epithelial structure (Fig. 3.5). Fig. 3.5 A shows that the epithelial structure in the small intestine was lost over time and that Lin9 deletion resulted

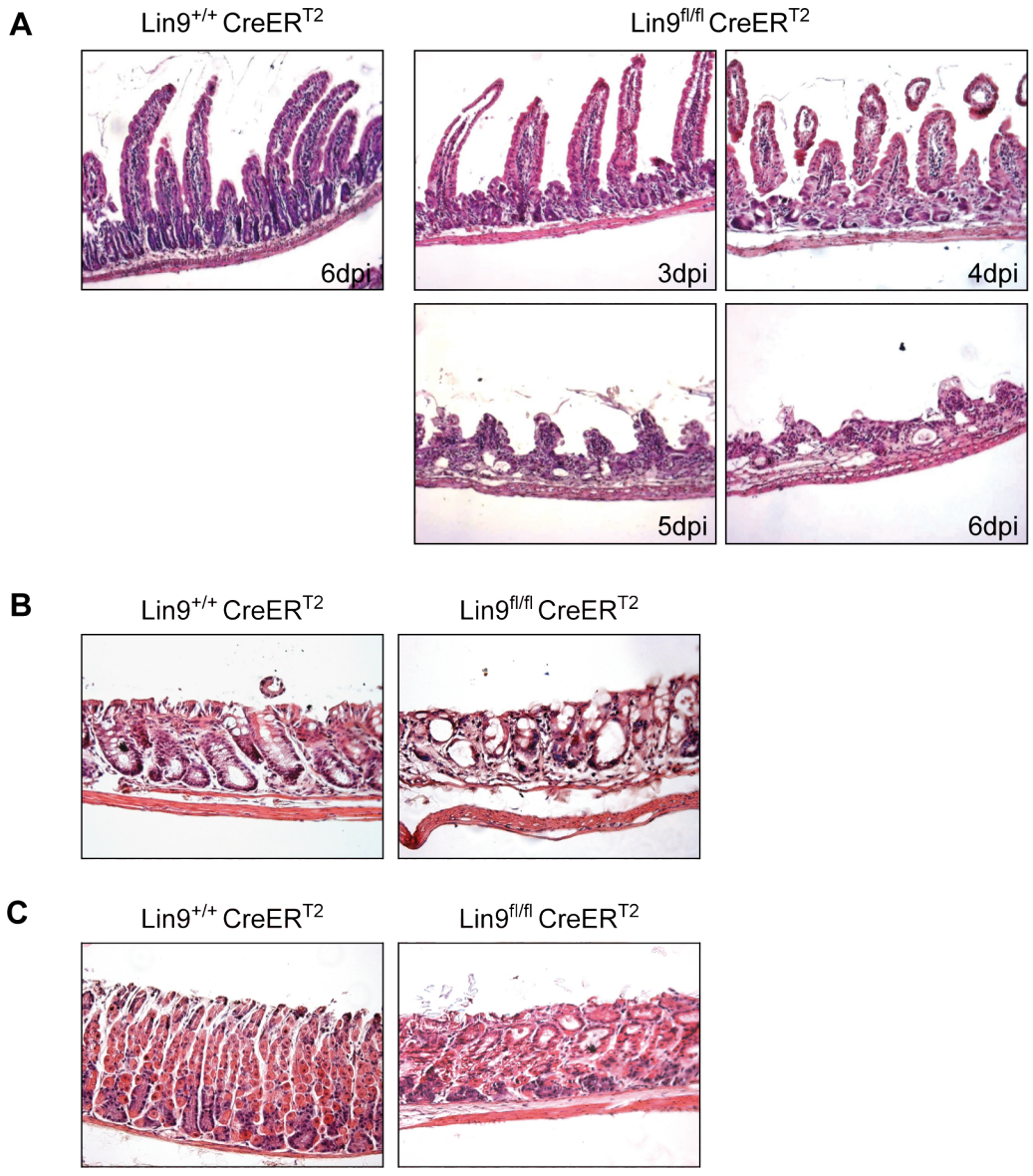

Fig. 3.5: Loss of Lin9 shows severe effects on the gastrointestinal epithelium
Lin9$^{fl/fl}$ CreER^{T2} and control Lin9$^{+/+}$CreER^{T2} mice were treated with 1mg tamoxifen by intraperitoneal injection for three consecutive days. At the indicated days post 1. injection (dpi) the mice were sacrificed and tissues were fixed. Paraffin embedded tissue sections were stainind with H&E. A) H&E staining of the small intestine. Magnification 100x. B) H&E staining of the colon at 6dpi, magnification 200x. C) H&E staining of the stomach at 6dpi, magnification 200x.

in nearly complete atrophy of the intestinal villi at 6dpi. The Lin9 depleted epithelium in the colon and stomach also displayed structural differences at 6dpi compared to control tissue. The crypts in the colon were entirely destroyed (Fig. 3.5 B) and the epithelial structure in the stomach was lost upon knockout of Lin9 (Fig. 3.5 C). This dramatic effect on the mouse gastrointestinal epithelium can be explained by the rapid renewal of this epithelium which is replaced every 3-5 days. In other tissues like kidney, liver, lung or heart no histological differences between $Lin9^{+/+}CreER^{T2}$ and $Lin9^{fl/fl}CreER^{T2}$ mice were found, which could be explained by the minimized proliferation in these tissues (data not shown).

3.2.3 Proliferation in the intestinal crypts is impaired upon deletion of Lin9

To find out if the atrophic phenotype observed in the gastrointestinal epithelium upon loss of Lin9 is due to proliferation defects, the amount of cycling cells in the intestinal crypts was analyzed. $Lin9^{fl/fl}CreER^{T2}$ mice and $Lin9^{+/+}CreER^{T2}$ were treated with tamoxifen for three days by i.p. injection. Tissues were taken at 3dpi and 4dpi as indicated and intestinal crypts were immunostained with the proliferation marker Ki-67. Haematoxyline was used as counterstain (Fig. 3.6 A). In control crypts high proliferation was detectable whereas Lin9

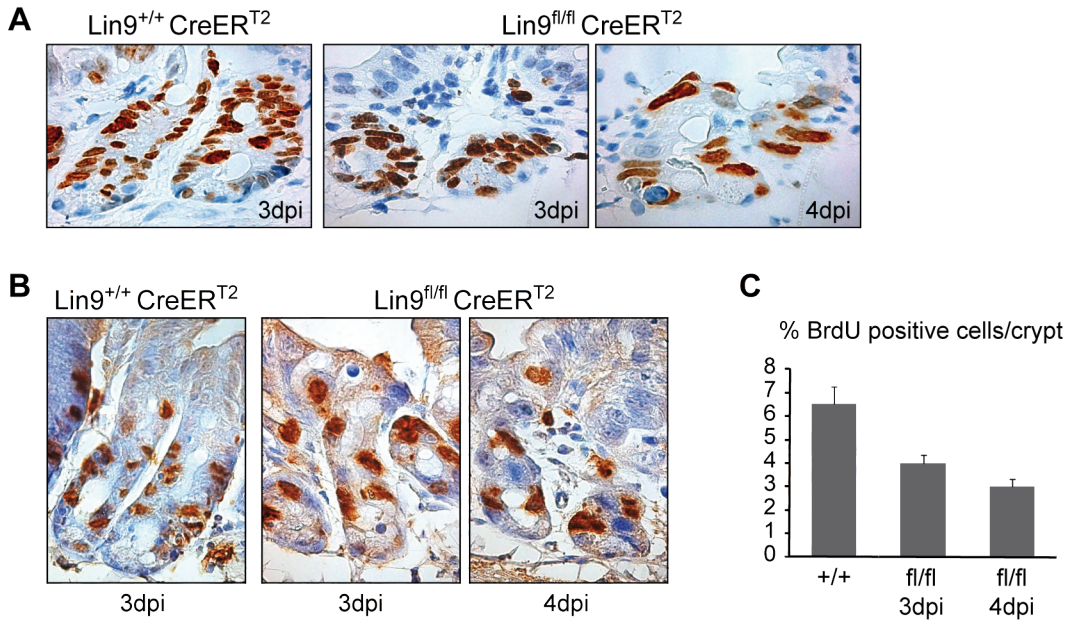

Fig. 3.6: Proliferation in the intestinal crypts is impaired upon Lin9 knockout
A) $Lin9^{fl/fl}CreER^{T2}$ and $Lin9^{+/+}CreER^{T2}$ mice were treated with 1mg tamoxifen for three days. Small intestine was taken at the indicated dpi and Ki-67 staining was performed. Haematoxyline was used as counterstain. B) Mice were treated with 1mg tamoxifen for three days and pulsed with 1mg BrdU 2h before sacrificing. BrdU antibody staining was performed using Haematoxyline as counterstaining. C) Quantification of BrdU positive cells per crypt. 25 crypts were analyzed per mouse, three mice were used for each time point.

depleted crypts depicted a strongly reduced cell proliferation. This loss of cycling cells was especially observed in the 4dpi crypts, where also cells with large and irregular nuclei were detected. The decreased proliferation rate was further confirmed by labeling S-phase cells with BrdU. On 3dpi or 4dpi Lin9$^{fl/fl}$CreER^{T2} mice and Lin9$^{+/+}$CreER^{T2} were treated with 1mg BrdU by i.p. injection 2 hours before sacrificing the mice. BrdU positive cells were detected using a specific BrdU antibody. Haematoxyline was used for counterstaining (Fig. 3.6 B). In Lin9 depleted mice the number of labeled S-phase cells per crypt was reduced to 4 (3dpi) and 3 (4dpi) in contrast to 6-7 BrdU positive cells in wild-type control mice (Fig. 3.6 C). These assays indicate that progression through the cell cycle is defective upon loss of Lin9 *in vivo*.

3.2.4 Reduced mitotic gene expression and binucleated cells in the small intestine after Lin9 knockout

When analyzing the enterocytes of the intestinal villi after Lin9 depletion in more detail, binucleated cells as well as cells with abnormal and huge nuclei were found in Lin9$^{fl/fl}$CreER^{T2} mice on 3dpi (Fig. 3.7 A) indicating abnormal cytokinesis. Furthermore, the mRNA expression levels of some selected DREAM target genes after Lin9 knockout in Lin9$^{fl/fl}$CreER^{T2} mice

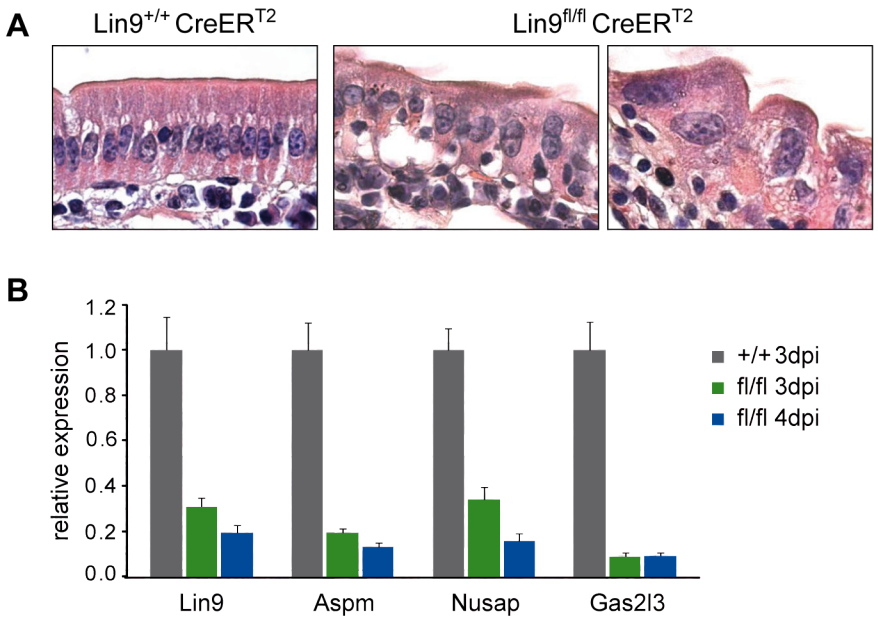

Fig. 3.7: Binucleated cells and abnormal nuclei in the small intestine due to down-regulated mitotic gene expression after loss of Lin9
Lin9$^{fl/fl}$ CreER^{T2} and Lin9$^{+/+}$ CreER^{T2} mice were treated with 1mg tamoxifen for three days. A) H&E staining of intestinal villi epithelium of control and lin9 knockout mice at 3dpi. 630x magnification. B) 3 and 4 days post injection (dpi) RNA was isolated from the small intestine and expression of Lin9 and DREAM target genes was determined using RT-qPCR.

were compared to Lin9$^{+/+}$CreER^{T2} mice. RNA was isolated from 3dpi and 4dpi small intestine and mRNA expression was determined by RT-qPCR. Upon reduction of Lin9 mRNA levels down to 20-30% after tamoxifen treatment, the expression levels of the mitotic genes Nusap, Aspm and Gas2l3 were decreased down to 10-30% (Fig. 3.7 B). Reduced expression of G2/M genes after loss of Lin9 may result in the formation of binucleated cells and abnormal nuclei *in vivo* which is consistent with the findings of Lin9 deletion *in vitro* (Reichert et al, 2010).

The same RNA was used for analyzing mRNA expression levels of the CDK inhibitors p16 and p21 after Lin9 knockout in the small intestine (Fig. 3.8). Compared to the control, both p16 and p21, were expressed to a higher extent when Lin9 was deleted. This gives a hint that mitotic defects that are induced upon Lin9 knockout in intestinal epithelium cells activate tumor suppressor pathways to arrest cells in the cell cycle and to stop proliferation.

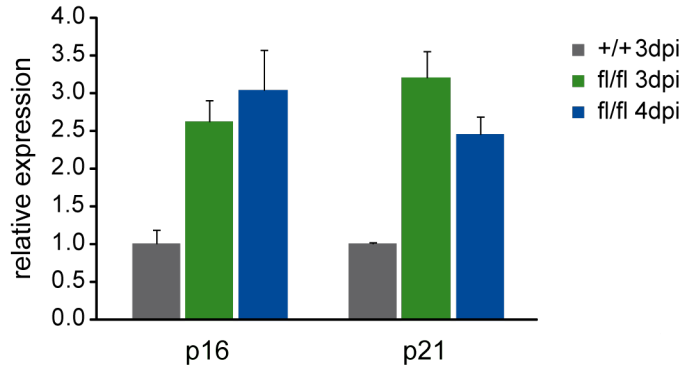

Fig. 3.8: p16 and p21 are upregulated in the small intestine upon Lin9 deletion
Lin9$^{fl/fl}$ CreER^{T2} and Lin9$^{+/+}$ CreER^{T2} mice were treated with 1mg tamoxifen for three days. 3dpi and 4dpi RNA was isolated from the small intestine and expression of p16 and p21 was determined using RT-qPCR.

3.2.5 Atrophic intestinal epithelium after Lin9 deletion in p16 knockout mice

In order to investigate if the atrophic intestinal phenotype can be prevented when the p16-pRB tumor suppressor pathway is blocked, Lin9$^{fl/fl}$CreER^{T2} mice were crossed to p16 null background (Krimpenfort et al., 2001). These mice were treated with tamoxifen for three days and the intestinal epithelium was analyzed by H&E staining at 6dpi (Fig. 3.9). Similarly to untreated control Lin9$^{fl/fl}$CreER^{T2} mice, proliferation defects upon Lin9 knockout resulted in atrophy of the intestinal epithelium in Lin9$^{fl/fl}$p16$^{-/-}$CreER^{T2} mice.
As the phenotype could not be restored when p16 was absent it can be concluded that inactivation of the tumor suppressor pathway p16-pRb is not sufficient to prevent degeneration of the intestinal epithelium induced by loss of Lin9. These data are in line with the findings

in vitro where inactivation of pRB did not prevent senescence after Lin9 depletion (Fig. 3.3).

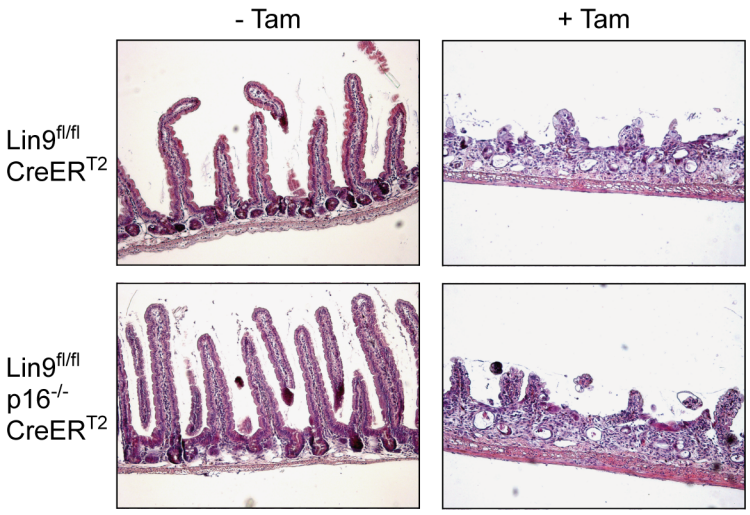

Fig. 3.9: Knockout of p16 does not prevent atrophy of the intestinal epithelium after loss of Lin9
$Lin9^{fl/fl}$ $CreER^{T2}$ and $Lin9^{fl/fl}$ $p16^{-/-}$ $CreER^{T2}$ mice were treated with 1mg tamoxifen or solvent (-Tam) for three days. 6dpi small intestine was stained with H&E.

3.3 Aurora B inhibition in U2OS cells - pretests for siRNA screen

After demonstrating that the p53 and pRB tumor suppressor pathways are activated upon knockout of Lin9 in MEFs (Fig. 3.2 and 3.3) it was now of interest to find out which proteins act upstream of these pathways. To identify proteins that are required for induction of cell proliferation arrest after defective mitosis or cytokinesis a high throughput siRNA screen targeting kinases and phosphatases was performed. The cellular system was switched from the primary mouse cell line (MEFs) to a human cancer cell line to provide a robust and reproducible cellular system for siRNA screening. The osteosarcoma cell line U2OS which expresses functional p53 and pRB proteins (Isfort et al., 1995), but lacks p16 (Miller et al., 1996) was chosen. In order to create defects in mitosis that resemble those induced by down-regulated mitotic gene expression upon Lin9 deletion, the Aurora kinase inhibitor ZM447439 was used. Inhibition of Aurora kinase activity results in defective chromosome alignment, chromosomal missegregation and failures in cytokinesis (Ditchfield et al., 2003). Although ZM447439 is a selective inhibitor of Aurora A and B, the cellular phenotypes after treatment with ZM447439 are similar to those observed upon single inhibition of Aurora B (Ditchfield et al., 2003; Girdler et al., 2006); therefore, ZM447439 is referred to as Aurora B inhibitor in the following work.

3.3.1 U2OS cells become polyploid after Aurora B inhibition

First, the cellular effects of Aurora B inhibition in U2OS cells were monitored. Cells were seeded on coverslips and treated with 1µM ZM447439 (from now on referred to as ZM) for 24 and 48 hours. Control cells were treated with DMSO. At the indicated time points cells were fixed with 3% PSP, the nuclei were stained with Hoechst 33258 and the nuclear shape was analyzed using a fluorescence phase contrast microscope (Fig. 3.10 A). Quantification of cells and nuclei demonstrated that about 50% of the cells became binucleated after 24h ZM treatment. Further 15% of the cells were multinucleated or showed multilobed nuclei at this time point. When cells were exposed to ZM for 48 hours about 40% of the cells were binucleated and further 40% were multinucleated or showed multilobular nuclei (Fig. 3.10 B). The formation of bi- and multinucleated cells over time was further investigated with propidiumiodide (PI) FACS analysis (Fig. 3.10 C). Cells were treated with ZM for 12 to 72 hours, fixed with ethanol and stained with PI. After 12h ZM treatment 75% of the cells accumulated in G2/M indicating that binucleated tetraploid cells arrest with a 4N DNA content in a pseudo-G1 state after cytokinesis failure (Lanni and Jacks, 1998). At the 24h time point 58% of the cells were found in the 4N fraction (G2/M) and 33% in the polyploid (8N) fraction. Upon prolonged ZM treatment (48h-72h) more and more cells became polyploid (up to 47%) suggesting that some cells were able to escape the G1-arrest and endoreduplicated as it has been shown in previous studies (Ditchfield et al.,

2003). Hence, the formation of binucleated and polyploid cells demonstrates that 1µM ZM completely inhibits cytokinesis in U2OS cells.

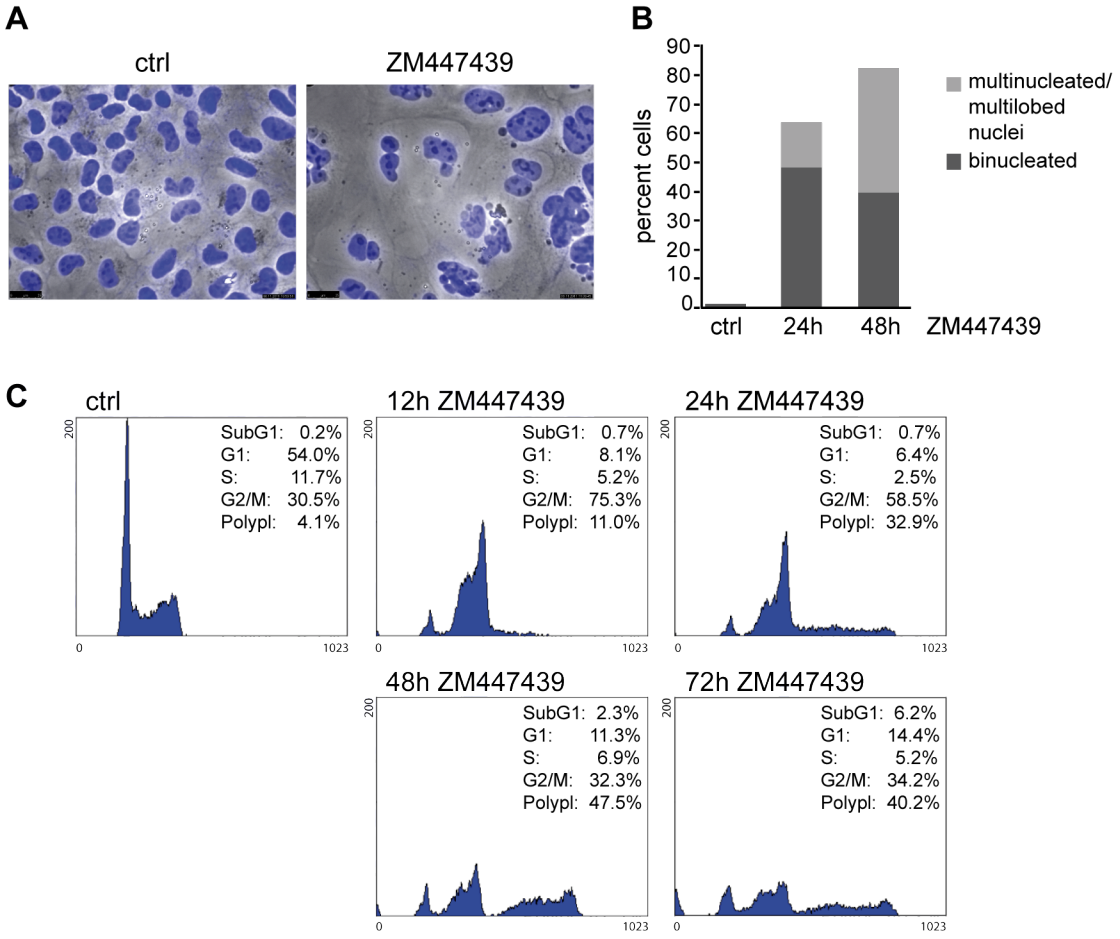

Fig. 3.10: Inhibition of AuroraB kinase results in polyploid cells
U2OS cells were treated with 1µM ZM447439 for the indicated times. A) Nuclei were stained with Hoechst 33258 after 24h ZM treatment. B) Quantification of bi- and multinucleated cells, 300 cells were counted. C) For FACS analysis cells were stained with propidiumiodide (PI) and cell cycle distribution was measured on a flow cytometer.

3.3.2 p53 dependent upregulation of p21 in response to Aurora B inhibition

Cell cycle arrest after Aurora B inhibition is due to upregulation of p53 and p21 as it has been reported by several groups (Dreier et al., 2009; Ditchfield et al., 2003; Gizatullin et al., 2006). Therefore, protein levels of p53 and its downstream target p21 in response to Aurora B inhibition in U2OS cells were tested. Cells were treated with DMSO or 1µM ZM for 24 hours and protein levels were determined by immunoblot analysis. Both proteins, p53 and p21, were upregulated after ZM treatment, suggesting that cytokinesis defects induced by Aurora B inhibition results in a postmitotic cell cycle arrest in the subsequent G1 phase (Fig. 3.11 A).

A stable cell line expressing shp53 was generated to investigate if p21 induction is dependent on p53. U2OS cells with an ecotrophic receptor (U2OS-EcoR) were infected retrovirally with a p53 specific shRNA or an empty vector (ctrl). After antibiotic selection U2OS-EcoR cells were treated with or without 1µM ZM for 24 hours and cells were harvested for protein and mRNA analyses. Reduction of p53 protein in p53 depleted cells correlated with decreased p21 levels (Fig. 3.11 B). RT-qPCR further confirmed that p53 shRNA prevented transcription of p21, indicating that p21 upregulation upon Aurora B inhibition is dependent on p53 (Fig. 3.11 C).

To investigate whether Aurora B inhibition in U2OS cells causes an irreversible cell cycle arrest and become senescent a SA-β - galactosidase staining was performed. Cells were exposed to 1µM ZM for 72 hours and 4 days later stained for SA-β - galactosidase. As depicted in Fig. 3.11 D the cells showed an enlarged and flattened morphology and were positive for SA-β - galactosidase.

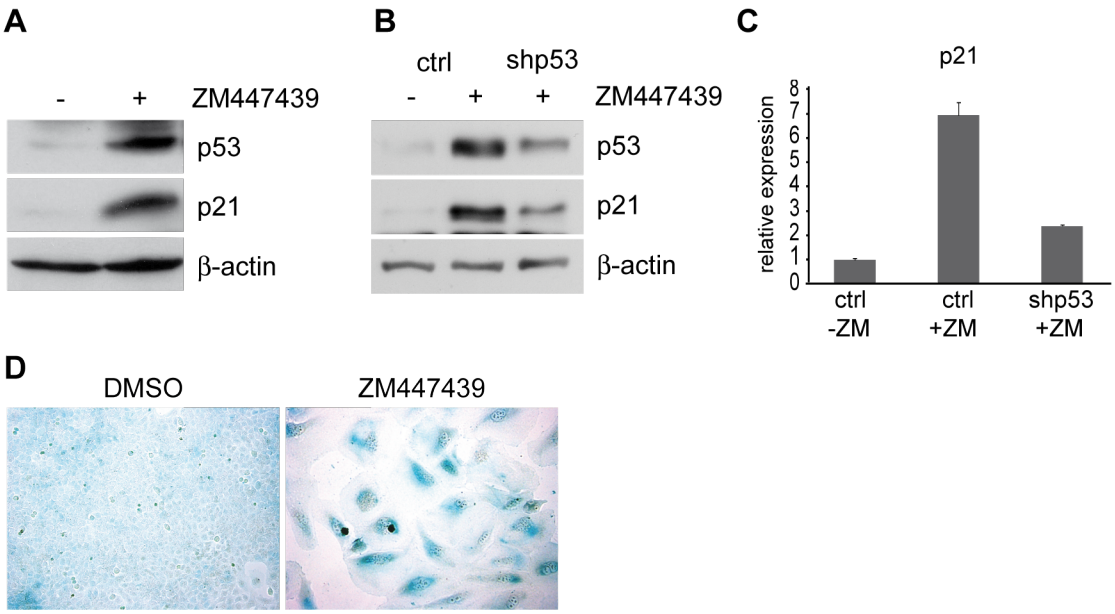

Fig. 3.11: AuroraB inhibition upregulates p53 and p21 and cells become senescent
U2OS were treated with 1µM ZM447439. A) p53 and p21 protein levels were detected by immunoblotting after 36h ZM treatment. B) U2OS-EcoR cells were infected with shp53 or control vector. After selection cells were treated with ZM for 24h and p53 and p21 protein levels were analyzed by immunoblotting. C) p21 mRNA expression levels were detected by RT-qPCR. D) U2OS cells were treated with ZM for 72h and 4 days later senescent cells were stained for SA-β-galactosidase.

3.3.3 Immunofluorescence staining of p21 is suitable as readout for the siRNA screen

For a successful siRNA screen a suitable readout system is necessary. Thus, p21 detection by immunofluorescence staining was validated as a possible assay. U2OS cells were seeded on coverslips and the next day cells were treated with 1µM for 36 hours. After fixation cells were stained with a polyclonal p21 antibody and immunofluorescently labeled with an anti-rabbit antibody. p21 upregulation due to Aurora B inhibition was detectable in immunofluorescence staining (Fig. 3.12 A). To test positive and negative controls for the use in the siRNA screen,

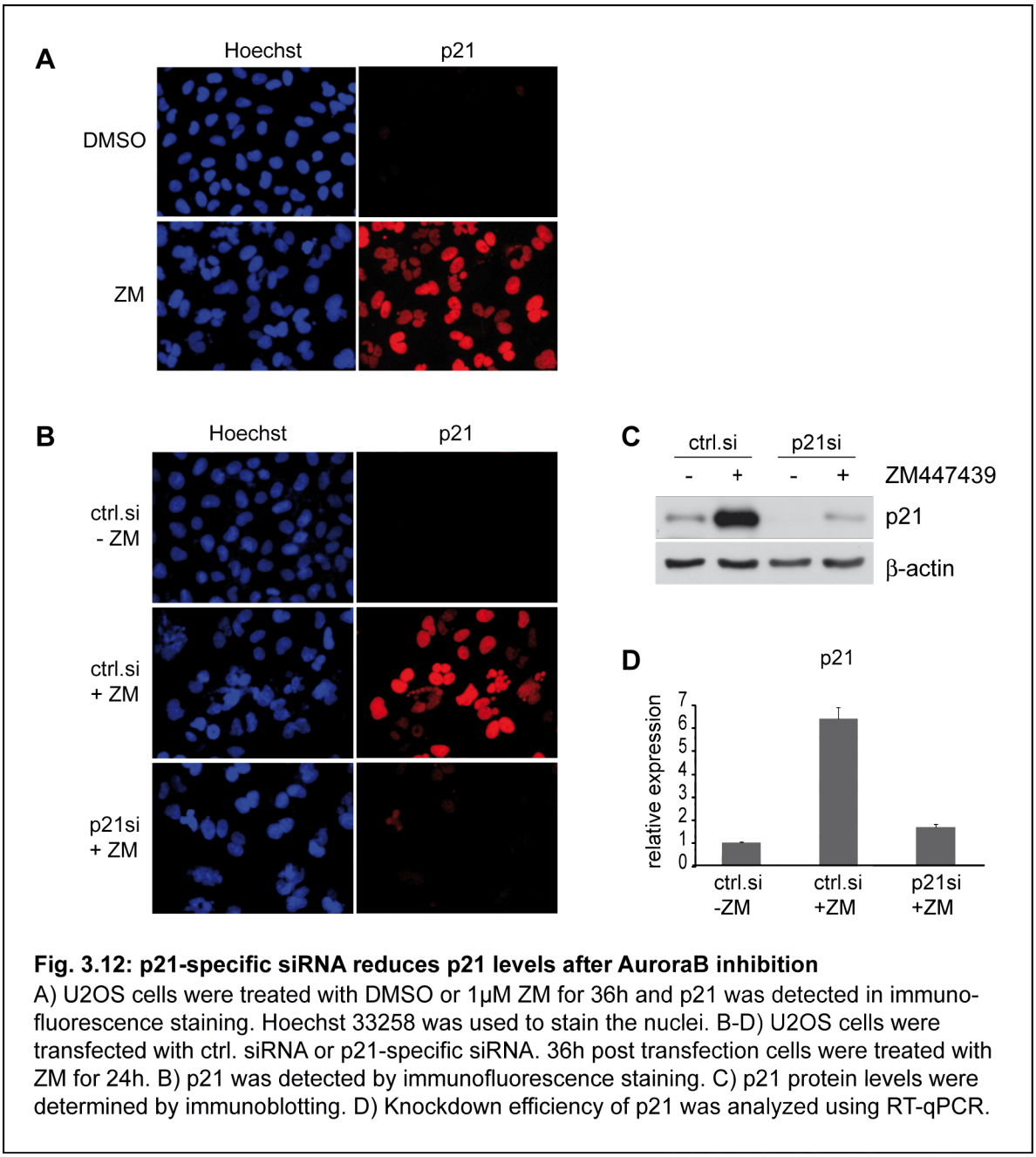

Fig. 3.12: p21-specific siRNA reduces p21 levels after AuroraB inhibition
A) U2OS cells were treated with DMSO or 1µM ZM for 36h and p21 was detected in immunofluorescence staining. Hoechst 33258 was used to stain the nuclei. B-D) U2OS cells were transfected with ctrl. siRNA or p21-specific siRNA. 36h post transfection cells were treated with ZM for 24h. B) p21 was detected by immunofluorescence staining. C) p21 protein levels were determined by immunoblotting. D) Knockdown efficiency of p21 was analyzed using RT-qPCR.

U2OS cells were transfected either with p21-specific or control siRNA (ctrl.siRNA). 36h post transfection cells were exposed to DMSO or ZM for 24 hours and immunofluoresence staining for p21 was performed (Fig. 3.12 B). Control siRNA transfected cells showed an increase in the p21 signal when treated with ZM whereas in p21 depleted cells the signal was reduced and hardly detectable anymore. The p21 protein levels after knockdown of p21 were further determined using immunoblot analysis. p21siRNA clearly diminished p21 protein levels in response to ZM treatment (Fig. 3.12 C). The knockdown efficiency of p21 siRNA was additionally proven on mRNA levels by RT-qPCR (Fig. 3.12 D).

In conclusion, these pretests suggest that inhibition of Aurora B in U2OS cells creates cytokinesis defects that result in tetraploid cells and a subsequent arrest in G1 induced by the p53-p21 pathway. Expression of p21 can be used as readout for a high throughput siRNA screen to identify proteins acting in the mitotic stress induced signaling pathway.

3.4 High throughput siRNA screening identifies MAP3K4 as a kinase acting in mitotic stress signaling pathways

The siRNA screening was performed using siRNAs targeting the human kinome and phosphatome (779 kinases, 130 phosphatases). U2OS cells were reversely transfected with the siRNA library in a 96 well format. Each well contained a pool of 4 single oligonucleotides against each target to exclude off-target effects. 30 hours post transfection cells were exposed to 1µM ZM447439 for 36 hours. The fluorescence signals of each well were measured by an automated microscope and the relative changes in the p21 fluorescence signals were determined by Z-score calculation (see 2.2.1.9).
Beside other kinases the MAP3 kinase MAP3K4 (also MEKK4, MTK1) showed strongly downregulated p21 levels after ZM treatment. As MAP3K4 is a known upstream activator of the MAP kinases signaling pathways p38 and JNK, that are both activated in response to certain stress stimuli (Hommes et al., 2003; Takekawa et al., 1997), this kinase was chosen for further analysis.

In order to validate the involvement of MAP3K4 in the stress signaling pathway that contributes to cell cycle arrest after Aurora B inhibition, U2OS cells were infected with the four specific single siRNAs used in the screen and a pool of these four siRNAs. 48 hours post transfection cells were treated with 1µM ZM for 24 hours. Immunofluorescence staining of p21 revealed that downregulation of MAP3K4 with each of the specific siRNAs prevented the induction of p21 after ZM treatment, compared to ctrl siRNA transfected cells treated with ZM (Fig. 3.13 A). Immunoblot analysis evidenced that MAP3K4 protein levels were reduced

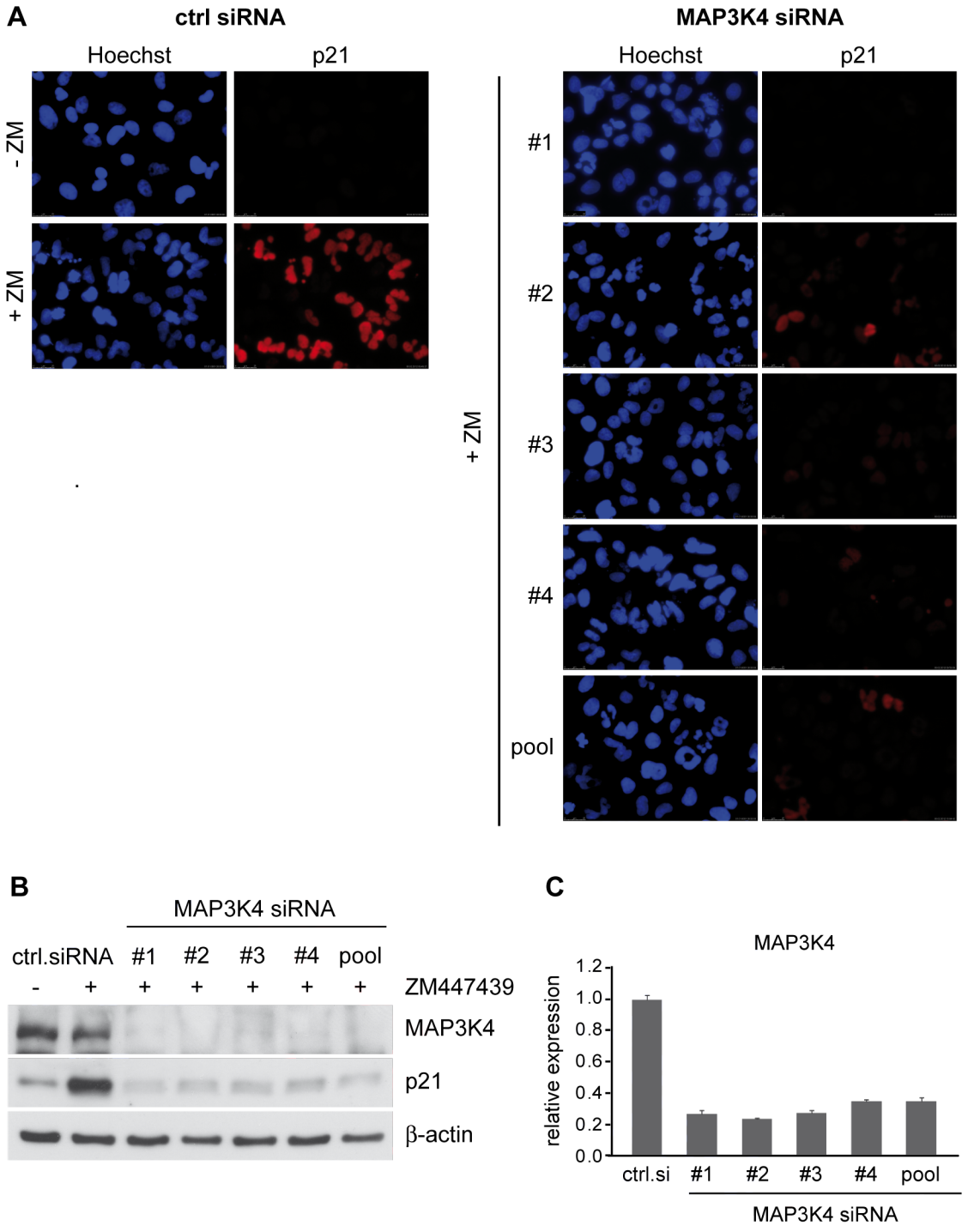

Fig. 3.13: MAP3K4 is involved in p21 upregulation after AuroraB inhibition
U2OS cells were transfected with ctrl.siRNA, specific MAP3K4 siRNAs and a pool of the four single MAP3K4 siRNAs. 48h after transfection cells were treated with 1µM ZM for 24h. A) p21 was detected by immunofluorescence staining. Hoechst 33258 was used for nuclear staining. B) p21 and MAP3K4 protein levels after MAP3K4 knockdown were determined by immunoblot analysis. C) Control of MAP3K4 knockdown on mRNA level using RT-qPCR analysis.

to a similar extend with all four individual siRNAs. This correlated well with decreased p21 expression levels upon Aurora B inhibition (Fig. 3.13 B). The knockdown of MAP3K4 was further confirmed on mRNA level using RT-qPCR (Fig. 3.13 C). MAP3K4 mRNA levels were reduced for all single siRNAs down to 20-30%.
Taken together, these validation studies indicate that MAP3K4 is required for p21 upregulation after Aurora B inhibition.

3.5 Analysis of downstream kinases of MAP3K4

3.5.1 The stress kinases p38 and JNK are activated upon Aurora B inhibition

The MAP3-kinase MAP3K4 phosphorylates and thereby activates the downstream MAP2-kinases MKK3/MKK6 and MKK4 (Takekawa et al., 1997). MKK3/MKK6 in turn phosphorylate the downstream stress kinases p38, MKK4 phosphorylates JNK as well as p38 (Dérijard et al., 1995; Han et al., 1996). To analyze if this downstream MAP kinase signaling cascades are also activated after cytokinesis failures upon Aurora B inhibition, immunoblot analysis with antibodies that specifically detect phosphorylated p38 and JNK was performed. After 24 hour treatment with 1µM ZM increased levels of phospho-p38 (pp38) and phospho-JNK (pJNK) were observed in U2OS cells, correlating with increased p53 and p21 protein levels (Fig. 3.14).
These data suggest that MAP3K4 transfers the mitotic stress signal after Aurora B inhibition to its downstream MAP kinases p38 and JNK.

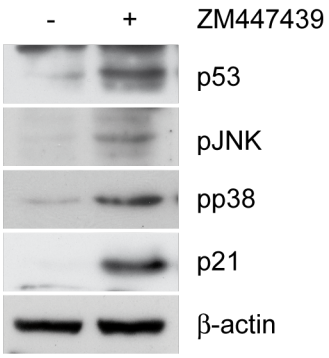

Fig. 3.14: AuroraB inhibition results in activation of p38 and JNK
U2OS cells were treated with 1µM ZM for 24h and protein levels of p53, phospho-JNK (pJNK), phospho-p38 (pp38) and p21 were analyzed by immunoblotting.

In the following, only involvement of the p38 pathway in regulating p21 after mitotic stress was further investigated, as treatment with the JNK inhibitor SP600125 itself blocked cells in the G2/M phase of the cell cycle (data not shown).

3.5.2 p38β, not p38α, is required for p21 activation after Aurora B inhibition

Next, it was examined if one or more of the p38 isoforms are involved in p21 upregulation after Aurora B inhibition. As p38α and p38β are ubiquitously expressed whereas p38γ and p38δ have a more tissue specific expression pattern (Zarubin and Han, 2005), only p38α and p38β were further analyzed.
U2OS cells were transfected with two specific siRNAs against both, p38α and p38β. 48 hours later the cells were exposed to 1μM ZM for 24 hours and protein expression level of p21 was analyzed by immunoblotting (Fig. 3.15 A). p21 expression was only affected when p38β was depleted by siRNA#1 and not when p38β siRNA#2 was used. As the available phospho-p38 antibody (Fig. 3.14) detects all phosphorylated p38 isoforms, knockdown of p38α and p38β was examined on mRNA level. RT-qPCR analysis revealed that p38β si#2 did not efficiently knockdown p38β in contrast to p38β si#1 (Fig. 3.15 B). Although the knockdown efficiency of both siRNAs against p38α was over 90%, this had no effect on the activation of p21, indicating that only p38β, but not p38α, is involved in upregulation of p21 upon Aurora B inhibition.

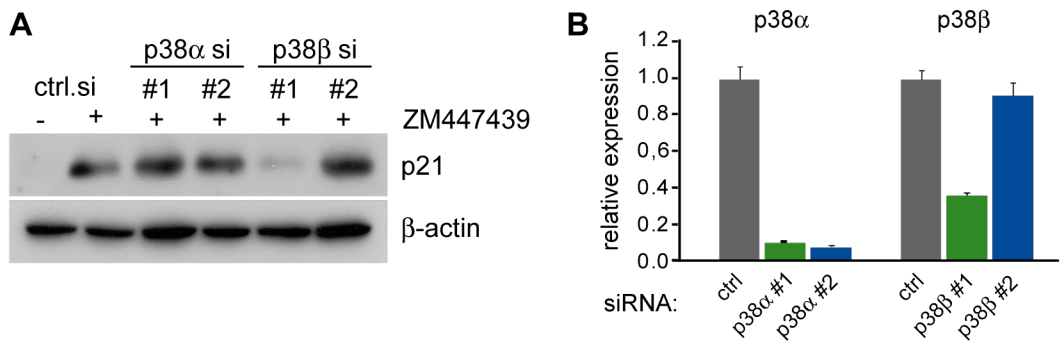

Fig. 3.15: p38β, not p38α regulates p21 in response to AuroraB inhibition
U2OS cells were transfected with ctrl.siRNA or specific siRNAs against p38α and p38β. 48h after transfection cells were treated with 1μM ZM for 24h. A) p21 protein levels were analyzed by immunoblotting. B) Knockdown efficiency of p38α and p38β siRNAs was tested by RT-qPCR.

3.6 Regulation of p53 activity by p38 after Aurora B inhibition

The finding that activation of p38 is required for p21 induction in response to Aurora B inhibition (Fig. 3.14 ,3.15) raised the question of how the p38 stress signaling pathway regulates the activity of p53 after mitotic stress. Therefore, assays that investigate the function of p38 on p53 stability, phosphorylation and cellular localization were performed.

3.6.1 The MAP3K4-p38 pathway is not required for p53 stabilization upon Aurora B inhibition

In response to cellular stress p53 is stabilized by posttranslational modifications on its N-terminal domain. Thereby the binding to its negative regulator Mdm2 is disrupted and p53 is no longer degraded and accumulates in the nucleus where it acts as transcription factor (Moll and Petrenko, 2003).

To investigate whether p38 plays a role in p53 stabilization after Aurora B inhibition, the potent p38 inhibitor SB202190, that specifically inhibits the kinase activity of p38α and p38β, was used. U2OS cells were pretreated with DMSO or 10 µM SB202190 (SB) for 2 hours followed by additional 24 h treatment with 1µM ZM. Immunoblot analysis revealed that p53 still accumulated when Aurora B and p38 were inhibited, although p21 levels were clearly reduced (Fig. 3.16 A). The same was observed when depleting either p38β or MAP3K4 with specific siRNAs (Fig. 3.16 B,C). 48 hours after siRNA transfection U2OS cells were exposed to 1µM ZM for 24 hours in both assays and immunoblot analysis was performed. p53 protein levels remained stable after ZM treatment when p38β was depleted (Fig. 3.16 B), confirming the finding made with the p38 inhibitor SB (Fig. 3.16 A). Also depletion of MAP3K4 did not change p53 accumulation after Aurora B inhibition (Fig. 3.16 C). Levels of phosphorylated p38 were reduced in MAP3K4 siRNA transfected cells compared to control cells (Fig. 3.16 C), indicating that activation of p38 after Aurora B inhibition is dependent on MAP3K4.

These assays indicate that the MAP3K4-p38 pathway is not required for p53 stability in response to Aurora B inhibition.

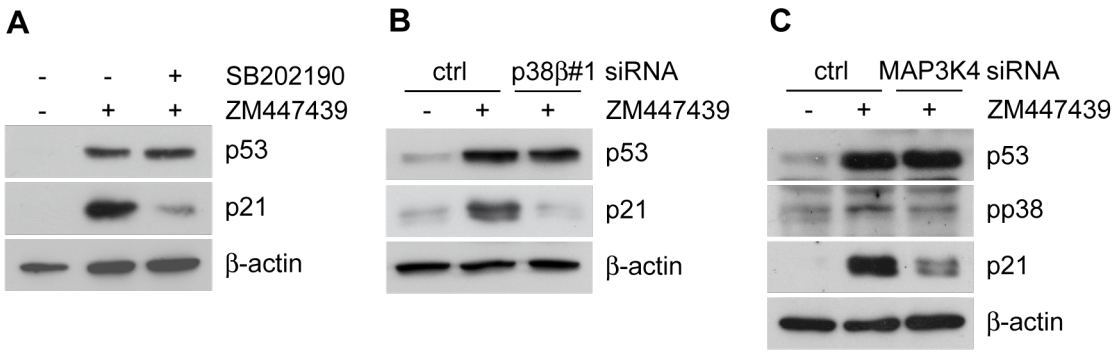

Fig. 3.16: MAP3K4-p38 pathway is not required for p53 stabilization after AuroraB inhibition

A) U2OS cells were pretreated with DMSO or with the p38 inhibitor SB202190 for 2h followed by an additional 24h treatment with 1µM ZM. p53 and p21 protein levels were detected by immunoblot analysis. B) +C) U2OS cells were transfected with ctrl siRNA or a specific siRNA against p38β (B) or MAP3K4 (C). 48h post transfection cells were treated with ZM for 24h and protein levels of p53, p21 and phospho-p38 (pp38) (C) were analyzed by immunoblotting.

3.6.2 p38 is not responsible for p53 phosphorylation in response to Aurora B inhibition

In response to different stress stimuli, like DNA damage or UV irradiation, p38 can directly regulate p53 by phosphorylating various serine residues. It has been reported that p38 can phosphorylate p53 on Ser15, Ser33, Ser46 and Ser392 *in vitro* (Bulavin et al., 1999; Keller et al., 1999; Huang et al., 1999; Sanchez-prieto et al., 2000; She et al., 2000). Furthermore, phosphorylation of Ser33 and Ser46 results in subsequent phosphorylation of Ser37 (Bulavin et al., 1999).

In order to find out if p38 is involved in p53 phosphorylation after inhibition of Aurora B, site- and phosphorylation specific antibodies for p53 were used. U2OS cells were pretreated with DMSO or SB for 2 hours followed by additional 24h treatment with 1µM ZM. Protein levels of p53, phosphorylated p53 and p21 were analyzed by immunoblotting (Fig. 3.17). Inhibition of Aurora B with ZM resulted in phosphorylation of all investigated p53 serine residues (Ser15, Ser20, Ser33, Ser37, Ser46, Ser392). Inhibition of p38 with SB did not alter the phosphorylation status of any of the investigated serine residues, although p21 induction was prevented. This assay suggests that p38 does not regulate p53 activity by direct phosphorylation.

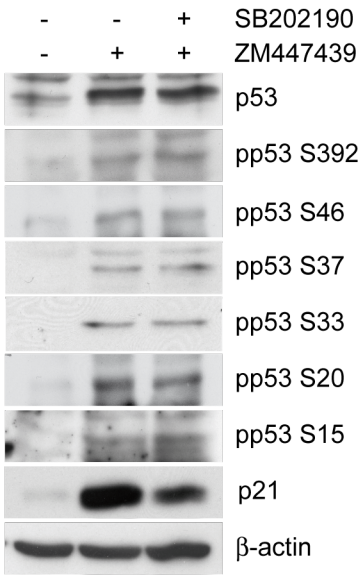

Fig. 3.17: Phosphorylation status of p53 after AuroraB inhibition is not altered when p38 is blocked
U2OS cells were pretreated with DMSO or the p38 inhibitor SB202190 for 2h followed by an additional 24h treatment with 1µM ZM. Protein levels of p53, phosphorylated p53 (pp53) at specific serin (S) residues and p21 were determined by immunoblot analysis.

3.6.3 p38 is required for transcriptional activity of p53 after Aurora B inhibition

In order to investigate whether p53 is still active or not when p38 signaling is blocked after Aurora B inhibition a luciferase reporter system was used to measure the trancriptional activity of p53. U2OS cells were transfected with the p53 reporter plasmid PG13-Luc containing 13 copies of the p53 response element, or with PM15-Luc, a construct with mutated p53 binding sites as negative control. As internal control the renilla luciferase construct pRL-TK was cotransfected. The next day, cells were pretreated with DMSO or SB for 2 hours and additionally treated with 1µM ZM. 24 hours later luciferase activity was measured. As shown in Fig. 3.18, inhibition of Aurora B resulted in increased activation of p53 compared to the DMSO control. Additional inhibition of p38 with SB reduced the activity of p53 to a similar basal level as untreated control cells. As expected no p53 activity was detectable when using the p53 mutant construct PM15-luc. This assay indicates that transcriptional activity of p53 is dependent on p38 when Aurora B is inhibited.

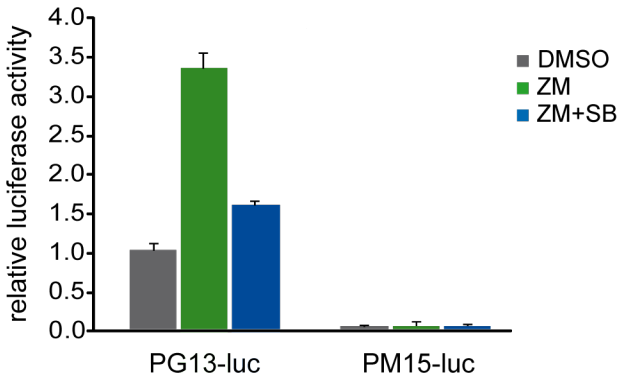

Fig. 3.18: Reduced p53 activity upon AuroraB and p38 co-inhibition
U2OS cells were transfected with the luciferase plasmids PG13-luc or PM15-luc. As internal control the renilla luciferase plasmid was cotransfected. 24h post transfection cells were pretreated with DMSO or SB followed by additional treatment with 1µM ZM. After 24 hours luciferase activity was measured on a luminometer.

3.6.4 Inhibition of p38 does not alter the nuclear localization and p21-promoter binding of p53 upon Aurora B inhibition

As p38 is required for activation of p53 in response to Aurora B inhibition the next step was to examine if the subcellular localization of p53 is altered when Aurora B and p38 are inhibited and p53 is not active any longer. After 2 h pretreatment with DMSO or SB U2OS cells were additionally treated with 1µM ZM. 24 hours later a p53 immunofluorescence staining was performed. p53 accumulated in the nucleus after ZM treatment and this localization was unchanged after co-treatment with the p38 inhibitor SB (Fig. 3.19 A), pointing out that p38

is not required for translocation of p53 to the nucleus after Aurora B inhibition.
Moreover, the binding of p53 to the p21 promoter was investigated with the same treatment conditions. DNA binding of p53 was analyzed by chromatin immunoprecipitation (ChIP) after cells were exposed to ZM or ZM+SB for 24 hours. Chromatin was immunoprecipitated with a specific p53 antibody or a nonspecific IgG antibody and bound p53 on the p21 and Gapdh2 promoter was examined by RT-qPCR (Fig. 3.19 B). As expected p53 was enriched on the p21 promoter upon Aurora B inhibition, which is consistent with the increased p21 expression. Additional inhibition of p38 with SB did not affect the binding of p53 to the p21 promoter. Binding of p53 to the p21 promoter is specific as no p53 binding to the Gapdh2 promoter was detectable. The ChIP data indicate that p38 is not necessary to recruit p53 to the p21 promoter in order to induce cell cycle arrest in response to Aurora B inhibition.

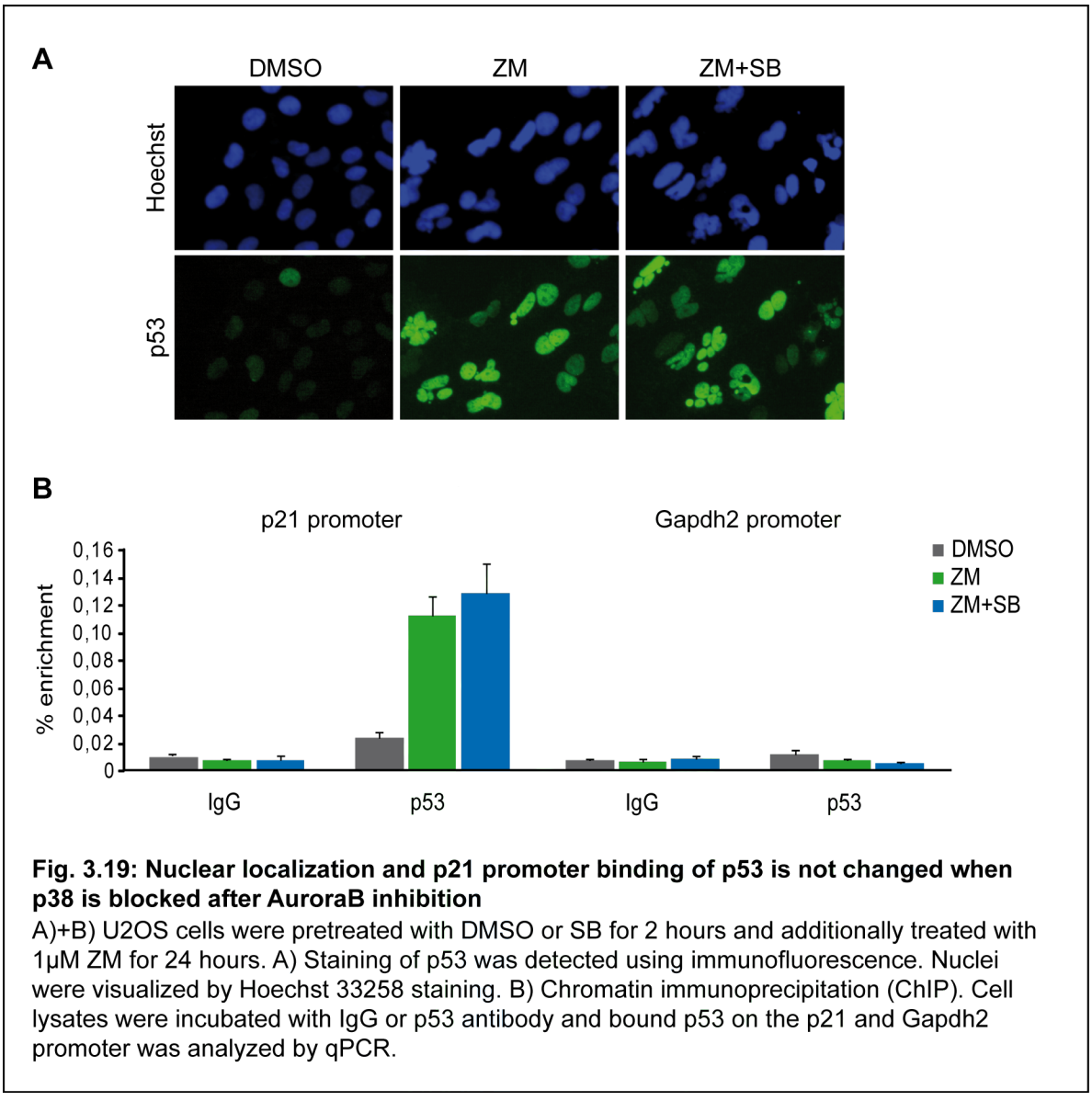

Fig. 3.19: Nuclear localization and p21 promoter binding of p53 is not changed when p38 is blocked after AuroraB inhibition
A)+B) U2OS cells were pretreated with DMSO or SB for 2 hours and additionally treated with 1µM ZM for 24 hours. A) Staining of p53 was detected using immunofluorescence. Nuclei were visualized by Hoechst 33258 staining. B) Chromatin immunoprecipitation (ChIP). Cell lysates were incubated with IgG or p53 antibody and bound p53 on the p21 and Gapdh2 promoter was analyzed by qPCR.

In summary, these data reveal that the p38 signaling pathway is required for transcriptional activity of p53 after Aurora B inhibition. However, p38 does not affect p53 stabilization, phosphorylation, subcellular localization and DNA binding.

3.7 p38 dependent and independent gene regulation after Aurora B inhibition

In order to examine if, besides p21, more genes are regulated in a p38 dependent manner after Aurora B inhibition, a genome-wide microarray analysis was performed. For this, U2OS cells were pretreated with DMSO or SB for 2 hours followed by additional treatment with 1μM ZM for 36 hours. Genes that were either activated or repressed more than 2 fold were analyzed. 636 genes were found upregulated after Aurora B inhibition. 62% of these genes were activated dependently of p38, 38% independently of p38. 399 genes were repressed in response to Aurora B inhibition and 72% of these downregulated genes were dependent on p38 signaling (Fig. 3.20 A).

Gene sets that were upregulated after Aurora B inhibition are involved in cell cycle arrest, cellular stress response, DNA repair and apoptosis. Several activated genes are known p53 targets such as Alox5, Rrad and Tp53inp1. RT-qPCR analysis confirmed that induction of these selected genes upon Aurora B inhibition was dependent on p38 as their expression was reduced when cells were additionally treated with SB (Fig. 3.20 B). This suggests that p38 dependent activation of p53 target genes in response to Aurora B inhibition is not resticted to p21.

Genes that were repressed after Aurora B inhibition have functions in cell cycle regulation and mitosis. Among these, many E2F target genes were found: genes that are important in G1/S-phase of the cell cycle (Cyclin A, Cdc6, p107) or genes necessary for the G2/M phase transition (CyclinB, Bub1, Birc5). Validation by RT-qPCR showed that Aurora B inhibition reduces the expression of these genes required for cell cycle progression (Fig. 3.20 C). Repression of these E2F target genes was dependent on p38 signaling as additional treatment of the cells with SB restored their expression levels, indicating that cells override the G1 arrest and further progress through the cell cycle when p38 function is blocked.

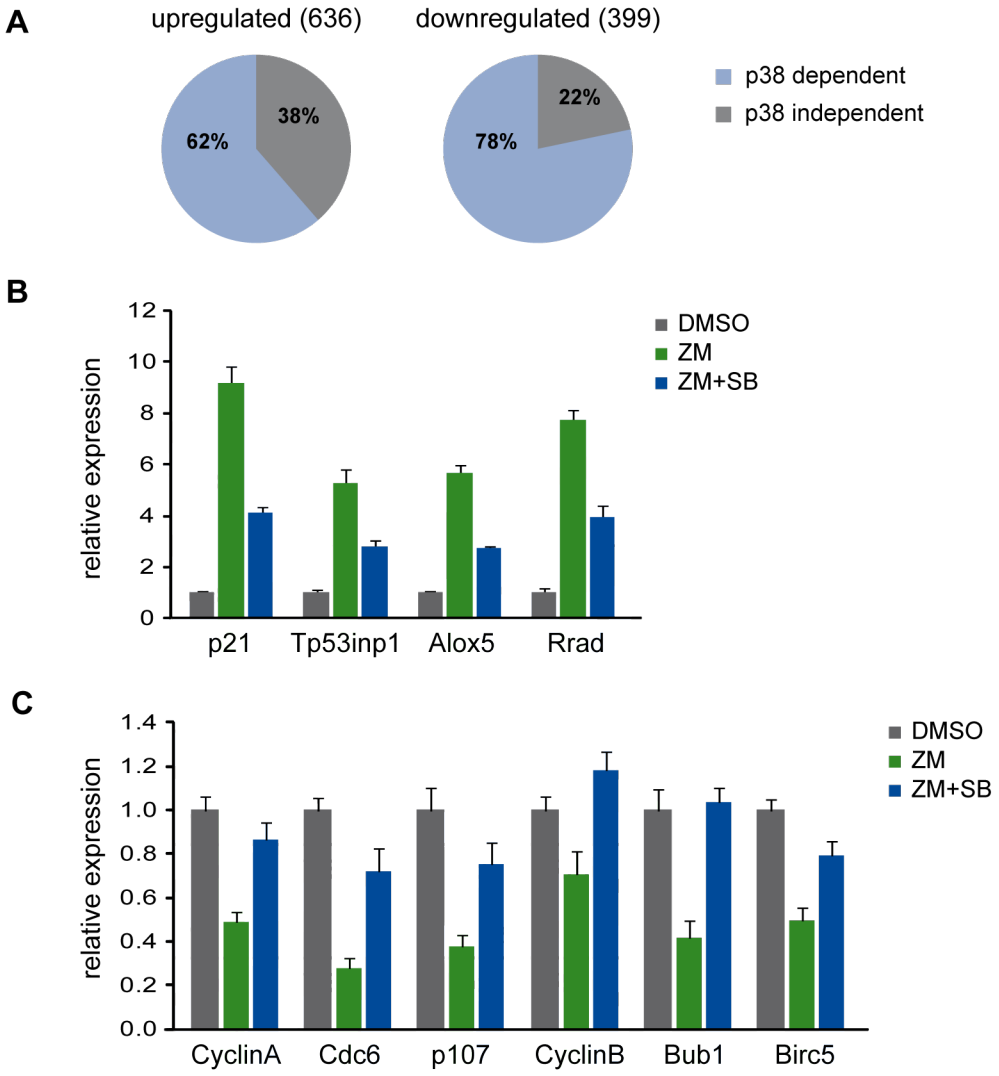

Fig. 3.20: p38-dependent and independent gene regulation in response to AuroraB inhibition
A) U2OS cells were pretreated with DMSO or SB for 2 hours followed by additional treatment with 1µM ZM for 36 hours. RNA was isolated and subjected to microarray analysis. Diagrams depict the percentage of genes that are up-or downregulated more than 2 fold dependent and independent of p38. B+C) Validation of microarray data. Cells were treated as above and gene expression was determined by RT-qPCR. B) p53 target genes. C) E2F-target genes.

3.8 Cellular outcome in response to partial Aurora B inhibition

3.8.1 Tetraploidization is not necessary to induce cell cycle arrest via the MAP3K4-p38 pathway

Next, it was of interest to find out whether cells have to become binucleated to induce cell cycle arrest or if more moderate failures in mitosis are also sufficient to activate p53 via the MAP3K4-p38 pathway. Thus, U2OS cells were treated with lower doses of the Aurora B inhibitor ZM. To study the extend of Aurora B inhibition with different ZM concentrations, the phosphorylation status of Serine 10 on histone H3 (phosho-H3), which is a mitotic substrate of Aurora B, was analyzed. For this purpose the cells were treated with 100ng/ml of the microtubule depolymerization drug nocodazole for 18 hours to synchronize cells in mitosis. One hour after exposure to 0.5 µM or 1 µM ZM mitotic cells were harvested and phospho-H3 was analyzed by immunoblotting (Fig. 3.21 A). Phospho-H3 levels were nearly completely absent when 1 µM ZM was used and were partially reduced with 0.5 µM ZM, suggesting that the lower amount of ZM inhibited Aurora B only in parts. Additionally the amount of bi- and multinucleated cells after 24h treatment with 0.5 µM or 1 µM ZM was

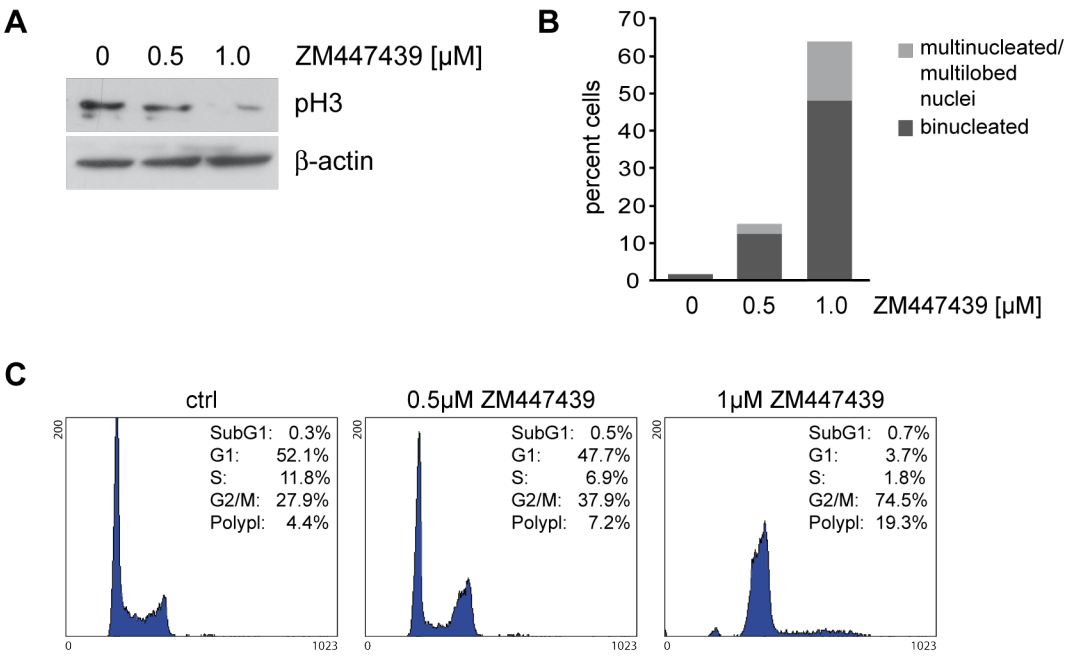

Fig. 3.21: Weak AuroraB inhibition results in fewer binucleated cells
A) To synchronize U2OS cells in mitosis, cells were treated with 100ng/ml nocodazole for 18h. 1h before harvesting mitotic cells, cells were additionally treated with 0.5 or 1µM ZM. pH3 levels were detected by immunoblotting. B)+C) Cells were treated with 0.5µM or 1µM ZM for 24h. B) Quantification of bi- and multinucleated cells, 200 cells were counted. C) Cell cycle distribution was determined using PI-FACS analysis.

counted (Fig. 3.21 B). Only 12% of the cells became binucleated and 3% multinucleated when 0.5 µM ZM was used, but over 60% bi- or multinucleated cells were found after exposure to 1 µM ZM. Analysis of cell cycle distribution with PI-FACS revealed that the fraction of cells with 4N DNA content in G2/M was only slightly increased when using 0.5 µM ZM compared to control cells, whereas over 70% of the cells accumulated with 4N DNA content after 1 µM ZM treatment (Fig. 3.21 C). These findings suggest that partial inhibition of Aurora B does not result in severe cytokinesis defects.

Although fewer cells showed binucleation after treatment with lower ZM concentration, cells also arrested in the cell cycle by induction of p21 (Fig. 3.22 A, B). After 24 hour treatment with different ZM concentrations the protein levels of p53, phospho-p38 (pp38) and p21 were analyzed by immunoblotting. 0.5 µM ZM treatment resulted in accumulation of p53 and activation of p38 and p21 to a similar extent to that when cells were treated with 1 µM ZM (Fig. 3.22 A). Immunofluorescence staining confirmed the activation of p21 with 0.5 µM ZM (Fig. 3.22 B). To further investigate if MAP3K4 is also involved in p21 induction upon partial Aurora B inhibition, p21 expression levels after depletion of MAP3K4 was determined

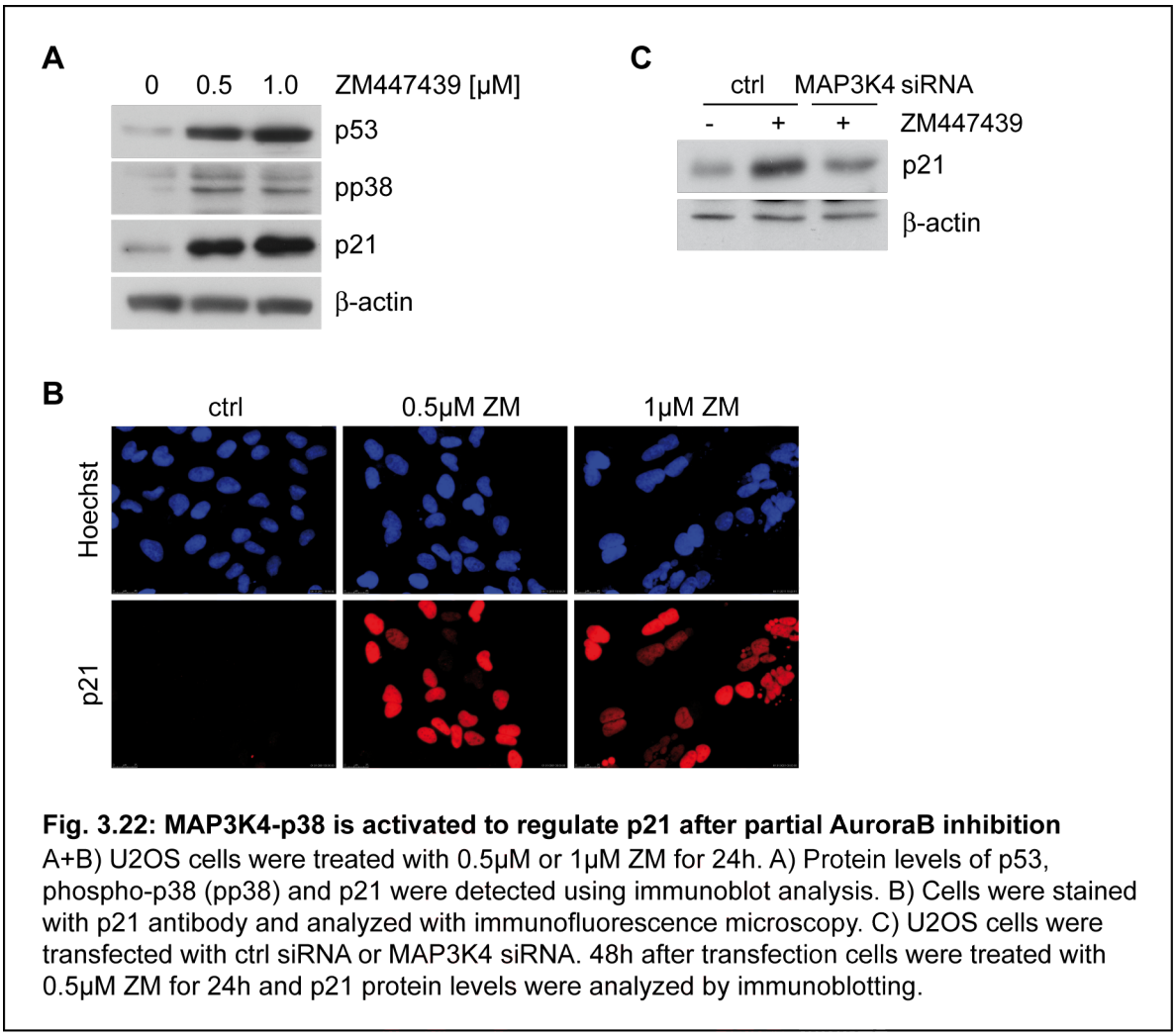

Fig. 3.22: MAP3K4-p38 is activated to regulate p21 after partial AuroraB inhibition
A+B) U2OS cells were treated with 0.5µM or 1µM ZM for 24h. A) Protein levels of p53, phospho-p38 (pp38) and p21 were detected using immunoblot analysis. B) Cells were stained with p21 antibody and analyzed with immunofluorescence microscopy. C) U2OS cells were transfected with ctrl siRNA or MAP3K4 siRNA. 48h after transfection cells were treated with 0.5µM ZM for 24h and p21 protein levels were analyzed by immunoblotting.

by immunoblot analysis (Fig. 3.22 C). 48 hours post transfection cells were exposed to 0.5 µM ZM for 24 hours. Reduced protein levels of p21 could be observed after MAP3K4 knockdown compared to ctrl siRNA treated cells.
These analyses suggest that not only tetraploidization but also subtle mitotic defects are sufficient to induce cell cycle arrest via the MAP3K4-p38 pathway in response to Aurora B inhibition.

3.8.2 Increase in chromosome missegregation after partial Aurora B inhibition

As visible in the immunofluorescence staining in Fig. 3.22 B, p21 is not only expressed in binucleated but also in mononucleated cells. This fact raised the question if induction of cell cycle arrest after partial inhibition of Aurora B might be due to chromosomal missegregation. In order to test this, centromere FISH (c-FISH) analysis in interphase cells was performed.

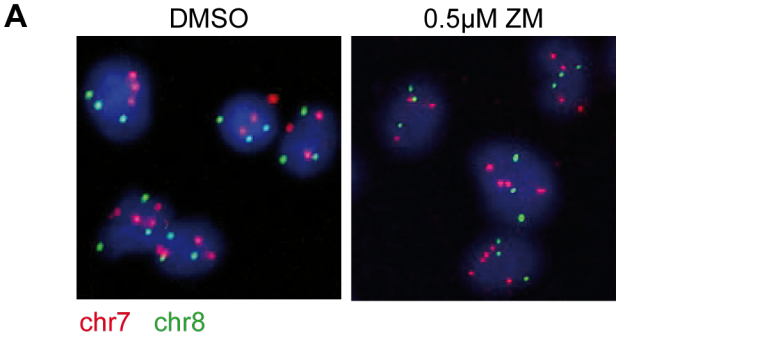

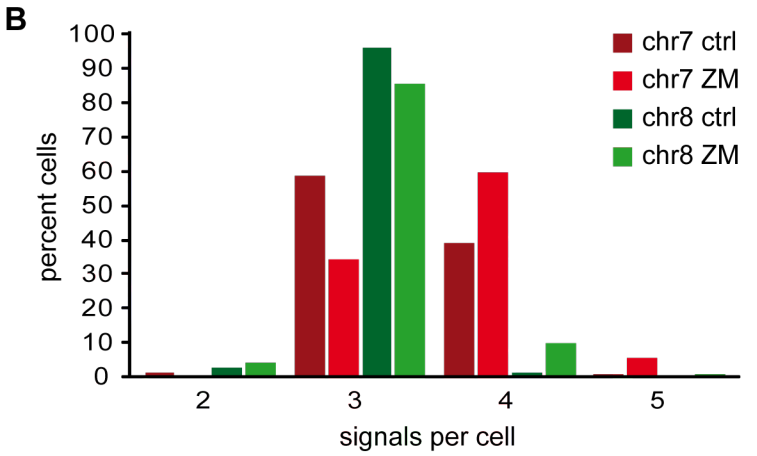

cells off the mode (%)

	ctrl	ZM
chr 7	41,2	64,5
chr 8	3,8	14,6

Fig. 3.23: Increase in chromosomal missegregation when AuroraB is partially inhibited
A) U2OS cells were treated with DMSO or 0.5µM ZM for 24h. Interphase cells were fixed and stained with centromere-specific, fluorescently-labeled probes against chromosome 7 (red) and 8 (green). Nuclei were visualized with Hoechst 33258 (blue). B) Quantification of FISH signals per cell. Table shows percentage of cells differing from the modal position (cells off the mode). The differences between DMSO and ZM treated cells were statistically significant for chromosome 7 and 8 ($p < 0.0001$, Fisher`s exact test). 650 cells were counted.

U2OS cells are aneuploid cells with a near triploid status (Niforou et al., 2008), but show only low chromosomal instability compared to other osteosarcoma cell lines (Al-Romaih et al., 2003). U2OS cells were either treated with 0.5 µM ZM or DMSO for 24 hours and c- FISH was carried out with probes specific for chromosome 7 and 8 to determine changes in chromosome numbers. Fig. 3.23 A shows examples for FISH signals in control and ZM treated cells. Quantification of FISH signals per cell revealed an increase in chromosome missegregation after Aurora B inhibition with 0.5 µM ZM (Fig. 3.23 B). Analysis of untreated control cells showed that chromosome 8 (green) is much more stable than chromosome 7 (red). Nearly 95% of control cells have three copies of chromosome 8 (3 signals) whereas chromosome 7 is less stable: 60% of the counted control cells showed three and 40% four signals for chromosome 7. When cells were treated with 0.5 µM ZM the numbers of FISH signals significantally changed for both investigated chromosomes. The deviation from the modal chromosome number was altered from 41.2% to 64.5% for chromosome 7 and from 3.8% to 14.6% for chromosome 8, suggesting that partial inhibition of Aurora B with low doses of ZM leads to increased chromosome missegregation and thereby causes a change in the ploidy status of U2OS cells.

In summary, partial Aurora B inhibition causes moderate mitotic defects resulting in chromosome missegregation and activation of the MAP3K4-p38 pathway that regulates p21 induction.

3.9 Consequences of Aurora B and p38 Co-inhibition

3.9.1 p38 inhibition overcomes the p21 induced G1 arrest upon Aurora B inhibition

As shown in Fig. 3.16, inhibition of p38 prevents p21 induction when Aurora B activity is blocked. Now it was of interest to analyze how cell cycle progression is affected when cells are treated with both, Aurora B and p38 inhibitors. To investigate cell cycle distribution with FACS analysis the lower ZM concentration (0.5 µM ZM) was chosen, as treatment with 1 µM ZM results in binucleated tetraploid cells that arrest with 4N DNA content in a pseudo-G1 state and that can not be distinguished from cells in G2/M phase (Fig. 3.10 C).
Therefore, cells were treated with 0.5 µM ZM with and without additional 2h SB pretreatment and cell cycle distribution was studied by FACS analysis (Fig. 3.24 A). Inhibition of Aurora B with 0.5 µM ZM resulted in the accumulation of 71% of the cells in G1 compared to control cells treated with DMSO or SB that showed about 60% cells in G1. The G1 arrest induced by ZM was overcome when cells were treated with ZM and SB (G1: 47%), indicating that p38 is essential for the G1 arrest induced by p21. Furthermore co-treatment with ZM and SB resulted in an increase in polyploid cells compared to ZM treated cells (ZM:

5.6%, ZM+SB: 12.3% polyploid cells). Analysis of DNA synthesis by BrdU incorporation assay further confirmed this finding. U2OS cells were pretreated with DMSO or SB for 2 hours followed by additional treatment with 0.5 µM ZM for 72 hours. 2 hours before fixation cells were labeled with BrdU to detect S-phase cells. BrdU positive cells were determined by immunofluorescence staining (Fig. 3.24 B). Cell counting demonstrated that Aurora B inhibition reduced the number of BrdU positive cells to 20%, in contrast to about 45% of BrdU-labeled control cells treated with DMSO or SB. Co-treatment with ZM and SB restored the number of cells that entered S-phase to nearly 40%.
The following experiment was performed to test whether the cells arrest in S-phase or proceed further through the cell cycle into mitosis when cells are exposed to both inhibitors: After 24 hour treatment with the indicated inhibitors cells were labeled with BrdU for 30 minutes and then treated with nocodacole for 8 hours. Cells were fixed and stained for BrdU and phospho-H3 and the number of the respective positive cells was determined by immunofluorescence microscopy. The number of BrdU positive cells as well as the number of mitotic cells (pH3 positive cells) was decreased in ZM treated cells (Fig. 3.24 C). The amount of mitotic cells after double treatment with ZM and SB nearly recovered to the level of control cells pointing out that cells with blocked p38 signaling pass through S-phase into mitosis. Furthermore, the amount of phospho-H3 positive cells that were BrdU labeled was similar for all three treatment conditions indicating that all cells that were labeled with BrdU did enter mitosis.

Taken together, these data indicate that p38 is required for induction of cell cycle arrest after chromosome missegregation or cytokinesis failures caused by Aurora B inhibition. Inhibiting p38 signaling prevents cells to arrest in G1 and cells are able to proceed through the cell cycle by entering S-phase and mitosis again. This is consistent with the restored gene expression of G1/S phase and G2/M phase genes after p38 inhibition found in Fig 3.20 C.

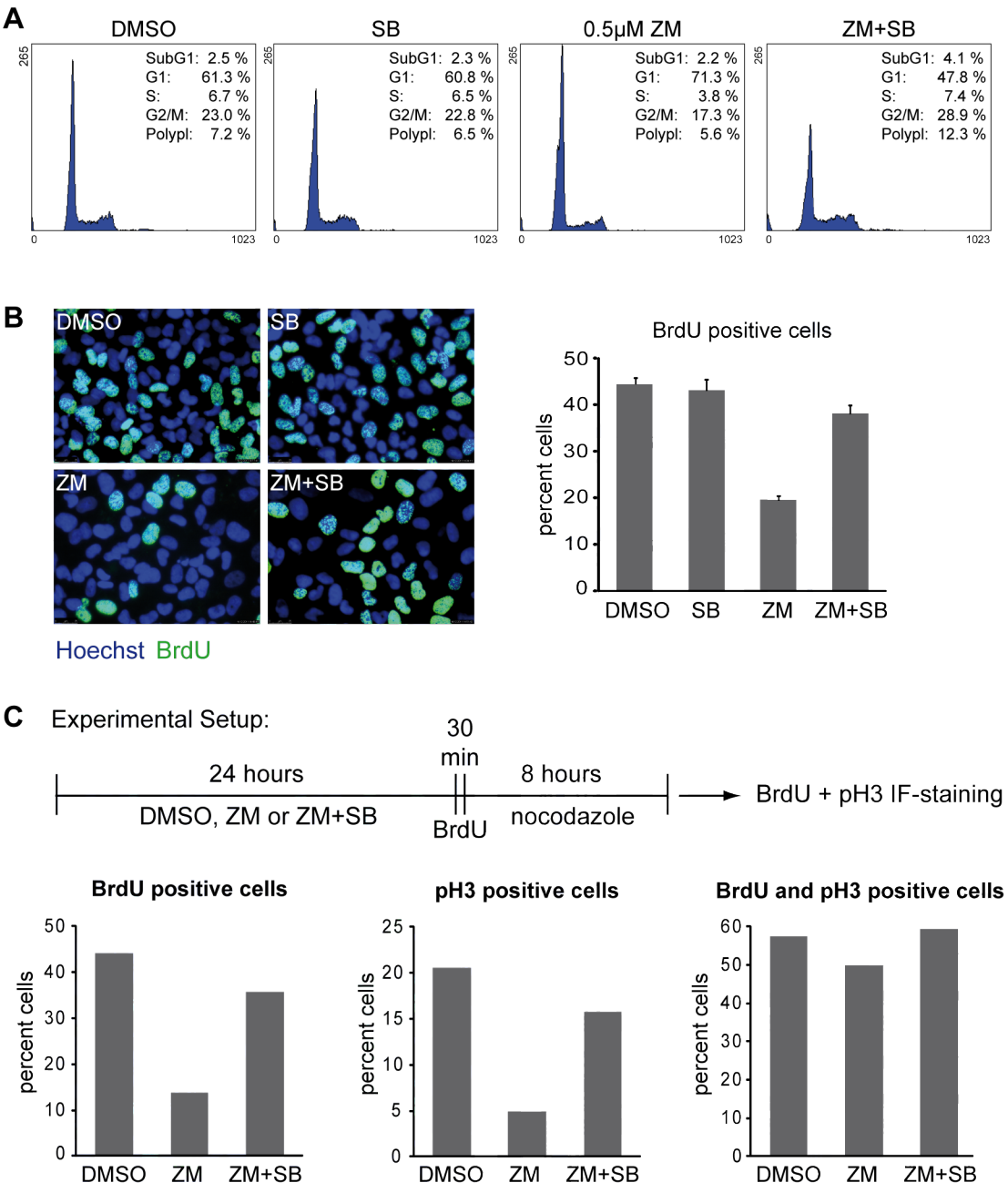

Fig. 3.24: p38-inhibition overcomes the G1-arrest induced by AuroraB inhibition
A) U2OS cells were pretreated with DMSO or SB for 2h followed by additional treatment with 0.5µM ZM for 72h. Cell cycle distribution was analyzed by PI-FACS analysis. B) U2OS cells were treated as in A) and additionally cells were labeled with BrdU for 2h and fixed for immunofluorescence staining. BrdU (green), Hoechst 33258 (blue). For quantification 600 cells in three independent experiments were counted. C) After 24h treatment with inhibitors as indicated, cells were pulsed with BrdU for 30min and afterwards treated with nozodacole for 8h. Cells were fixed and immunofluorescence staining for BrdU and pH3 was performed. 100 cells were counted.

3.9.2 Impaired cell proliferation in response to Aurora B and p38 Co-inhibition

In order to study the long term consequence of Aurora B inhibition as well as of Aurora B and p38 co-inhibition, a colony formation assay was performed to analyze cell proliferation. Therefore, cells were plated in a very low density (6000 cells) on 10 cm dishes and treated with 0.5 µM or 1 µM ZM alone or additionally with SB for 72 hours. After 10 days colonies were stained with crystal violet (Fig. 3.25). Treatment with 1 µM ZM almost entirely prevented colony formation. Cells treated with the lower ZM concentration (0.5 µM) were still able to form colonies but in a reduced manner compared to DMSO treated control cells. Interestingly, cells that were co-treated with ZM and SB showed impaired proliferation in contrast to ZM treatment alone, although single SB treatment had no effect on colony formation. This effect was especially observed when cells were exposed to 0.5 µM ZM.

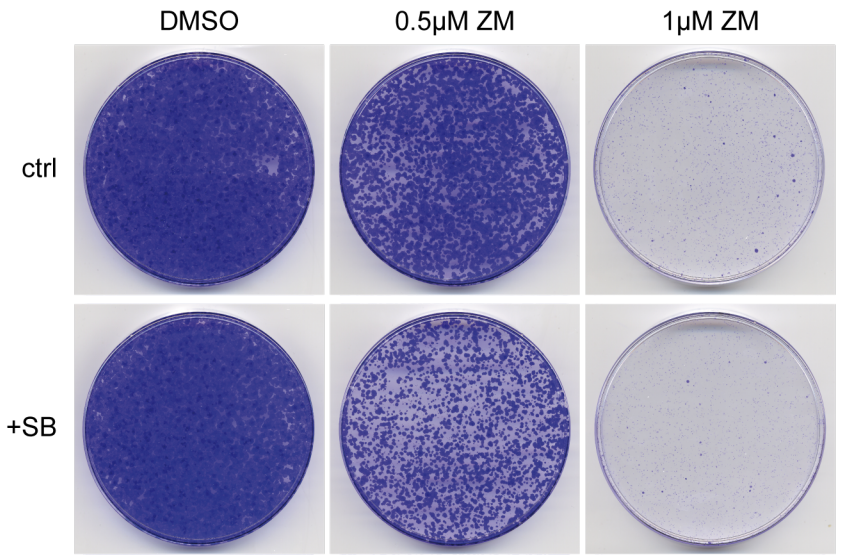

Fig. 3.25: Co-inhibition of AuroraB and p38 leads to reduced proliferation
6000 cells were plated on 10cm dishes and treated with DMSO or SB for 2h and additionally treated with 0.5µM or 1µM ZM for 72h. 10 days later cells were fixed and stained with crystal violet.

To investigate if apoptosis could explain the reduced proliferation after co-treatment of ZM with SB, an AnnexinV staining was carried out. U2OS cells were pretreated with DMSO or SB for 2 hours and additionally exposed to 0.5 µM for 72 hours and stained for AnnexinV, a marker for apoptotic cells. AnnexinV positive cells were analyzed by flow cytometry. Treatment of cells with both inhibitors, ZM and SB, resulted in a significant higher number of apoptotic cells (about 14%) when compared to cells treated with ZM only (8%) (Fig. 3.26). This increase in apoptotic cells might explain the reduced proliferation rate of cells when p38 is inhibited additionally to Aurora B.

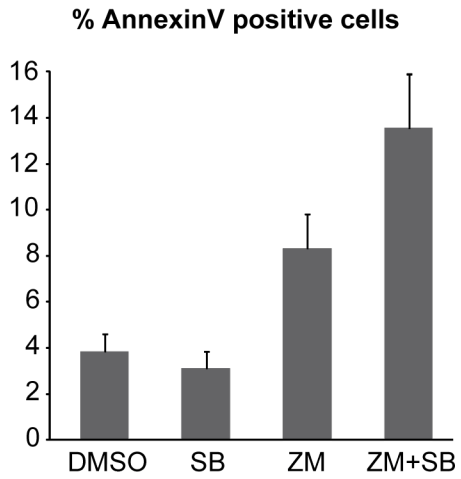

Fig. 3.26: Increase of apoptotic cells upon co-treatment with AuroraB and p38 inhibitor
U2OS cells were treated with DMSO or SB for 2h followed by additional treatment with 0.5µM ZM for 72h. Cells were harvested and stained with AnnexinV. The number of AnnexinV positive cells was detected by flow cytometry (FACS). Three independent experiments were performed. The differences between ZM and ZM+SB treated cells were statistically significant (p=0.03, Students t-test).

3.10 Lin9 depletion in U2OS cells activates p38 and JNK to induce cell cycle arrest

Assays performed so far investigated signaling pathways that are activated upon defects in mitosis and/or cytokinesis due to inhibition of Aurora B. As cytokinesis failures and p21 upregulation were also found in Lin9 depleted MEFs (Reichert et al., 2010) and (Fig. 3.2 B), it was now of interest to determine if the pathways that are activated after Lin9 depletion and Aurora B inhibition are the same.

Therefore, U2OS cells were transfected with a specific Lin9 siRNA or ctrl siRNA. 48 hours after transfection cells were harvested and protein levels of p53, p21, phospho-p38 and phospho-JNK was analyzed by immunoblotting. The active phosphorylated forms of p38 and JNK proteins were detectable and this activation correlated with the induction of p53 and p21 (Fig. 3.27 A). Knockdown of Lin9 was controlled by RT-qPCR and showed 80% reduction of Lin9 mRNA (Fig. 3.271 B).

As both, p38 and JNK, act downstream of MAP3K4 it can be speculated that depletion of Lin9 and the resulting mitotic defects leads to activation of the same pathways as observed after Aurora B inhibition.

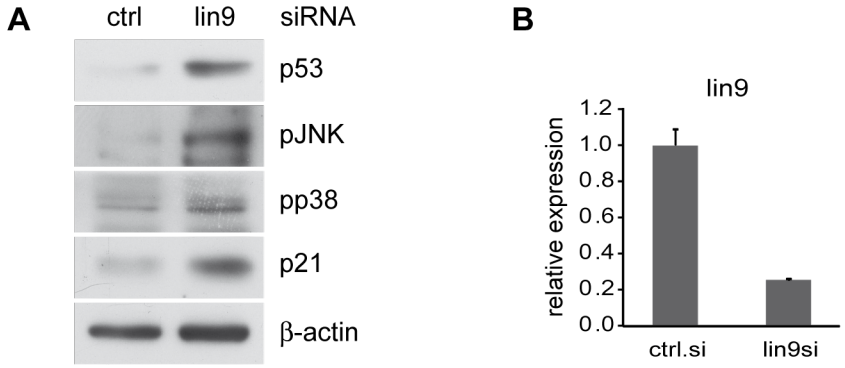

Fig. 3.27: Lin9 depletion activates p38 and JNK to induce cell cycle arrest
U2OS cells were transfected with ctrl or lin9si RNA. A) 48h post transfection cells were lysed and protein expression of p53, p21 phospho-p38 (pp38), phospho-JNK (pJNK) was determined by immunoblot analysis. B) 24h after transfection knockdown of Lin9 was analyzed by RT-qPCR.

4 Discussion

4.1 Analysis of the senescence phenotype after Lin9 knockout

Analysis of the function of Lin9, a core-subunit of the DREAM complex, demonstrated that loss of Lin9 in MEFs results in reduced mitotic gene expression and in the formation of binucleated cells. Due to this cytokinesis defect cells undergo premature senescence, a permanent cell growth arrest (Reichert et al., 2010).
The first part of this work investigated the tumor suppressor pathways that are activated in response to Lin9 deletion in order to induce senescence.

The CDK inhibitors p16 and p21, that are linked to permanent cell cycle arrest, were up-regulated after deletion of Lin9 in MEFs before cells became senescent (Fig. 3.2). As both, p16 and p21, function in two different tumor suppressor pathways, it was analyzed whether senescence induced upon Lin9 deletion is mediated by the p53-p21 and/or the p16-pRB pathway. Expression of SV40 LargeT antigen, that binds p53 and pRB and thereby inhibits their functions, no longer resulted in senescent cells, indicating that senescence is overcome when both pathways are blocked (Fig. 3.3). It was further of interest whether p53 and pRB act together in one linear senescence pathway (p53-p21-pRB) or if both pathways are independently required for senescence induction after Lin9 deletion. Assays with SV40 LargeT mutants, that can no longer bind either to pRB and the related pocket proteins 107 and p130 (SV40 LT-K1) or to p53 (SV40 LT Δ434-444) (Kierstead and Tevethia, 1993; Stubdal et al., 1997) revealed that the senescence phenotype could no longer be prevented when only one of the tumor suppressors is inhibited (Fig. 3.3). Inactivation of either p53 or pRB was therefore not sufficient to bypass induction of senescence, suggesting that Lin9 deletion in MEFs does not activate one single linear p53-p21-pRB pathway, but that both pathways, p53-p21 and p16-pRB, independently mediate senescence.

These data indicate that, dependent on the nature of stress, different pathways are responsible for inducing senescence in mouse fibroblasts. In contrast to the parallel activation of both tumor suppressor pathways after mitotic stress induced by Lin9 deletion, premature senescence caused by oncogenic activation is regulated via one linear pathway (p19ARF-p53-p21-pRB) (Serrano et al., 1997).
Whether p19ARF, that is known to stabilize p53 and is linked to senescence phenotype in mouse cells (Ben-Porath and Weinberg, 2005; Dimri, 2005), also functions in premature senescence due to Lin9 deletion has to be further analyzed. In order to examine whether the p53-p21 pathway leading to senescence depends on p19ARF or not, one could use conditional Lin9 knockout MEFs stably expressing shp19ARF and inhibit pRB using SV40 LT Δ434-444 (LT p53-bdg. mutant). Another option would be to cross conditional Lin9 knockout mice

with mice deficient for the INK4a locus, that encodes p16 and p19ARF. MEFs derived from these mice would elucidate the involvement of p19ARF in premature senescence caused by Lin9 deletion.

4.2 Function of Lin9 *in vivo*

Using a constitutive Lin9 knockout mouse model, previous work in our group revealed that Lin9 is required for mouse development, as loss of Lin9 caused early embryonic lethality. In order to study the role of Lin9 in adult mice a conditional Lin9 knockout mouse model was generated to circumvent this embryonic lethality phenotype (Reichert et al., 2010).

Deletion of Lin9 in 8-week-old mice resulted in rapid death of the mice within 6-7 days (3.2.2). This dramatic effect indicates that Lin9 is also essential for the survival of adult mice. The Lin9 knockout mice exhibited an almost complete atrophy of the intestinal epithelium and showed destroyed and abnormal looking epithelium of the colon and stomach (Fig. 3.5). In contrast, histological analysis of other tissues like lung, heart, kidney or liver did not depict abnormalities in Lin9 knockout mice (data not shown).
Loss of the epithelium in the small intestine after Lin9 deletion (Fig. 3.5 A) can be explained by the continuous and rapid renewal of the gastro-intestinal epithelium in mice. In the small intestine proliferation occurs within the crypt compartment. Rapidly cycling transit-amplifying cells (TA), that are derived from intestinal stem cells, undergo several rounds of cell division before they terminally differentiate at the crypt-villus junction. Within 3-5 days the TA cells migrate to the top of the villus where they are removed by apoptosis or cell shedding (Barker et al., 2008). The atrophic phenotype observed upon loss of Lin9 in the small intestine pointed to proliferation errors in the intestinal crypts. Defects in cell cycle progression were confirmed by the reduced number of proliferating cells observed with Ki-67 staining and the decreased amount of S-phase cells in Lin9 deleted crypts (Fig. 3.6). Accordingly, it can be assumed that the diminished proliferation rate in Lin9 deficient crypts prevents the development of new villus epithelium thereby creating the atrophic phenotype. Lin9 knockout resulted in binucleated cells and abnormally huge nuclei in the intestinal epithelium indicating failures in cytokinesis (Fig. 3.7 A). This binucleation phenotype might be due to the reduced expression of DREAM target genes (Aspm, Nusap, Gas2l3) that was found upon loss of Lin9 (Fig. 3.7 B). Increased expression of p16 and p21 in the intestinal tissue of Lin9 knockout mice suggests that the tumor suppressor pathways p16-pRB and p53-p21 are activated in order to induce cell cycle arrest and thereby avoid cell cycle progression after loss of Lin9 *in vivo* (Fig. 3.8). Deletion of Lin9 in $p16^{-/-}$ mice did not prevent the atrophic phenotype (Fig. 3.9), indicating that besides the p16-pRB pathway the p53-21 signaling might also lead to reduced proliferation in the intestinal crypts after Lin9 knockout. This would be consistent with the findings *in vitro* where the single blocking of either p53

or pRB did not overcome the cell growth arrest (Fig. 3.3). To address if the atrophy of the intestinal epithelium after Lin9 deletion occurs via both tumor suppressor pathways, a conditional Lin9 knockout mouse model with p16/p21 or p16/p19 null background could be generated.

In summary, the reduced expression of mitotic genes, the cytokinesis defects as well as the increased expression of p16 and p21 observed upon Lin9 deletion *in vivo* are consistent with the previous *in vitro* findings in conditional Lin9 knockout MEFs (Reichert et al., 2010), (Fig. 3.2 B).
As the DREAM complex is required for mitotic gene expression (Schmit et al., 2007), the reduced expression of DREAM target genes after loss of Lin9 could possibly be due to an impaired or missing binding of the DREAM complex to target gene promoters. It could be speculated that Lin9 depletion results in disruption of the DREAM complex and/or degradation of DREAM subunits as it has been shown for the homolog DRM/synMuv complex in C. elegans (Harrison et al., 2006).

Taken together, these studies in Lin9 knockout mice show the essential role of Lin9 in the regulation of proper mitotic gene expression and proliferation *in vivo*. This is consistent with previous Lin9 *in vivo* studies in zebrafish that also demonstrated the important function of Lin9 as regulator of mitotic progression (Kleinschmidt et al., 2009).

4.3 Analysis of pathways activating p53 after cytokinesis failures

Failures in cell division result in tetraploid cells that arrest in a p53 dependent manner to prevent aneuploidy and tumorigenesis. The upstream pathways that are involved in the activation of p53 following cytokinesis defects are not well understood so far (Ganem and Pellman, 2007; Stukenberg, 2004). In order to examine the regulation of these pathways more precisely, inhibition of the mitotic kinase Aurora B in U2OS cells was used as a robust and reproducible cellular system. Inhibiting Aurora B function causes defective chromosome alignment, chromosome missegregation and failures in cytokinesis (Ditchfield et al., 2003).

Using the potent Aurora B inhibitor ZM447439 in U2OS cells resulted in a high fraction of bi- and multinucleated cells (Fig. 3.10 A,B), assuming a complete inhibition of cytokinesis. FACS analysis revealed an increase in polyploidy over time (Fig. 3.10 C), indicating that some cells did not directly arrest as tetraploid cells but escaped the G1 arrest and endoreduplicated before they arrest with DNA content $>$ 8N. This effect has been reported earlier in different cell lines treated with the Aurora B inhibitor ZM (Ditchfield et al., 2003). There was only a slight increase in the amount of cells in the Sub-G1 fraction observed with FACS analysis (Fig. 3.10 C), suggesting that Aurora B inhibition does not strongly induce apoptosis in U2OS cells. Instead, U2OS cells underwent senescence when treated with the Aurora B inhibitor

(Fig. 3.11 D) in order to prevent cellular proliferation after cytokinesis errors. The response to Aurora B inhibition seems to depend on the cell type, as ZM treatment in other cell lines like HCT116 cells leads to induction of apoptosis (Li et al., 2010).
Aurora B inhibition in U2OS cells caused accumulation of p53 and its downstream target p21 (Fig. 3.11 A). Using a p53-specific shRNA prevented upregulation of p21 after ZM treatment and confirmed that p21 induction is dependent on p53 (Fig. 3.11 B,C).

Thus, it can be concluded that tetraploidization in U2OS cells in response to Aurora B inhibition results in activation of p53 followed by p21 mediated cell cycle arrest. This cellular system seemed suitable for analyzing the upstream pathways that activate p53 due to failed cytokinesis in more detail.

4.3.1 MAP3K4-p38 regulates activation of p21 upon Aurora B inhibition

A high throughput siRNA screen was performed to identify kinases that are required for p21 activation after Aurora B inhibition. Induction of p21 by immunofluorescence staining was used as readout for the screen (Fig. 3.12 A). p21 specific siRNA and control siRNA were taken as positive and negative controls because validation showed a strongly reduced expression of p21 in cells transfected with a p21 specific siRNA compared to the control siRNA transfected cells in response to Aurora B inhibition (Fig. 3.12 B).

The siRNA screen identified those kinases as potential hits, that showed strongly reduced p21 levels after Aurora B inhibition when downregulated with their specific siRNAs. Beside other kinases, MAP3K4 (also MEKK4, MTK1) was one of these potential hits. This kinase was selected as it is a known activator of the stress MAP kinases p38 and JNK. Validation with the four specific MAP3K4 siRNAs, that were used in the screen, revealed that MAP3K4 is required for p21 induction when Aurora B is inhibited (Fig. 3.13). Each of the four individual siRNAs reduced the expression of MAP3K4 and p21 to a similar extent, for which reason off-target effects could be excluded.

MAP3K4 is a MAP3 kinase that is found on top of the stress MAPK signaling cascade and phosphorylates the MAP2 kinases MKK3/6 and MKK4 that in turn activate the stress MAP kinases p38 and JNK, respectively (Takekawa et al., 1997) (see Fig 1.1). Both downstream targets of MAP3K4, p38 and JNK, were activated after Aurora B inhibition, as determined with phospho-specific antibodies (Fig. 3.14). Phosphorylation of p38 and JNK correlated with increased p53 and p21 levels, suggesting that mitotic stress induced by inhibiting Aurora B activates MAP3K4 and the downstream stress kinases.
Using the p38 inhibitor SB202190, that blocks the isoforms p38α and p38β, revealed that p38 is required for p21 activation after Aurora B inhibiton, as expression of p21 was strongly reduced when cells were treated with ZM and SB (Fig. 3.16 A). To address whether p38α

and p38β are both involved in the activation of p21 after ZM treatment, specific siRNAs against these p38 isoforms were used. Interestingly, this assay showed that only p38β, but not p38α, regulates the induction of p21 in response to Aurora B inhibition (Fig. 3.15). As depletion of MAP3K4 prevented p38 phosphorylation after ZM treatment (Fig. 3.16 C), it is assumable that in response to Aurora B inhibition MAP3K4 and p38 actually act in one stress signaling pathway that mediates induction of p21. Involvement of p38 in inducing cell cycle arrest after Aurora B inhibition is consistent with recent findings that showed that the p38 stress kinase is implicated in cell growth arrest of aneuploid cells (Thompson and Compton, 2010).
How the JNK kinase is involved in regulating the downstream pathways after mitotic stress could not be analyzed in more detail since the specific JNK inhibitor SP600125 itself caused cell cycle arrest in G2/M phase (data not shown). This is consistent with studies in different tumor cell lines that demonstrated that SP600125 is implicated in inhibition of proliferation and G2/M arrest (Du et al., 2004; Mingo-Sion et al., 2004).

The mechanism of MAP3K4 activation in response to Aurora B inhibition requires further investigation. In general, MAP3K4 exists in an auto-inhibited state and activation of MAP3K4 is controlled by interaction with other proteins (Bettinger and Amberg, 2007). In unstressed cells the N-terminal autoinhibitory domain of MAP3K4 is bound to its C-terminus thereby inhibiting the C-terminal kinase domain (Miyake et al., 2007).
One protein that has been linked to the activation of MAP3K4 is the stress sensor protein GADD45 (growth arrest and DNA-damage inducible protein) (Takekawa and Saito, 1998). The GADD45 proteins (GADD45 α,-β,-γ) play important roles in cellular stress responses like cell cycle arrest, DNA repair and apoptosis and are induced upon DNA damage or other environmental stress signals (Liebermann and Hoffman, 2008). GADD45 can bind to the N-terminus of MAP3K4 thereby interrupting the N-C interaction and mediating the dimerization of MAP3K4. Dimerization facilitates the autophosphorylation in the kinase domain of MAP3K4 leading to full catalytic activation (Miyake et al., 2007).
It has recently been reported that missegregated chromosomes can be damaged during cytokinesis resulting in DNA double-strand break induced stress response (Janssen et al., 2011). However, in response to mitotic stress caused by Aurora B inhibition no evidence for DNA damage could be provided. In cells treated with the Aurora B inhibitor neither DNA damage positive γ-H2AX foci nor a clear involvement of ATM could be determined (data not shown). Whether GADD45 is induced independently of DNA damage upon Aurora B inhibition and whether it is involved in activation of MAP3K4 needs to be further analyzed.

MAP3K4 activation in response to Aurora B inhibition could also be triggered by other known MAP3K4 interacting proteins, like the scaffold proteins Axin and TRAF4 or the Rho-GTPases Cdc42/Rac. Axin and TRAF4 have been shown to bind the kinase domain of MAP3K4 leading to MAP3K4 oligomerization and activation of p38 and JNK (Abell et al.,

2005, 2007). Axin, a negative regulator of the Wnt signaling pathway, has been reported to be a microtubule-associated protein and to localize to centrosomes and to the mitotic spindle during mitosis (Kim et al., 2009). Conceivably, disruption of the mitotic spindle apparatus due to Aurora B inhibition might be sensed by Axin resulting in MAP3K4 activity.
Cdc42 and Rac are GTPases that are associated with actin cytoskeletal structures and were found to bind to MAP3K4 and to activate downstream MAP kinases (Fanger et al., 1997; Zhang et al., 1995). Cdc42 might also be attributed a role in mitosis, as it was concidered to regulate microtubules attachment to kinetochors (Narumiya and Yasuda, 2006). Thus, it could be speculated that Cdc42 senses either mitotic spindle damage or disruption of the actin cytoskeleton leading to MAP3K4 activation after Aurora B inhibition.
Further investigations are needed to elucidate whether one of these described MAP3K4 interacting proteins functions as signal transducer regulating MAP3K4's activity in response to defective mitosis.

Other possible mechanisms mediating activation of MAP3K4 might be metabolic changes or proteomic stress due to extra chromosomes in aneuploid or polyploid cells after incorrect mitosis.

4.3.2 Regulation of p53 activity by p38 after Aurora B inhibition

After demonstrating that the MAP3K4-p38 pathway is required for p53 mediated p21 upregulation after inhibition of Aurora B (Fig. 3.13, 3.14, 3.15), it was of interest to analyze how p38 regulates the function and activity of p53 and the induction of p21.
It could be shown that phosphorylation, stabilization, nuclear accumulation and promoter binding of p53 occur independently of p38 signaling, whereas the transcriptional activition of p53 target genes requires the activated p38 pathway.

When p38 was inhibited by SB202190 or when either p38β or MAP3K4 were depleted with specific siRNA in addititon to Aurora B inhibition, p21 transactivation was prevented although p53 was still accumulated (Fig. 3.16). These assays indicate that p38 signaling is indeed necessary for p53 activity but not for its stabilization. Therefore, stabilization of p53 seems to be meditated via a second, p38-independent pathway in response to Aurora B inhibition.
p53 is a substrate of JNK, the second stress kinase activated by MAP3K4. It has been reported that JNK phosphorylates p53 leading to increased stabilization and transcriptional activity of p53 in response to different stress stimuli (Buschmann et al., 2001). Even though the direct evidence that phosphorylation of JNK is prevented when MAP3K4 is depleted could not be shown, the fact that p53 is still stabilized upon MAP3K4 depletion (Fig. 3.16 C) might exclude the possibility of JNK stabilizing p53 after Aurora B inhibition.
Instead, stabilization of p53 could even occur directly through inhibition of Aurora B. It

has recently been shown that Aurora B and p53 exist in one complex and that Aurora B can phosphorylate p53 thereby facilitating its ubiquitin dependent degradation (Gully et al., 2012; Wu et al., 2011). Inhibiting the Aurora B function with ZM might therefore lead to accumulation of p53. Another possible p38-independent mechanism triggering the stabilization of p53 might be the disruption of the mitotic spindle apparatus. It is assumable that mitotic proteins sense the spindle damage after Aurora B inhibition leading to p53 stabilization. For instance, the spindle checkpoint protein BubR1 has been proposed to be important for phosphorylation and stability of p53 in response to spindle damage (Ha et al., 2007).

Assays with p53 site- and phosphospecific antibodies revealed that p53 was phosphorylated at all investigated serine residues (Ser15, Ser20, Ser33, Ser37, Ser46 and Ser392) after Aurora B inhibition (Fig. 3.17). This phosphorylation status of p53 was not altered when p38 was inhibited, demonstrating that p38, although it is required for p21 induction (Fig. 3.15, 3.16), does not regulate the activity of p53 by direct phosporylation. This result was unexpected, as it has been reported in several studies that p38 can directly phosphorylate p53 leading to its activation in response to different kinds of stress signals. For instance, p53 is phosphorylated by p38 on Ser33 when cells are exposed to UV light, osmotic shock or chemotherapeutic agents (Bulavin et al., 1999; Kishi et al., 2001; Sanchez-prieto et al., 2000). UV irradiation also leads to p38 mediated phosphorylation of p53 on Ser15, Ser46 and Ser392 (Bulavin et al., 1999; Huang et al., 1999; Keller et al., 1999; She et al., 2000). Furthermore, phosphorylation of Ser37 is facilitated through previous phosphorylation of Ser33 and Ser46 by p38 after UV irradiation (Bulavin et al., 1999). Ser20 of p53 is not phosphorylated by p38 directly but by its downstream target MAPKAPK2 (She et al., 2002). As the assays in the studies mentioned above were performed using p38 inhibitors that target p38α and p38β , it cannot be ruled out that p53 phosphorylation is mediated only by one of these isoforms. The fact that only p38β and not p38α regulates p21 activation after Aurora B inhibition (Fig. 3.15) leads to the assumption that in general phosphorylation of p53 might be mediated by p38α and that p38β *per se* does not phosphorylate p53.
Thus, it seems likely that other stress kinases act in parallel to p38 in order to phosphorylate p53 in response to mitotic failures. These phosphorylations are not sufficient to activate p53 but might rather lead to further stabilization and/or DNA binding of p53. As the nuclear localization as well as the p21 promoter binding of p53 was not influenced by the p38 pathway after inhibition of Aurora B (Fig. 3.19), it can be supposed that p53 is stabilized, translocated to the nucleus and recruited to the p21 promoter by p38 independent pathways.

p38 has been shown to regulate p21 stability through phosphorylation of the RNA binding protein HuR after γ-irradiation (Lafarga et al., 2009). However, in response to Aurora B inhibition the half-life of p21 mRNA was not changed when cells were additionally treated with the p38 inhibitor SB (data not shown). This excluded the possibility of p38 affecting the stability of p21 mRNA when Aurora B is inhibited.

Instead, p38 is required for transcriptional activity of p53 as it could be examined with a p53-responsive reporter assay (Fig. 3.18). Aurora B inhibition resulted in increased activity of a p53 reporter construct and this activity was remarkably impaired when both, Aurora B and p38, were blocked, indicating that transcriptional activity of p53 depends on the p38 signaling pathway upon Aurora B inhibition.
p38 might indirectly regulate the activity of stabilized promoter-bound p53 by targeting one of the transcriptional co-factors of p53 that are required for p53 induced gene expression. The transcriptional co-factor PGC1α could be a possible target of p38 in order to regulate p53 activity after Aurora B inhibition. PGC1α has been shown to bind to p53 and to enhance p53-mediated transactivation of pro-arrest target genes among others of p21 (Sen et al., 2011). p38 can directly phosphorylate PGC1α leading to stabilization and enhanced transcriptional activity of this co-activator (Fan and Rhee, 2004; Puigserver et al., 2001). Whether PGC1α is actually required as co-factor of p53 in the mitotic stress induced pathway remains to be further investigated.

4.3.3 Chromosomal missegregation is sufficient to activate the MAP3K4-p38-p53 pathway upon partial Aurora B inhibition

Complete inhibition of Aurora B with 1 µM ZM resulted in failed cytokinesis with bi- and multinucleated cells and activation of the MAP3K4-p38-p53 pathway in order to induce cell cycle arrest via p21 upregulation (Fig. 3.10, 3.13, 3.16, 3.18).
The complete inhibition of Aurora B's kinase activity was verified by analyzing the phosphorylation status of the Aurora B substrate histone H3 (Fig. 3.21 A). When lower ZM concentrations were used (0.5 µM), Aurora B was only partially blocked and this caused only few binucleated and polyploid cells as compared to complete Aurora B inhibition (Fig. 3.21 B, C). However, in response to partial Aurora B inhibition p53 was stabilized, p38 phosphorylated and p21 upregulated to an extent similar to that observed after complete inhibition of Aurora B (Fig. 3.22 A). Depletion of MAP3K4 and partial inhibition of Aurora B further led to reduced p21 expression levels suggesting that the same MAP3K4-p38-p53 pathway is activated under these conditions (Fig. 3.22 C). Immunofluorescence staining revealed that p21 was not only expressed in binucleated but also in mononucleated cells after partial Aurora B inhibition (Fig. 3.22 B), leading to the assumption that chromosomal missegregation could lead to the activation of the mitotic stress signaling pathway. FISH analysis confirmed this surmise (Fig. 3.23): When Aurora B was partially blocked, cells exhibited a significant increase in the number of chromosomal missegregation for the investigated chromosomes 7 and 8, as compared to untreated cells, indicating that induction of the MAP3K4-p38-p53 pathway is due to these subtle defects occurring in mitosis.

These data reveal that not only tetraploid cells that arise from cytokinesis failure activate

the p53-mediated cell cycle arrest but that also chromosomal missegregation is sufficient to induce the mitotic stress signaling pathway. Thus, these results support the challenge of the existence of an independent 'tetraploidy checkpoint' (Uetake and Sluder, 2004; Wong and Stearns, 2005), that was proposed to monitor chromosome or centrosome number to induce p53 mediated G1 arrest after cytokinesis failure (Andreassen et al., 2001). The results are also consistent with the finding of Thompson and Compton (2010), who reported that missegregation of single chromosomes in diploid cells activates the p53 pathway to induce cell cycle arrest and to limit proliferation of aneuploid cells.

Recent work in our group could show that although Aurora B is already inhibited in interphase, induction of p21 only occurs when cells have passed mitosis (G.Kumari, unpublished data), evidencing that the MAP3K4-p38-p53 pathway is indeed activated by defects in mitosis or cytokinesis.

4.3.4 Consequences of Aurora B and p38 co-inhibition

The essential function of p38 in inducing p53 mediated G1 arrest following defects in mitosis or cytokinesis was further demonstrated with analyses of Aurora B and p38 co-inhibition (Fig. 3.24). When both kinases, Aurora B and p38, were inhibited, cells overcame the G1 arrest resulting in increased polyploidization (Fig. 3.24 A). The inhibition of DNA synthesis in S-phase and the reduced number of cells in mitosis after Aurora B inhibition was restored when p38 signaling was additionally blocked (Fig. 3.24 B, C), indicating that cells continue to proliferate. The progression through the cell cycle observed after co-inhibition of Aurora B and p38 was further confirmed by restored expression of E2F regulated genes, that were found in microarray-analysis to be induced in a p38 dependent manner (Fig. 3.20 C). Expression of G1/S genes (CyclinA, Cdc6, p107) and G2/M genes (CyclinB, Bub1, Birc5) was decreased when cells were treated with the Aurora B inhibitor and repression of these genes was abolished when p38 was inhibited in addition. Repression of E2F target gene induction might by regulated by p38 via activation of the p53-p21 pathway. p21 prevents the release of E2Fs from repressive E2F/pRB complexes by inhibiting cyclin-CDK complexes (Polager and Ginsberg, 2009). When the p38 pathway is blocked, activation of p21 and thus repression of E2F/pRB is prevented, leading to expression of E2F target genes and to further progression through the cell cycle.

The cellular outcome of long term inhibition of Aurora B and p38 was analyzed using colony formation assay (Fig. 3.25). Treatment of cells with 1 μM ZM resulted in nearly complete prevention of colony formation, whereas partial inhibition of Aurora B with 0.5 μM ZM showed only a slight reduction in formation of colonies as compared to the control. Interestingly, combined inhibition of Aurora B and p38 did not augment colony formation although the cells had overcome the G1 arrest (Fig. 3.24). In contrast, co-inhibition resulted in impaired

cell proliferation. This reduced proliferation could be explained by the increased number of apoptotic cells after co-inhibition of Aurora B and p38 (Fig. 3.26). Thus, p38 seems to have an anti-apoptotic function what is consistent with studies reporting that p38 inhibition enhances the apoptotic effect of DNA damaging agents (Cappellini et al., 2005; Kurosu et al., 2005). It is supposable that cells, that overcome the G1 arrest induced by Aurora B inhibition, progress further through the cell cycle and undergo cell death, possibly via mitotic catastrophe, due to severe cellular damage.
The finding of a synergistic effect on cancer cell proliferation with combined inhibition of Aurora B and p38 might provide an approach for cancer therapy. Several Aurora kinase inhibitors have already been tested in preclinical and clinical trials. Although preclinial studies were promising, in clinical studies the effects in patients with solid tumors were not satisfying. Thus, combined therapy of Aurora kinase inhibitors with chemotherapy or other anticancer agents seems to be a more efficient strategy (Boss et al., 2009). The combined treatment with Aurora B and p38 inhibitors might therefore offer a possible way to a more efficient cancer therapy.

4.3.5 MAP3K4-p38-p53 - a common pathway activated after cytokinesis failure?

In order to address whether the MAP3K4-p38-p53 signaling is a common pathway activated after mitosis or cytokinesis failure to induce cell cycle arrest or whether it is only restricted to Aurora B inhibition, a Lin9 depletion assay was performed.

Depletion of Lin9 with specific siRNA in U2OS cells resulted in accumulation of p53 and increased expression of its target p21, which is consistent with findings in senescent Lin9 knockout MEFs (Fig. 3.2, 3.3). Further the MAP3K4 downstream targets p38 and JNK were phosphorylated and activated which makes MAP3K4 likely to be activated in response to Lin9 depletion in order to trigger the p38-p53 pathway. Whether MAP3K4 is actually involved in the stress pathway, that is induced after mitotic failures due to downregulated Lin9, needs to be further investigated with Lin9 and MAP3K4 co-depletion assays.
It is conceivable that mitotic errors due to Lin9 depletion activate the same MAP3K4-p38 pathway as observed upon Aurora B inhibition. Mitotic genes regulated by Lin9/DREAM have functions in chromosome segregation, spindle checkpoint and cytokinesis (Osterloh et al., 2007; Reichert et al., 2010) (Fig. 1.2). Therefore, downregulated expression of Lin9 target genes might cause damage to the mitotic spindle or to the cytoskeleton, that was discussed as a possible trigger for MAP3K4 activation (4.3.1). Altered expression of some Lin9 target genes have been implicated in inducing a p53 responsive cell cycle arrest. For instance, reduced expression of either the spindle checkpoint proteins Bub1 or the centromere

protein CENP-A results in p53 activation (Gjoerup et al., 2007; Maehara et al., 2010), possible due to disruption of the mitotic spindle apparatus.

It can be hypothesized that the MAP3K4-p38-p53 signaling serves as a common pathway that is activated after defects in mitosis or cytokinesis in order to prevent cell cycle progression of aneuploid or polyploid cells.

4.3.6 Model of the mitotic stress induced pathway

The findings of these studies can be summarized in a model of the mitotic stress induced pathway (Fig. 4.1): Partial or complete inhibition of the mitotic kinase Aurora B results in chromosome missegregation or cytokinesis failure. In order to limit the proliferation of aneuploid, a p53 mediated cell cycle arrest is induced. In this process the function of p53 is regulated by two separate pathways: p53 is possibly stabilized by inhibition of Aurora B itself or by damage of the mitotic spindle apparatus. This stabilization event is not sufficient to activate p53 and a second pathway, the MAP kinase signaling pathway MAP3K4-p38, is required for transcriptional activation of p53. MAP3K4 might be activated by mitotic spindle disruption and trigger the signal to p38β. Presumably, p38β targets a transcriptional co-factor of p53 leading to full activity of p53 and induction of p21.
The cell growth arrest induced by these pathways might prevent chromosomal instability and might therefore suppress tumorigenesis.

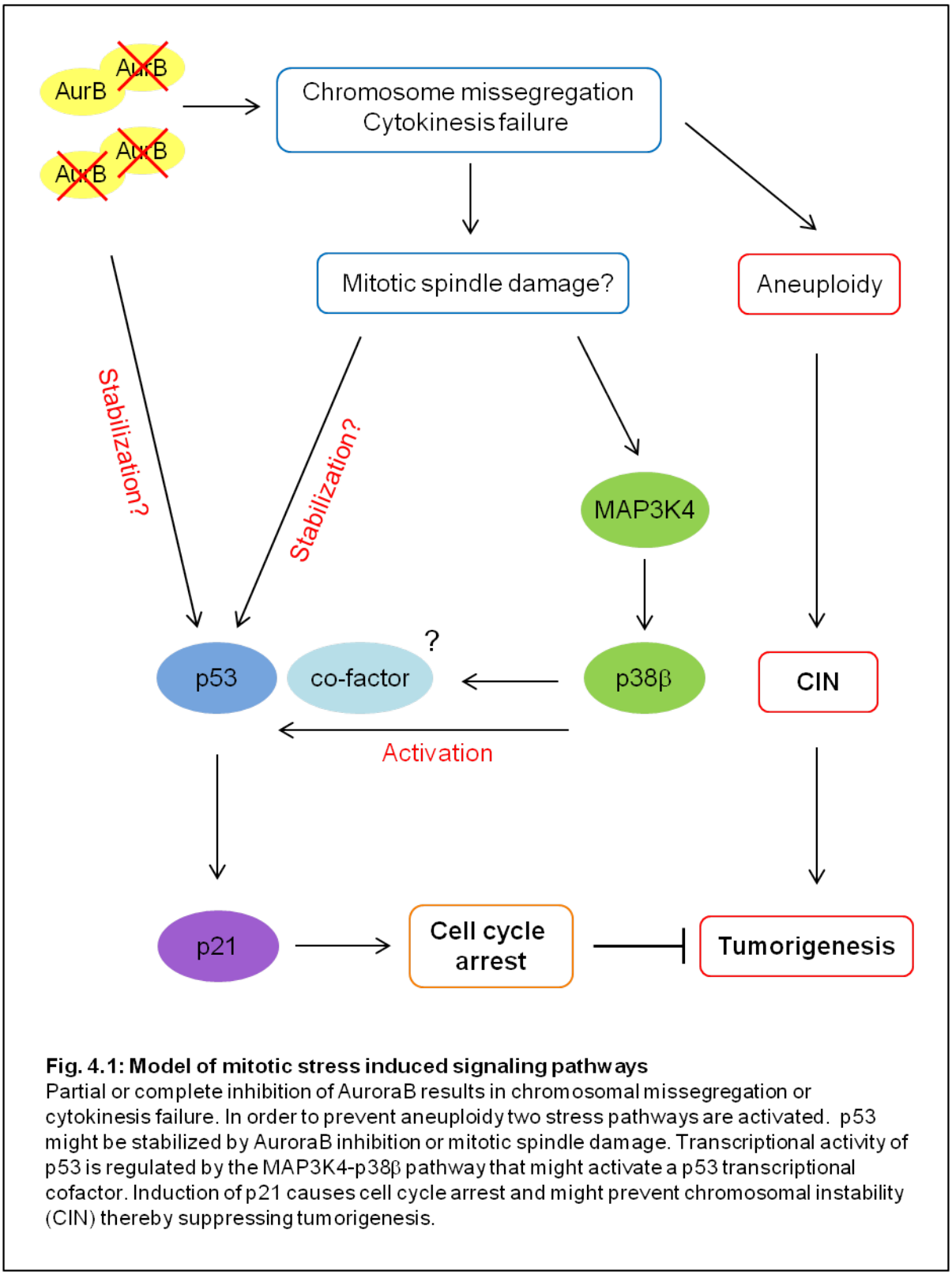

Fig. 4.1: Model of mitotic stress induced signaling pathways
Partial or complete inhibition of AuroraB results in chromosomal missegregation or cytokinesis failure. In order to prevent aneuploidy two stress pathways are activated. p53 might be stabilized by AuroraB inhibition or mitotic spindle damage. Transcriptional activity of p53 is regulated by the MAP3K4-p38β pathway that might activate a p53 transcriptional cofactor. Induction of p21 causes cell cycle arrest and might prevent chromosomal instability (CIN) thereby suppressing tumorigenesis.

5 Summary

Precise control of progression through mitosis is essential to maintain genomic stability and to prevent aneuploidy. The DREAM complex is an important regulator of mitotic gene expression. Depletion of Lin9, one core-subunit of DREAM, leads to reduced expression of G2/M genes and impaired proliferation. In conditional mouse knockout cells (MEFs) Lin9 deletion causes defects in mitosis and cytokinesis and cells undergo premature senescence in order to prevent further proliferation.

In this work it could be shown that the senescence phenotype in Lin9 knockout MEFs is independently mediated by the two tumor suppressor pathways p53-p21 and p16-pRB.
Studies using the conditional Lin9 knockout mouse model demonstrated an important function of Lin9 in the regulation of mitotic gene expression and proliferation *in vivo*. Deletion of Lin9 caused reduced proliferation in the intestinal crypts resulting in atrophy of the intestinal epithelium and in rapid death of the animals.

In the second part of this work, the pathways leading to p53 mediated G1 arrest after failed cytokinesis were analyzed by using a chemical inhibitor of the mitotic kinase Aurora B. In a high throughput siRNA screen the MAP kinase MAP3K4 was identified as an upstream activator of p53. It could be shown that MAP3K4 activates the downstream stress kinase p38β to induce the p53 mediated cell cycle arrest of tetraploid cells. p38β was required for the transcriptional activation of the p53 target gene p21 in response to Aurora B inhibition. In contrast, phosphorylation, stabilization and recruitment of p53 to the p21 promoter occured independently of p38 signaling. Partial inhibition of Aurora B demonstrated that chromosome missegregation also activates the MAP3K4-p38-p53 pathway, suggesting that subtle defects in mitosis are sufficient for inducing this stress signaling pathway. Although p38 was required for the G1 cell cycle arrest after mitotic failures, long-term co-inhibition of p38 and Aurora B resulted in reduced proliferation probably due to increased apoptosis.
Presumably, MAP3K4-p38-p53 signaling is a common pathway that is activated after errors in mitosis or cytokinesis to arrest cells in G1 and to prevent chromosomal instability.

6 Zusammenfassung

Eine genaue Kontrolle des Verlaufs durch die Mitose ist entscheidend für die Gewährleistung genomischer Stabilität und für die Vermeidung von Aneuploidy. Der DREAM Komplex ist ein wichtiger Regulator der Expression von mitotischen Genen. Die Depletion der DREAM-Untereinheit Lin9, führt zu einer verrminderten Expression von G2/M Genen und beeinträchtigt die Proliferation. In konditionellen knockout Mauszellen (MEFs) verursacht das Ausschalten von Lin9 Defekte in Mitose und Zytokinese und löst vorzeitige Seneszenz aus, um eine weitere Zellproliferation zu verhindern.

In dieser Arbeit konnte gezeigt werden, dass der seneszente Phänotyp in Lin9 knockout MEFs unabhängig von den beiden Tumorsuppressor-Signalwegen p53-p21 und p16-pRB induziert wird. Untersuchungen mit dem konditionellen Lin9 knockout Mausmodell verdeutlichten die wichtige Funktion von Lin9 in der Regulierung der mitotischen Genexpression und der Proliferation *in vivo*. Das Fehlen von Lin9 führte zu einer verringerten Proliferation in den Krypten des Dünndarms und verursachte eine Atrophie des Darmepithels und einen schnell eintretenden Tod der Tiere.

Im zweiten Teil der Arbeit wurden Signalwege untersucht, die nach fehlerhafter Zytokinese zu einem p53 vermittelten G1-Arrest führen. Hierfür wurde ein chemischer Inhibitor der mitotischen Kinase Aurora B verwendet. Mit Hilfe eines Hochdurchsatz siRNA Screens wurde die MAP Kinase MAP3K4 als Aktivator des p53 Signalwegs identifiziert. Es konnte gezeigt werden, dass MAP3K4 die Stresskinase p38β aktiviert, um den p53 vermittelten Zellzyklusarrest in tetraploiden Zellen auszulösen. Dabei wurde p38β nach Hemmung von Aurora B für die transkriptionelle Aktivierung des p53 Zielgens p21 benötigt. Im Gegenteil dazu erfolgte die Phosphorylierung, Stabilisierung und die Rekrutierung von p53 an den p21 Promoter unabhängig von p38. Die teilweise Hemmung von Aurora B zeigte, dass fehlerhafte Segregation von Chromosomen auch den MAP3K4-p38-p53 Signalweg aktiviert und lässt darauf schließen, dass subtile Defekte in der Mitose ausreichen diesen Stress-Signalweg zu induzieren. Obwohl p38 für den G1 Zellzyklusarrest nach mitotischen Schäden erforderlich war, führte die gleichzeitige Inhibierung von p38 und Aurora B über einen längeren Zeitraum zu einer verringerten Proliferation, vermutlich aufgrund verstärkter Apoptose.
Es ist anzunehmen, dass der MAP3K4-p38-p53 Signalweg generell nach Defekten in der Mitose oder Zytokinese aktiviert wird um Zellen in G1 zu arretieren und um chromosomale Instabilität zu vermeiden.

7 References

Abell A N, Granger D a and Johnson G L (2007). MEKK4 stimulation of p38 and JNK activity is negatively regulated by GSK3beta. J Biol Chem 282, 30476–84.

Abell A N, Rivera-perez J A, Cuevas B D, Uhlik M T, Sather S, Johnson N L, Minton S K, Lauder J M, Winter-vann A M, Nakamura K, Magnuson T, Vaillancourt R R, Heasley L E and Johnson G L (2005). Ablation of MEKK4 Kinase Activity Causes Neurulation and Skeletal Patterning Defects in the Mouse Embryo. Mol Cell Biol 25, 8948–8959.

Al-Romaih K, Bayani J, Vorobyova J, Karaskova J, Park P, Zielenska M and Squire J (2003). Chromosomal instability in osteosarcoma and its association with centrosome abnormalities. Cancer Genet Cytogenet 144, 91–99.

Alberts B (2002). *Molecular Biology of the Cell, 4th edition*. New York: Garland Science.

Allsopp R C and Harley C B (1995). Evidence for a critical telomere length in senescent human fibroblasts. Exp Cell Res 219, 130–6.

Andreassen P R, Lohez O D, Lacroix F B and Margolis R L (2001). Tetraploid state induces p53-dependent arrest of nontransformed mammalian cells in G1. Mol Biol Cell 12, 1315–28.

Ashcroft M, Taya Y and Vousden K H (2000). Stress signals utilize multiple pathways to stabilize p53. Mol Cell Biol 20, 3224–33.

Baker D J, Jeganathan K B, Cameron J D, Thompson M, Juneja S, Kopecka A, Kumar R, Jenkins R B, de Groen P C, Roche P and van Deursen J M (2004). BubR1 insufficiency causes early onset of aging-associated phenotypes and infertility in mice. Nat Genet 36, 744–9.

Baker D J, Jeganathan K B, Malureanu L, Perez-Terzic C, Terzic A and van Deursen J M a (2006). Early aging-associated phenotypes in Bub3/Rae1 haploinsufficient mice. J Cell Biol 172, 529–40.

Barker N, van de Wetering M and Clevers H (2008). The intestinal stem cell. Genes Dev 22, 1856–64.

Barrett M T, Pritchard D, Palanca-Wessels C, Anderson J, Reid B J and Rabinovitch P S (2003). Molecular phenotype of spontaneously arising 4N (G2-tetraploid) intermediates of neoplastic progression in Barrett's esophagus. Cancer research 63, 4211–7.

Beckerman R and Prives C (2010). Transcriptional regulation by p53. Cold Spring Harb Perspect Biol 2, a000935.

Ben-Porath I and Weinberg R A (2005). The signals and pathways activating cellular senescence. Int J Biochem Cell Biol 37, 961–76.

Bettinger B T and Amberg D C (2007). The MEK kinases MEKK4/Ssk2p facilitate complexity in the stress signaling responses of diverse systems. J Cell Biochem 101, 34–43.

Bode A M and Dong Z (2004). Post-translational modification of p53 in tumorigenesis. Nat Rev Cancer 4, 793–805.

Bode A M and Dong Z (2007). The functional contrariety of JNK. Mol Carcinog 46, 591–8.

Bogoyevitch M a and Kobe B (2006). Uses for JNK: the many and varied substrates of the c-Jun N-terminal kinases. Microbiol Mol Biol Rev 70, 1061–95.

Boss D S, Beijnen J H and Schellens J H M (2009). Clinical experience with aurora kinase inhibitors: a review. Oncologist 14, 780–93.

Boveri T (2008). Concerning the Origin of Malignant Tumours by Theodor Boveri. Translated and annotated by Henry Harris. J Cell Sci 121, 1–84.

Brancho D, Tanaka N, Jaeschke A, Ventura J J, Kelkar N, Tanaka Y, Kyuuma M, Takeshita T, Flavell R A and Davis R J (2003). Mechanism of p38 MAP kinase activation in vivo. Genes Dev 17, 1969–78.

Bulavin D V, Saito S, Hollander M C, Sakaguchi K, Anderson C W, Appella E and Fornace a J (1999). Phosphorylation of human p53 by p38 kinase coordinates N-terminal phosphorylation and apoptosis in response to UV radiation. EMBO J 18, 6845–54.

Buschmann T, Potapova O, Bar-shira A, Ivanov V N, Fuchs S Y, Henderson S, Fried V A, Minamoto T, Alarcon-vargas D, Pincus M R, Gaarde W A, Holbrook N J, Shiloh Y and Ronai Z E E V (2001). Jun NH 2 -Terminal Kinase Phosphorylation of p53 on Thr-81 Is Important for p53 Stabilization and Transcriptional Activities in Response to Stress. Mol Cell Biol 21, 2743–2754.

Cappellini a, Tazzari P L, Mantovani I, Billi a M, Tassi C, Ricci F, Conte R and Martelli a M (2005). Antiapoptotic role of p38 mitogen activated protein kinase in Jurkat T cells and normal human T lymphocytes treated with 8-methoxypsoralen and ultraviolet-A radiation. Apoptosis 10, 141–52.

Carmena M and Earnshaw W C (2003). The cellular geography of aurora kinases. Nat Rev Mol Cell Biol 4, 842–54.

Carnero A and Hannon G (1994). The INK4 family of CDK inhibitors. Cell 78, 59–66.

Castro A, Arlot-Bonnemains Y, Vigneron S, Labbé J C, Prigent C and Lorca T (2002). APC/Fizzy-Related targets Aurora-A kinase for proteolysis. EMBO Rep 3, 457–62.

Chen Q, Fischer A, Reagan J D, Yan L J and Ames B N (1995). Oxidative DNA damage and senescence of human diploid fibroblast cells. Proc Natl Acad Sci USA 92, 4337–41.

Cuenda A and Rousseau S (2007). p38 MAP-kinases pathway regulation, function and role in human diseases. Biochim Biophys Acta 1773, 1358–75.

Cuevas B D, Abell a N and Johnson G L (2007). Role of mitogen-activated protein kinase kinase kinases in signal integration. Oncogene 26, 3159–71.

Dérijard B, Raingeaud J, Barrett T, Wu I H, Han J, Ulevitch R J and Davis R J (1995). Independent human MAP-kinase signal transduction pathways defined by MEK and MKK isoforms. Science 267, 682–5.

Dimri G P (2005). What has senescence got to do with cancer? Cancer cell 7, 505–12.

Dimri G P, Lee X, Basile G, Acosta M, Scott G, Roskelley C, Medrano E E, Linskens M, Rubelj I and Pereira-Smith O (1995). A biomarker that identifies senescent human cells in culture and in aging skin in vivo. Proc Natl Acad Sci USA 92, 9363–7.

Ditchfield C, Johnson V L, Tighe A, Ellston R, Haworth C, Johnson T, Mortlock A, Keen N and Taylor S S (2003). Aurora B couples chromosome alignment with anaphase by targeting BubR1, Mad2, and Cenp-E to kinetochores. J Cell Biol 161, 267–80.

Dreier M R, Grabovich A Z, Katusin J D and Taylor W R (2009). Short and long-term tumor cell responses to Aurora kinase inhibitors. Exp Cell Res 315, 1085–99.

Du L, Lyle C S, Obey T B, Gaarde W a, Muir J a, Bennett B L and Chambers T C (2004). Inhibition of cell proliferation and cell cycle progression by specific inhibition of basal JNK activity: evidence that mitotic Bcl-2 phosphorylation is JNK-independent. J Biol Chem 279, 11957–66.

El-Deiry W S, Tokino T, Velculescu V E, Levy D B, Parsons R, Trent J M, Lin D, Mercer W E, Kinzler K W and Vogelstein B (1993). WAF1, a potential mediator of p53 tumor suppression. Cell 75, 817–25.

Enslen H, Brancho D M and Davis R J (2000). Molecular determinants that mediate selective activation of p38 MAP kinase isoforms. EMBO J 19, 1301–11.

Fan M and Rhee J (2004). Suppression of mitochondrial respiration through recruitment of p160 myb binding protein to PGC-1a: modulation by p38 MAPK. Genes Dev 18, 278–289.

Fang S, Jensen J P, Ludwig R L, Vousden K H and Weissman a M (2000). Mdm2 is a RING finger-dependent ubiquitin protein ligase for itself and p53. J Biol Chem 275, 8945–51.

Fanger G R, Johnson N L and Johnson G L (1997). MEK kinases are regulated by EGF and selectively interact with Rac/Cdc42. EMBO J 16, 4961–72.

Fu J, Bian M, Jiang Q and Zhang C (2007). Roles of Aurora kinases in mitosis and tumorigenesis. Mol Cancer Res 5, 1–10.

Ganem N J and Pellman D (2007). Limiting the proliferation of polyploid cells. Cell 131, 437–40.

Ganem N J, Storchova Z and Pellman D (2007). Tetraploidy, aneuploidy and cancer. Curr Opin Genet Dev 17, 157–62.

Gautschi O, Heighway J, Mack P C, Purnell P R, Lara P N and Gandara D R (2008). Aurora kinases as anticancer drug targets. Clin Cancer Res 14, 1639–48.

Girard F, Strausfeld U, Fernandez a and Lamb N J (1991). Cyclin A is required for the onset of DNA replication in mammalian fibroblasts. Cell 67, 1169–79.

Girdler F, Gascoigne K E, Eyers P a, Hartmuth S, Crafter C, Foote K M, Keen N J and Taylor S S (2006). Validating Aurora B as an anti-cancer drug target. J C 119, 3664–75.

Gisselsson D, Hå kanson U, Stoller P, Marti D, Jin Y, Rosengren A H, Stewénius Y, Kahl F and Panagopoulos I (2008). When the genome plays dice: circumvention of the spindle assembly checkpoint and near-random chromosome segregation in multipolar cancer cell mitoses. PloS One 3, e1871.

Gizatullin F, Yao Y, Kung V, Harding M W, Loda M and Shapiro G I (2006). The Aurora kinase inhibitor VX-680 induces endoreduplication and apoptosis preferentially in cells with compromised p53-dependent postmitotic checkpoint function. Cancer Res 66, 7668–77.

Gjoerup O V, Wu J, Chandler-Militello D, Williams G L, Zhao J, Schaffhausen B, Jat P S and Roberts T M (2007). Surveillance mechanism linking Bub1 loss to the p53 pathway. Proc Natl Acad Sci USA 104, 8334–9.

Glotzer M (2003). Cytokinesis: progress on all fronts. Curr Opin Cell Biol 15, 684–690.

Gully C P, Velazquez-Torres G, Shin J H, Fuentes-Mattei E, Wang E, Carlock C, Chen J, Rothenberg D, Adams H P, Choi H H, Guma S, Phan L, Chou P C, Su C H, Zhang F, Chen J S, Yang T Y, Yeung S C J and Lee M H (2012). Aurora B kinase phosphorylates and instigates degradation of p53. Proc Natl Acad Sci USA 109, 1513–1522.

Ha G H, Baek K H, Kim H S, Jeong S J, Kim C M, McKeon F and Lee C W (2007). p53 activation in response to mitotic spindle damage requires signaling via BubR1-mediated phosphorylation. Cancer Res 67, 7155–64.

Han J, Lee J D, Jiang Y, Li Z, Feng L and Ulevitch R J (1996). Characterization of the structure and function of a novel MAP kinase kinase (MKK6). J Biol Chem 271, 2886–91.

Harper J W, Elledge S J, Keyomarsi K, Dynlacht B, Tsai L h, Zhang P, Dobrowolski S, Bai C, Connell-crowley L, Swindell E, Fox M P and Wei N (1995). Inhibition of Cyclin-dependent Kinases by p21. Mol Cell Biol 6, 387–400.

Harrison M M, Ceol C J, Lu X and Horvitz H R (2006). Some C. elegans class B synthetic multivulva proteins encode a conserved LIN-35 Rb-containing complex distinct from a NuRD-like complex. Proc Natl Acad Sci USA 103, 16782–7.

Hartwell L H and Weinert T a (1989). Checkpoints: controls that ensure the order of cell cycle events. Science 246, 629–34.

Haruki N, Harano T, Masuda A, Kiyono T, Takahashi T, Tatematsu Y, Shimizu S, Mitsudomi T, Konishi H, Osada H and Fujii Y (2001). Persistent increase in chromosome instability in lung cancer: possible indirect involvement of p53 inactivation. Am J Pathol 159, 1345–52.

Hauf S, Cole R W, LaTerra S, Zimmer C, Schnapp G, Walter R, Heckel A, van Meel J, Rieder C L and Peters J M (2003). The small molecule Hesperadin reveals a role for Aurora B in correcting kinetochore-microtubule attachment and in maintaining the spindle assembly checkpoint. J Cell Biol 161, 281–94.

Hommes D W, Peppelenbosch M P and van Deventer S J H (2003). Mitogen activated protein (MAP) kinase signal transduction pathways and novel anti-inflammatory targets. Gut 52, 144–51.

Horn H F and Vousden K H (2007). Coping with stress: multiple ways to activate p53. Oncogene 26, 1306–16.

Howman E V, Fowler K J, Newson a J, Redward S, MacDonald a C, Kalitsis P and Choo K H (2000). Early disruption of centromeric chromatin organization in centromere protein A (Cenpa) null mice. Proc Natl Acad Sci USA 97, 1148–53.

Huang C, Ma W Y, Maxiner A, Sun Y and Dong Z (1999). p38 kinase mediates UV-induced phosphorylation of p53 protein at serine 389. J Biol Chem 274, 12229–35.

Hunter T and Pinest J (1994). Cyclins and Cancer II : Cyclin D and CDK Inhibitors Come of Age. Cell 79, 573–582.

Isfort R J, Cody D B, Lovell G and Doersen C J (1995). Analysis of oncogenes, tumor suppressor genes, autocrine growth-factor production, and differentiation state of human osteosarcoma cell lines. Mol Carcinog 14, 170–8.

Itahana K, Campisi J and Dimri G P (2004). Mechanisms of cellular senescence in human and mouse cells. Biogerontology 5, 1–10.

Iwanaga Y, Chi Y H, Miyazato A, Sheleg S, Haller K, Peloponese J M, Li Y, Ward J M, Benezra R and Jeang K T (2007). Heterozygous deletion of mitotic arrest-deficient protein 1 (MAD1) increases the incidence of tumors in mice. Cancer Res 67, 160–6.

Janssen A, Burg M V D, Szuhai K and Kops G J P L (2011). Chromosome Segregation Errors as a Cause of DNA Damage and Structural. Science 333, 1895–1898.

Jiang Y (1997). Characterization of the Structure and Function of the Fourth Member of p38 Group Mitogen-activated Protein Kinases, p38delta. J Biol Chem 272, 30122–30128.

Johnson D G and Walker C L (1999). Cyclins and cell cycle checkpoints. Annu Rev Pharmacol Toxicol 39, 295–312.

Kamb A (1998). Cyclin-dependent kinase inhibitors and human cancer. Curr Top Microbiol Immunol 227, 139–48.

Kang J and Yu H (2009). Kinase signaling in the spindle checkpoint. J Biol Chem 284, 15359–63.

Kastan M B and Bartek J (2004). Cell-cycle checkpoints and cancer. Nature 432, 316–23.

Katayama H, Brinkley W R and Sen S (2003). The Aurora kinases: role in cell transformation and tumorigenesis. Cancer Metastasis Rev 22, 451–64.

Katayama H and Sen S (2010). Aurora kinase inhibitors as anticancer molecules. Biochim Biophys Acta 1799, 829–39.

Keesler G A, Bray J, Hunt J, Johnson D A, Gleason T, Yao Z, Wang S W, Parker C, Yamane H, Cole C and Lichenstein H S (1998). Purification and activation of recombinant p38 isoforms alpha, beta, gamma, and delta. Protein Expression Purif 14, 221–8.

Keller D, Zeng X, Li X, Kapoor M, Iordanov M S, Taya Y, Lozano G, Magun B and Lu H (1999). The p38MAPK inhibitor SB203580 alleviates ultraviolet-induced phosphorylation at serine 389 but not serine 15 and activation of p53. Biochem Biophys Res Commun 261, 464–71.

Kierstead T D and Tevethia M J (1993). Association of p53 binding and immortalization of primary C57BL/6 mouse embryo fibroblasts by using simian virus 40 T-antigen mutants bearing internal overlapping deletion mutations. J Virol 67, 1817–29.

Kim S M, Choi E J, Song K J, Kim S, Seo E, Jho E H and Kee S H (2009). Axin localizes to mitotic spindles and centrosomes in mitotic cells. Exp Cell Res 315, 943–54.

King R W, Jackson P K and Kirschner M W (1994). Mitosis in Transition Review. Cell 79, 563–571.

Kishi H, Nakagawa K, Matsumoto M, Suga M, Ando M, Taya Y and Yamaizumi M (2001). Osmotic shock induces G1 arrest through p53 phosphorylation at Ser33 by activated p38MAPK without phosphorylation at Ser15 and Ser20. J Biol Chem 276, 39115–22.

Kleinschmidt M a, Wagner T U, Liedtke D, Spahr S, Samans B and Gaubatz S (2009). Lin9 Is Required for Mitosis and Cell Survival During Early Zebrafish Development. J Biol Chem 284, 13119–27.

Korenjak M, Taylor-Harding B, Binné U K, Satterlee J S, Stevaux O, Aasland R, White-Cooper H, Dyson N and Brehm A (2004). Native E2F/RBF complexes contain Myb-interacting proteins and repress transcription of developmentally controlled E2F target genes. Cell 119, 181–93.

Krimpenfort P, Quon K C, Mooi W J, Loonstra A and Berns A (2001). Loss of p16Ink4a confers susceptibility to metastatic melanoma in mice. Nature 413, 83–6.

Kruse J P and Gu W (2009). Modes of p53 regulation. Cell 137, 609–22.

Kuilman T, Michaloglou C, Mooi W J and Peeper D S (2010). The essence of senescence. Genes Dev 24, 2463–79.

Kurosu T, Takahashi Y, Fukuda T, Koyama T, Miki T and Miura O (2005). p38 MAP kinase plays a role in G2 checkpoint activation and inhibits apoptosis of human B cell lymphoma cells treated with etoposide. Apoptosis 10, 1111–20.

Kyriakis J M and Avruch J (2001). Mammalian mitogen-activated protein kinase signal transduction pathways activated by stress and inflammation. Physiol Rev 81, 807–69.

Lafarga V, Cuadrado A, Lopez de Silanes I, Bengoechea R, Fernandez-Capetillo O and Nebreda A R (2009). p38 Mitogen-activated protein kinase- and HuR-dependent stabilization of p21(Cip1) mRNA mediates the G1/S checkpoint. Mol Cell Biol 29, 4341–51.

Lanni J S and Jacks T (1998). Characterization of the p53-Dependent Postmitotic Checkpoint following Spindle Disruption. Mol Cell Biol 18, 1055–1064.

Lavin M F and Gueven N (2006). The complexity of p53 stabilization and activation. Cell Death Differ 53, 941–950.

Lawler S, Fleming Y, Goedert M and Cohen P (1998). Synergistic activation of SAPK1/JNK1 by two MAP kinase kinases in vitro. Current Biology 8, 1387–1391.

Lee H, Lee D J, Oh S P, Park H D, Nam H H, Kim J M and Lim D S (2006). Mouse emi1 has an essential function in mitotic progression during early embryogenesis. Mol Cell Biol 26, 5373–81.

Lee M H, Reynisdottir I and Massague J (1995). Cloning of p57KIP2, a cyclin-dependent kinase inhibitor with unique domain structure and tissue distribution. Genes Dev 9, 639–649.

Lee W H, Bookstein R, Hong F, Young L J, Shew J Y and Lee E Y (1987). Human retinoblastoma susceptibility gene: cloning, identification, and sequence. Science 235, 1394–9.

Lees E (1995). Cyclin dependent kinase regulation. Curr Opin Cell Biol 7, 773–780.

Lengauer C (1997). Genetic instability in colorectal cancer. Nature 386, 623–627.

Lewis P W, Beall E L, Fleischer T C, Georlette D, Link A J and Botchan M R (2004). Identification of a Drosophila Myb-E2F2/RBF transcriptional repressor complex. Genes Dev 18, 2929–40.

Li M, Jung A, Ganswindt U, Marini P, Friedl A, Daniel P T, Lauber K, Jendrossek V and Belka C (2010). Aurora kinase inhibitor ZM447439 induces apoptosis via mitochondrial pathways. Biochem Pharmacol 79, 122–9.

Liebermann D a and Hoffman B (2008). Gadd45 in stress signaling. J Mol Signal 3, 15.

Lindström M S and Nistér M (2010). Silencing of ribosomal protein S9 elicits a multitude of cellular responses inhibiting the growth of cancer cells subsequent to p53 activation. PloS One 5, e9578.

Lingle W L, Barrett S L, Negron V C, D'Assoro A B, Boeneman K, Liu W, Whitehead C M, Reynolds C and Salisbury J L (2002). Centrosome amplification drives chromosomal instability in breast tumor development. Proc Natl Acad Sci USA 99, 1978–83.

Litovchick L, Florens L a, Swanson S K, Washburn M P and DeCaprio J a (2011). DYRK1A protein kinase promotes quiescence and senescence through DREAM complex assembly. Genes Dev 25, 801–13.

Litovchick L, Sadasivam S, Florens L, Zhu X, Swanson S K, Velmurugan S, Chen R, Washburn M P, Liu X S and DeCaprio J a (2007). Evolutionarily conserved multisubunit RBL2/p130 and E2F4 protein complex represses human cell cycle-dependent genes in quiescence. Mol Cell 26, 539–51.

Lu L Y, Wood J L, Minter-Dykhouse K, Ye L, Saunders T L, Yu X and Chen J (2008). Polo-like kinase 1 is essential for early embryonic development and tumor suppression. Mol Cell Biol 28, 6870–6.

Maehara K, Takahashi K and Saitoh S (2010). CENP-A reduction induces a p53-dependent cellular senescence response to protect cells from executing defective mitoses. Mol Cell Biol 30, 2090–104.

Michel L S, Liberal V, Chatterjee A, Kirchwegger R, Paschek B, Gerald W, Dobles M, Sorger P K, Murty V V V S and Benezra R (2001). MAD2 haplo-insufficiency causes premature anaphase and chromosome instability in mammalian cells. Nature 409, 355–359.

Miller C W, Aslo A, Campbell M J, Kawamata N, Lampkin B C and Koeffler H P (1996). Alterations of the p15, p16,and p18 genes in osteosarcoma. Cancer Genet Cytogenet 86, 136–42.

Mingo-Sion A M, Marietta P M, Koller E, Wolf D M and Van Den Berg C L (2004). Inhibition of JNK reduces G2/M transit independent of p53, leading to endoreduplication, decreased proliferation, and apoptosis in breast cancer cells. Oncogene 23, 596–604.

Miyake Z, Takekawa M, Ge Q and Saito H (2007). Activation of MTK1/MEKK4 by GADD45 through induced N-C dissociation and dimerization-mediated trans autophosphorylation of the MTK1 kinase domain. Mol Cell Biol 27, 2765–76.

Moll U M and Petrenko O (2003). The MDM2-p53 interaction. Mol Cancer Res 1, 1001–8.

Morgan D O (1997). CYCLIN-DEPENDENT KINASES : Engines , Clocks , and Microprocessors. Ann Rev Cell Dev Biol 13, 261–91.

Murray-Zmijewski F, Slee E A and Lu X (2008). A complex barcode underlies the heterogeneous response of p53 to stress. Nat Rev Mol Cell Biol 9, 702–12.

Musacchio A and Hardwick K G (2002). The spindle checkpoint: structural insights into dynamic signalling. Nat Rev Mol Cell Biol 3, 731–41.

Narumiya S and Yasuda S (2006). Rho GTPases in animal cell mitosis. Curr Opin Cell Biol 18, 199–205.

Nguyen H, Chinnappan D and Urano T (2005). Mechanism of Aurora-B degradation and its dependency on intact KEN and A-boxes: identification of an aneuploidy-promoting property. Mol Cell Biol 25, 4977–4992.

Niforou K M, Anagnostopoulos A K, Vougas K, Kittas C, Gorgoulis V G and Tsangaris G T (2008). The proteome profile of the human osteosarcoma U2OS cell line. Cancer Genomics Proteomics 5, 63–78.

Ohtsubo M, Theodoras a M, Schumacher J, Roberts J M and Pagano M (1995). Human cyclin E, a nuclear protein essential for the G1-to-S phase transition. Mol Cell Biol 15, 2612–24.

Olaharski A J, Sotelo R, Solorza-Luna G, Gonsebatt M E, Guzman P, Mohar A and Eastmond D a (2006). Tetraploidy and chromosomal instability are early events during cervical carcinogenesis. Carcinogenesis 27, 337–43.

Ono K and Han J (2000). The p38 signal transduction pathway: activation and function. Cell Signal 12, 1–13.

Osterloh L, von Eyss B, Schmit F, Rein L, Hübner D, Samans B, Hauser S and Gaubatz S (2007). The human synMuv-like protein LIN-9 is required for transcription of G2/M genes and for entry into mitosis. EMBO J 26, 144–57.

Pan Z Q, Reardon J T, Li L, Flores-Rozas H, Legerski R, Sancar A and Hurwitz J (1995). Inhibition of nucleotide excision repair by the cyclin-dependent kinase inhibitor p21. J Biol Chem 270, 22008–16.

Pearson G, Robinson F, Beers Gibson T, Xu B E, Karandikar M, Berman K and Cobb M H (2001). Mitogen-activated protein (MAP) kinase pathways: regulation and physiological functions. Endocr Rev 22, 153–83.

Pilkinton M, Sandoval R, Song J, Ness S a and Colamonici O R (2007). Mip/LIN-9 regulates the expression of B-Myb and the induction of cyclin A, cyclin B, and CDK1. J Biol Chem 282, 168–75.

Planas-Silva M D and Weinberg R a (1997). The restriction point and control of cell proliferation. Curr Opin Cell Biol 9, 768–72.

Polager S and Ginsberg D (2009). p53 and E2f: partners in life and death. Nat Rev Cancer 9, 738–48.

Puigserver P, Rhee J, Lin J and Wu Z (2001). Cytokine stimulation of energy expenditure through p38 MAP kinase activation of PPAR coactivator-1. Mol Cell 8, 971–982.

Rajagopalan H and Lengauer C (2004). Aneuploidy and cancer. Nature 432, 338–41.

Reichert N, Wurster S, Ulrich T, Schmitt K, Hauser S, Probst L, Götz R, Ceteci F, Moll R, Rapp U and Gaubatz S (2010). Lin9, a subunit of the mammalian DREAM complex, is essential for embryonic development, for survival of adult mice, and for tumor suppression. Mol Cell Biol 30, 2896–908.

Riley T, Sontag E, Chen P and Levine A (2008). Transcriptional control of human p53-regulated genes. Nat Rev Mol Cell Biol 9, 402–12.

Ruchaud S, Carmena M and Earnshaw W C (2007). Chromosomal passengers: conducting cell division. Nat Rev Mol Cell Biol 8, 798–812.

Sancar A, Lindsey-Boltz L a, Unsal-Kaçmaz K and Linn S (2004). Molecular mechanisms of mammalian DNA repair and the DNA damage checkpoints. Annu Rev Biochem 73, 39–85.

Sánchez I and Dynlacht B D (2005). New insights into cyclins, CDKs, and cell cycle control. Semin Cell Dev Biol 16, 311–21.

Sanchez-prieto R, Rojas J M and Taya Y (2000). A Role for the p38 Mitogen-activated Protein Kinase Pathway in the Transcriptional Activation of p53 on Genotoxic Stress by Chemotherapeutic Agents. Cancer Res 60, 2464–2472.

Saunders W (2005). Centrosomal amplification and spindle multipolarity in cancer cells. Semin Cancer Biol 15, 25–32.

Schliekelman M, Cowley D O, O'Quinn R, Oliver T G, Lu L, Salmon E D and Van Dyke T (2009). Impaired Bub1 function in vivo compromises tension-dependent checkpoint function leading to aneuploidy and tumorigenesis. Cancer Res 69, 45–54.

Schmit F, Mannefeld M, Schmitt K, Franke C, Hänel F, Brehm A and Gaubatz S (2007). LINC , a Human Complex That is Related to pRB-Containing Complexes RIB. Cell Cycle 6, 1903–1913.

Sen N, Satija Y K and Das S (2011). PGC-1α, a key modulator of p53, promotes cell survival upon metabolic stress. Mol Cell 44, 621–34.

Serrano M, Lin A W, Mccurrach M E, Beach D and Lowe S W (1997). Oncogenic ras Provokes Premature Cell Senescence Associated with Accumulation of p53 and p16 INK4a. Cell 88, 593–602.

She Q B, Chen N and Dong Z (2000). ERKs and p38 kinase phosphorylate p53 protein at serine 15 in response to UV radiation. J Biol Chem 275, 20444–9.

She Q B, Ma W Y and Dong Z (2002). Role of MAP kinases in UVB-induced phosphorylation of p53 at serine 20. Oncogene 21, 1580–9.

Sherr C J (1996). Cancer Cell Cycles. Science 3788, 1672–1677.

Skop A R, Liu H, Yates J, Meyer B J and Heald R (2004). Dissection of the mammalian midbody proteome reveals conserved cytokinesis mechanisms. Science 305, 61–6.

Steigemann P, Wurzenberger C, Schmitz M H a, Held M, Guizetti J, Maar S and Gerlich D W (2009). Aurora B-mediated abscission checkpoint protects against tetraploidization. Cell 136, 473–84.

Stevaux O and Dyson N J (2002). A revised picture of the E2F transcriptional network and RB function. Curr Opin Cell Biol 14, 684–691.

Storchová Z, Breneman A, Cande J, Dunn J, Burbank K, O'Toole E and Pellman D (2006). Genome-wide genetic analysis of polyploidy in yeast. Nature 443, 541–7.

Storchova Z and Pellman D (2004). From polyploidy to aneuploidy, genome instability and cancer. Nat Rev Cancer 5, 45–54.

Stubdal H, Zalvide J, Campbell K S, Schweitzer C, Roberts T M and DeCaprio J a (1997). Inactivation of pRB-related proteins p130 and p107 mediated by the J domain of simian virus 40 large T antigen. Mol Cell Biol 17, 4979–90.

Stukenberg P T (2004). Triggering p53 after cytokinesis failure. J Cell Biol 165, 607–8.

Takekawa M, Posas F and Saito H (1997). A human homolog of the yeast Ssk2/Ssk22 MAP kinase kinase kinases, MTK1, mediates stress-induced activation of the p38 and JNK pathways. EMBO J 16, 4973–82.

Takekawa M and Saito H (1998). A family of stress-inducible GADD45-like proteins mediate activation of the stress-responsive MTK1/MEKK4 MAPKKK. Cell 95, 521–30.

Thompson S L, Bakhoum S F and Compton D a (2010). Mechanisms of chromosomal instability. Curr Biol 20, R285–95.

Thompson S L and Compton D a (2010). Proliferation of aneuploid human cells is limited by a p53-dependent mechanism. J Cell Biol 188, 369–81.

Trimarchi J M and Lees J a (2002). Sibling rivalry in the E2F family. Nat Rev Mol Cell Biol 3, 11–20.

Uetake Y and Sluder G (2004). Cell cycle progression after cleavage failure: mammalian somatic cells do not possess a "tetraploidy checkpoint". J Cell Biol 165, 609–15.

Vader G and Lens S M A (2008). The Aurora kinase family in cell division and cancer. Biochim Biophys Acta 1786, 60–72.

Vader G, Medema R H and Lens S M A (2006). The chromosomal passenger complex: guiding Aurora-B through mitosis. J Cell Biol 173, 833–7.

Vermeulen K, Van Bockstaele D R and Berneman Z N (2003). The cell cycle: a review of regulation, deregulation and therapeutic targets in cancer. Cell Prolif 36, 131–49.

Vogelstein B, Lane D and Levine A J (2000). Surfing the p53 network. Nature 408, 307–10.

Vousden K H and Lu X (2002). Live or let die: the cell's response to p53. Nat Rev Cancer 2, 594–604.

Wälchli S, Skanland S S, Gregers T F, Lauvrak S U, Torgersen M L, Ying M, Kuroda S and Sandvig K (2008). The Mitogen-activated Protein Kinase p38 Links Shiga Toxin-dependent Signaling and Trafficking Se. Mol Biol Cell 19, 95–104.

Weaver B a a and Cleveland D W (2006). Does aneuploidy cause cancer? Curr Opin Cell Biol 18, 658–67.

Weaver B A A and Cleveland D W (2009). The role of aneuploidy in promoting and suppressing tumors. J Cell Biol 185, 935–7.

Wei W, Herbig U, Wei S, Dutriaux A and Sedivy J M (2003). scientific report. EMBO Rep 4, 1061–1066.

Wong C and Stearns T (2005). Mammalian cells lack checkpoints for tetraploidy, aberrant centrosome number, and cytokinesis failure. BMC Cell Biol 6, 6.

Wu L, Ma C a, Zhao Y and Jain A (2011). Aurora B interacts with NIR-p53, leading to p53 phosphorylation in its DNA-binding domain and subsequent functional suppression. J Biol Chem 286, 2236–44.

Yang K, Li S, Chang C and Tang C (2010). Aurora-C kinase deficiency causes cytokinesis failure in meiosis I and production of large polyploid oocytes in mice. Mol Biol Cell 21, 2371–2383.

Ye X, Zerlanko B, Zhang R, Somaiah N, Lipinski M, Salomoni P and Adams P D (2007). Definition of pRB- and p53-dependent and -independent steps in HIRA/ASF1a-mediated formation of senescence-associated heterochromatin foci. Mol Cell Biol 27, 2452–65.

Yoon D S, Wersto R P, Zhou W, Chrest F J, Garrett E S, Kwon T K and Gabrielson E (2002). Variable levels of chromosomal instability and mitotic spindle checkpoint defects in breast cancer. Am J Pathol 161, 391–7.

Yu H (2002). Regulation of APC-Cdc20 by the spindle checkpoint. Curr Opin Cell Biol 14, 706–14.

Zachariae W (1999). Progression into and out of mitosis. Curr Opin Cell Biol 11, 708–16.

Zarubin T and Han J (2005). Activation and signaling of the p38 MAP kinase pathway. Cell Res 15, 11–8.

Zhang H (2007). Molecular signaling and genetic pathways of senescence: Its role in tumorigenesis and aging. J Cell Physiol 210, 567–74.

Zhang S, Han J, Ann M, Chernoffe J, Knaus U G, Ulevitch R J and Bokoch G M (1995). Rho Family GTPases Regulate p38 Mitogen-activated Protein Kinase through the Downstream Mediator Pak1. J Biol Chem 10, 23934–23936.

8 Appendix

8.1 List of Figures

8.2 Abbreviations

APC/C	Anaphase promoting complex/Cyclosome
APS	Ammonium persulfate
bp	base pairs
BSA	Bovine serum albumine
CDK	Cyclin dependent kinase
ChIP	Chromotin immunoprecipitation
DMSO	Dimethylsuloxyde
DNA	Deoxyribonucleotide acid
dNTP	Deoxyribonucleeotide triphosphate
dpi	days post injection
DREAM	DP, RB-like, E2F and MuvB complex
ECL	Enhanced chemiluminescence
EDTA	Ethylendiaminetetraacetic acid
ESB	Electrophoresis sample buffer
FACS	Fluorescence-associated cell sorting
FCS	Fetal calf serum
Fig.	Figure
G0,G1,G2	Gap phases
GAPDH	Glyceraldehyde-3-phosphate dehydrogenase
h	hours
H&E	Haemotoxylin & Eosin
HRP	Horseradish peroxydase
IF	Immunofluorescence
i.p.	intraperitoneal injection
kDa	kiloDalton
LINC	LIN complex
MAPK	Mitogen-activated protein kinase
M phase	Mitosis and cytokinesis
NP-40	Nonylphenoxylpolyethoxyl- ethanol
0/N	over night
4-OHT	4-Hydroxytamoxifen
PBS	Phosphate buffer saline
PFA	Paraformaldehyde
PH3	Phosphorylated histone H3 (ser10)
PI	Protease inhibitor
	Propidium iodide
shRNA	short hairpin RNA

siRNA	small interfering RNA
rpm	Revolutions per minute
RT	Reverse transcription
	Room temperature
SCS	Sodium dodecyl phosphate
TAE	Tris-acetate-EDTA
TBS	Tris-buffered saline
WB	Western blot
wt	wilde type

8.3 Own Publications

submitted	Ulrich T, Kumari G, Günster R, Krause M, Finkernagel F and Gaubatz S. p53 mediated cell cycle arrest in response to Aurora B inhibition requires signaling through MAP3K4 and p38β.
2011	Hauser S, Ulrich T, Wurster S, Schmitt K, Reichert N and Gaubatz S. Loss of LIN9, a member of the DREAM complex, cooperates with SV40 large T antigen to induce genomic instability and anchorage-independent growth. Oncogene April 2011; 31(14): 185968.
2010	Reichert N, Wurster S, Ulrich T, Schmitt K, Hauser S, Probst L, Götz R, Ceteci F, Moll R, Rapp U and Gaubatz S. LIN9, a subunit of the mammalian DREAM complex is essential for embryonic development, for survival of adult mice and for tumor suppression. Molecular and Cellular Biology 2010 June; 30(12): 2896-908.

Conference attribution (Talks & Posters)

13.-15.02.2012	Retreat of the Integrated Graduate College of the SFB Transregio 17, Schöntal *Talk:* Mitotic segregation defects activate the MAP3K4-p38-p53 pathway to induce cell cycle arrest
10.-13.04.2011	Joint meeting of SFB Transregio 17 & LOEWE *Poster:* Ulrich T, Hauser S, Reichert N, Spahr S, Gaubatz S. Loss of Lin9 causes senescence and aneuploidy in vitro and results in atrophy of the mouse intestinal epithelium
06.-08.10.2010	Meeting The Puzzling World of Cancer,Integrated Graduate College of the SFB Transregio 17, Würzburg *Poster:* Ulrich T, Gaubatz S. LIN9 is essential for proliferation in the intestinal epithelium
01.-04-04-2009:	Meeting of the SFB Transregio 17, Beilengries *Talk:* Mouse models to analyze the role of LIN-9 in differentiation and tumorigenesis

8.4 Lebenslauf

8.5 Danksagung

Zunächst möchte ich mich herzlichst bei Prof. Dr. Stefan Gaubatz für die Betreuung meiner Doktorarbeit bedanken. Vielen Dank für die wissenschaftliche Unterstützung und die hilfreichen Diskussionen, die zum Gelingen meiner Doktorarbeit beigetragen haben.

Außerdem danke ich den Mitgliedern meines Thesis Committees, Prof. Dr. Thorsten Stiewe und Dr. Daniel Murphy, die mich mit hilfreichen Vorschlägen zu meiner Arbeit unterstützt haben.

Ich danke Prof. Dr. Georg Krohne vielmals für die kurzfristige und unkomplizierte Übernahme des Zweitgutachtens.

Dr. Michael Krause aus dem IMT in Marburg möchte ich für die Auswertung des siRNA Screens und die Durchführung des Microarrays danken. Auch danke ich Florian Finkernagel aus dem IMT in Marburg für die Microarray-Auswertung.

Herzlichen Dank an alle aktuellen und ehemaligen Kollegen aus meiner Arbeitsgruppe für die nette Arbeitsatmosphäre und Unterstützung im Labor: Jasmina Esterlechner, Piero Ocone, Marc Fackler, Fabian Iltsche, Patrick Wolter, Geeta Kumari, Susi Spahr, Adelgunde Wolpert, Steffi Hauser, Nina Reichert, Mirijam Mannefeld, Kathrin Schmitt, Leona Probst und Regina Günster. Insbesondere möchte ich mich bei Susi für ihre Hilfe beim Mausprojekt, Jasmina für das Korrekturlesen dieser Arbeit und Regina für ihre Vorversuche für das Screen-Projekt bedanken.
Außerdem möchte ich mich bei allen Kollegen aus der PCI, EBC und PCII für ihre Unterstützung und Hilfe bedanken. Hierbei danke ich besonders Katrin Wiese für das Korrekturlesen dieser Arbeit.

Im Besonderen möchte ich mich bei meinen Eltern und meinen Schwestern bedanken, die mich immer unterstützt und ermutigt haben. Meinem Freund Philipp danke ich herzlichst, dass er mich stets motiviert hat, immer an mich geglaubt hat und ich mich immer auf ihn verlassen kann.

8.6 Eidesstattliche Erklärung

Hiermit erkläre ich an Eides statt, dass ich die vorliegende Dissertation selbständig verfasst habe und dabei keine anderen als die von mir angegebenen Hilfsmittel und Quellen benutzt habe. Zitate sind als solche gekennzeichnet.

Ich erkläre außerdem, dass die vorliegende Dissertation weder in gleicher noch in ähnlicher Form bereits in einem anderen Prüfungsverfahren vorgelegen hat.

Ich habe früher, außer den mit dem Zulassungsantrag urkundlich vorgelegten Graden, keine weiteren akademischen Grade erworben oder zu erwerben versucht.

Würzburg, den

_____

Tanja Ulrich